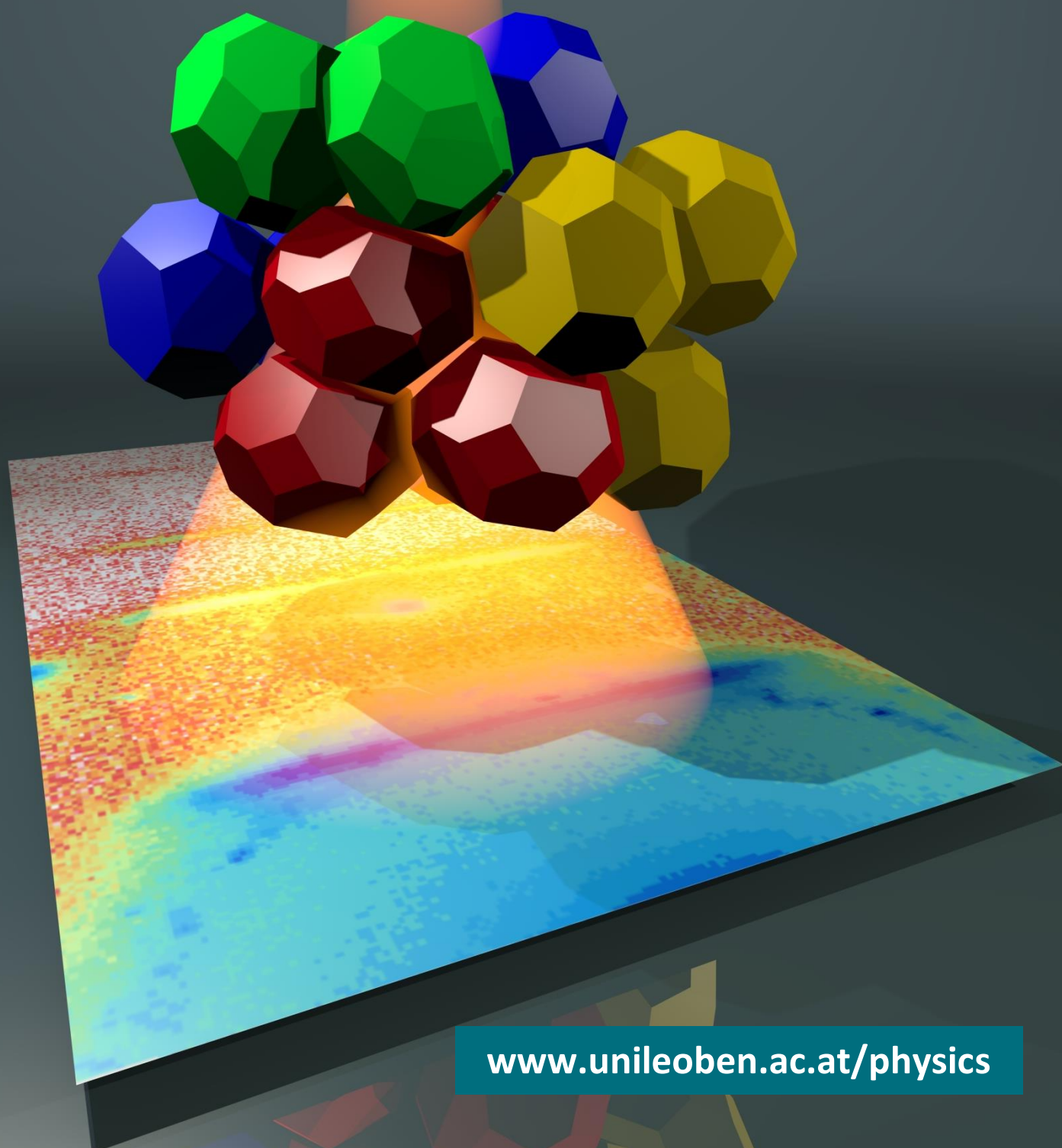


BI-ANNUAL REPORT

2016 and 2017





First row from left: Oswald, Moharitsch, Gratwohl, Czibula, Kirchberger, Paris, Kratzer, Teichert, Pirker
Second row from left: Genser, Koczwarra, Morak, Ludescher, Prehal, Stock, Meisels
Third row from left: Kuchar, Lin, Lechner, Matković

Impressum

Editor: Oskar Paris

Layout and Production: Heide Kirchberger
Gerhard Popovski
Oskar Paris

Contact

Institute of Physics
Montanuniversität Leoben
Franz Josef Straße 18
A-8700 Leoben

Phone: +43 (0)3842 402-4601

Fax: +43 (0)3842 402-4602

e-mail: physics@unileoben.ac.at

<http://www.unileoben.ac.at/physics>

Cover image (Design © M. Burian):

Colloidal nanocrystal in the synchrotron beam (M. Burian & R.T. Lechner et al., *Advanced Materials* 2018)

BI-ANNUAL REPORT

2016 / 2017

CONTENTS

		Page
	Preface	3
1.	Personnel	5
2.	Research	9
3.	Publication List	47
4.	Presentations	51
5.	Research Projects	56
6.	Teaching	60
7.	Bachelor-, Diploma- and Doctoral Theses	68
8.	Incomings: Invited Guests	70
9.	Outgoings: Foreign Stays of Institute Members	75
10.	Conference Organisation	77
11.	University Administration	78
12.	Advisory- & Editorial Boards, Review Committees, Memberships, etc	78
13.	Picture Gallery	80

Preface

Dear colleagues and friends,

It is a great pleasure to share with you the biannual report 2016/2017 of the Institute of Physics at the Montanuniversität Leoben. Our mission is to perform cutting-edge fundamental research related to the physics of functional materials. Moreover, the basic physics education for Bachelor students and several advanced physics related courses for Master/PhD students continue to keep us busy also in teaching. In this report we present our main scientific and teaching activities during the reporting period, the core being 18 scientific reports on the diverse activities of the four research groups at the institute.

Research: some facts and figures in brief

The publication output during the reporting period was 67 scientific articles (thereof 51 in SCI journals) and 86 presentations at international conferences and at external universities or research institutions. The impressive number of 14 high-impact publications (SCI Impact-Factor > 7), among them papers in *Science*, *Nature Energy*, and *Advanced Materials*, demonstrates that the Institute acts at the real forefront of international scientific research in materials physics. A quite significant number of press articles, e.g. in "Die Krone", "Der Standard" or "Kleine Zeitung" shows that we have also quite some public outreach with our work. Members of the institute have been invited to write a "News and Views" article in *Nature Materials*, have obtained prestigious awards, or have received international grants for research stays abroad. Not to forget, a large amount of time and effort was invested by institute members in serving the international scientific community with the organization of conferences and schools, editorial work and service in boards and review committees, and acting as reviewers for grant applications and research manuscripts. A number of FWF-projects (fundamental research), FFG-projects (applied research), participation in a Christian Doppler laboratory, and several ÖAD projects, ensured the third party financing of 3 Postdocs and 6 PhD students as well as several student workers during the reporting period. This means that slightly more than half of the scientific employees are financed from research grants. Moreover, 11 projects at large scale synchrotron and neutron facilities with a total of 56 days of beamtime were granted to members of the Institute in a competitive international peer review process. It should also be mentioned that new investments in infrastructure have been made in collaboration with other Chairs at MUL and supported by the rectorate, such as a new X-ray diffractometer, a tip-enhanced Raman spectroscopy AfM, and the participation in the new high-performance computing cluster.

In terms of promotion of young academics, one Habilitation, two PhD theses and six Master theses were completed at the institute during the reporting period. We are also delighted on the ongoing success of our research seminar on "Semiconductor Physics and Nanotechnology" with 47 lectures given by external guests during the reporting period, roughly half of the lecturers coming from outside Austria.

Teaching: the foremost obligation

Although the overall load was slightly released as compared to the previous reporting period, we still had a considerable teaching and examination obligation. The institute provides roughly 20 full courses each semester with around 20 parallel groups for the Physics I exercises course and 15 parallel groups for the Physics I practical training course in the respective winter terms, and only slightly lower numbers for the courses in the summer terms. This adds up to an average of almost 100 semester hours (semester hours are 45 Minute units given each week during the semester) over the reporting period. The highest load was on the two senior lecturers with up to 14 semester hours. By October 2017 a third senior lecturer was employed, which should help redistributing this load a bit, giving also the senior lecturers the possibility to advance their research portfolio towards habilitation. The fact that all freshmen Bachelor students have to pass three main physics courses in their first year, results in an enormous number of exams which have to be corrected essentially by the faculty staff. In total, 7826 individual exams were taken by the institute of physics in 2016/2017. This means close to 4000 exams each year, adding some more "semester hours" on teaching activity particularly for the faculty staff members.

All our progress and achievements strongly rely on the motivation and creativity of the individuals involved. I am very grateful to all members of the institute, who contributed in one or another way to make the successful work documented in this report happen. I am particularly also grateful to all those who contributed actively to this report.

I hope you enjoy reading this report and keep in touch with the Institute of Physics

August 2018

Univ.-Prof. Dr. Oskar Paris



1. Personnel

Faculty: Science and Teaching

Professors



Univ.-Prof. Dr. Oskar PARIS
(Chair)



Ao.Univ.-Prof. Dr. Christian
TEICHERT
(Vice-Chair)

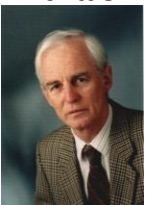


Ao.Univ.-Prof. Dr. Josef
OSWALD



Ao.Univ.-Prof. Dr. Ronald
MEISELS

Emeritus



Em. O.Univ.-Prof. Dr. Friedemar
KUCHAR

Assistants



Dr. Rainer LECHNER
Assistant/Senior Lecturer



Dr. Markus KRATZER
Assistant/Senior Lecturer



Dipl. Ing. Christian KOCZWARA
Assistant/PhD Student



Dr. Roland MORAK
Assistant/PhD Student

Faculty: Administration and Technical Support



Heide KIRCHBERGER
(Secretary)



Peter MOHARITSCH
(Mechanical Engineer)



Thomas JUD
(Apprentice to the Secretariat)



Ing. Heinz PIRKER
(Electrical Engineer)

Research Associates

Postdoc



Aleksandar MATKOVIC
Postdoc



Doz. Dr. Gerhard POPOVSKI
(Postdoc until 12/2016)

Assistant/Senior Lecturer
(since 10/2017)



Dr. Christian GANSER
Doctoral student
(until 03/2017)

PhD students



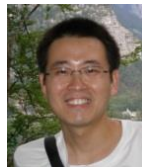
MSc Benjamin KAUFMANN
(until 08/2016)



Dr. Christian PREHAL
Doctoral student



Dipl. Ing. Lukas LUDESCHER
Diploma thesis (until 03/2016)
Doctoral student (since 07/2016)



Dipl. Ing. Quan SHEN
Doctoral student



Dipl.-Ing. Catherina CZIBULA
Diploma thesis (until 06/2016)
Doctoral student (since 08/2016)

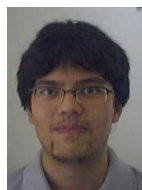


Dr. Monika MIRKOWSKA
joint with Chair of Mineral
Processing (until 12/2016)

Diploma / Master thesis



Dipl.-Ing. Jakob Alexander
GENSER
Student Worker,
Diploma thesis (until 12/2016)



Dipl.-Ing. Patrice KREIML
Student Worker,
Diploma thesis (until 6/2016)



Dipl.-Ing. Michael LASNIK
Student Worker
Diploma thesis (until 10/2016)



Michael HUSZAR
Diploma thesis (since 6/2015)



Dipl.-Ing. Guanpeng LIN
Diploma thesis (until 09/2017)

Student workers



Kevin-Peter GRADWOHL
Student Worker (since 10/2016)



Aydan CICEK
Student Worker (until 10/2017)



Hanno Lorenz HOLZINGER
Student Worker (since 10/2017)



Hannah SCHÖNMAIER
Student Worker (until 2/2017)



Sebastian Manfred STOCK
Student Worker (since 04/2017)



Lisa Weniger
Student Worker (since 12/2017)



Lorenz HAMMERSCHMIDT
Student Worker (since 10/2017)

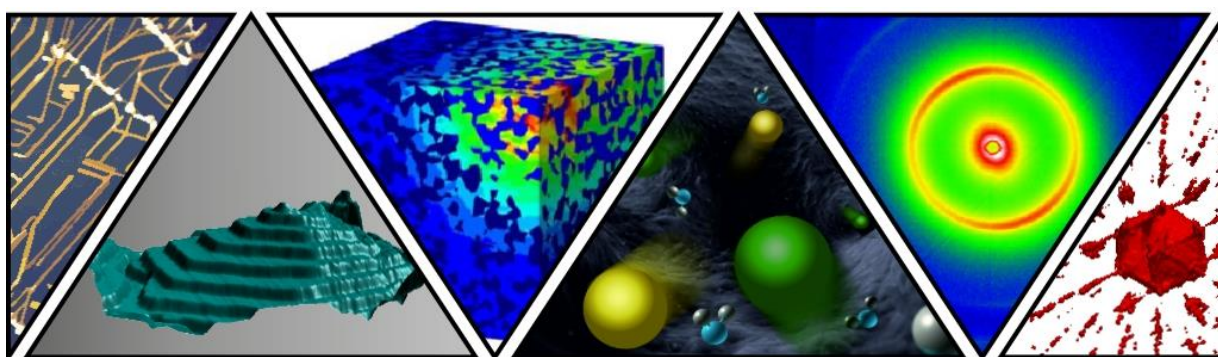


Maximilian RITTER
Student Worker (since 10/2017)

2. Research

Research at the Institute of Physics is dedicated to the physics of functional materials. Actual research topics include the study of nanostructured surfaces, nanoparticles and nanoporous materials, as well as biological, bio-inspired and bio-based systems. We investigate for instance the (nano-) structure and functional properties of a wide range of materials and material systems such as molecular semiconductors on 2D materials, semiconductor nanoparticles, ordered nanoporous silica and -carbons, paper fibers, and teeth. Potential application fields are in microelectronics (including electronic transport phenomena), photonics, energy conversion (e.g. solar cells), and energy storage (supercapacitors and batteries).

Two major experimental techniques are employed and continuously further developed, namely scanning probe microscopy and X-ray / neutron scattering including the extensive use of synchrotron- and neutron radiation at large-scale facilities. In particular, we develop new measurement techniques for the characterization of materials and devices at work, e.g., in-situ X-ray scattering during charging/discharging of operating supercapacitor cells. Experimental work is complemented by a range of numerical simulation tools such as atomistic Monte Carlo simulations, finite difference time domain (FDTD) calculations, or quantum mechanical (Hartree Fock) simulations.



2.1 High-impact publications

First author	Co-authors from the Institute of Physics	Journal	SCI Impact Factor 2017
Prehal	Koczwar, Paris	Nature Energy	46.86
Natalio	Popovski, Paris	Science	41.06
Teichert		Nature Materials	39.23
Van Opendenbosch	Popovski, Paris	Advanced Materials	21.95
Sytnykt	Lechner, Ludescher	ACS Nano	13.71
Kostoglou	Koczwar, Prehal, Paris	Nano Energy	13.20
Herbig	Teichert	Nano Letters	12.08
Putz	Morak, Paris	Chem. Mater.	9.89
Prinz	Matkovic	Small	9.60
Samusjew	Kratzer, Teichert	ACS Appl. Mater. Interface	8.09
Koczwar	Prehal, Paris	ACS Appl. Mater. Interface	8.09
Zhang	Paris	Nanoscale	7.23
Vasić	Matkovic	Carbon (2 times)	7.08

The table highlights the high-impact publications (SCI Impact Factor > 7) from- or with participation of the Institute of Physics within the reporting period. Names in bold indicate that the first author / corresponding author is from the Institute of Physics.

2.2 Public outreach / press reports

1. APA: 'Neue Einblicke in das Innere von Superkondensatoren', 06.03.2017
2. APA: 'Nanoporöser Kohlenstoff für die Energiespeicherung', 09.11.2017
3. Der Standard: 'Magnetische und fluoreszierende Baumwolle erzeugt', 17.09.2017, <https://derstandard.at/2000064080957/Forscher-erzeugen-magnetische-und-fluoreszierende-Baumwolle>
4. Der Standard Print Ausgabe: 'Röntgenblick ins Innere von Superkondensatoren mit Teilchenbeschleuniger', 22. Februar 2017, F5
5. Der Standard Online Ausgabe: 'Forschern gelingt neuer Einblick ins Innere von Superkondensatoren', 06.03.2017, <https://derstandard.at/2000053657776/Forschern-gelingt-neuer-Einblick-ins-Innere-von-Superkondensatoren>
6. Forbes online: 'This Cotton Is Grown To Glow', 14.09.2017, <https://www.forbes.com/sites/samlemonick/2017/09/14/this-cotton-is-grown-to-glow/#563b07424184>
7. Kleine Zeitung Print Ausgabe: Erfolgreiche Forschung bei Energiespeicherung, 10.11.2017
8. Kleine Zeitung Print Ausgabe: Energie speichern mit Nano-Kohlenstoff, 10.11.2017
9. Kleine Zeitung Online Ausgabe: Superkondensatoren auf der Spur, 02.02.2017, https://www.kleinezeitung.at/steiermark/leoben/5163694/Montanuni-Leoben_Superkondensatoren-auf-der-Spur
10. Kronen Zeitung Print Ausgabe: T-Shirt auch nach 30 Mal waschen wie neu, Kronen Zeitung, 15.19.2017, 40f
11. Nature Chemical Biology: 'Biomaterials: Cotton gets superpowers', 18.09.2017, <https://www.nature.com/articles/nchembio.2505>
12. New York Times: 'A Glowing Cotton Study That Might Have Deserved Less Glowing Reviews', 21.09.2017, <https://www.nytimes.com/2017/09/21/science/glowing-cotton-study.html>
13. ORF online: 'Baumwolle, die leuchtet und magnetisch ist', 15.09.2017, <https://science.orf.at/stories/2866262/>
14. ORF Steiermark: 'Leobner erforschen Superkondensatoren', 06.03.2017, <https://steiermark.orf.at/news/stories/2829316/>
15. Pro-Physik: 'Bessere Simulation von Energiespeichern', 01.02.2017, http://www.pro-physik.de/details/news/10460652/Bessere_Simulation_von_Energiespeichern.html
16. Spektrum online: 'Leuchtende Wolle', 15.09.2017, <https://www.spektrum.de/news/leuchtende-wolle/1502211>
17. New Business: 'Auf grünen Pfaden', 4.5.2017, <https://www.newbusiness.at/magazin/new-business-innovations/nr-04--mai-2017/auf-gruenen-pfaden>

2.3 New Research Infrastructure

Considerable investments in new research infrastructure (mostly together with other MUL-Chairs) have been made, with the help of partial funding by the infrastructure program of the rectorate. The numbers denote the total investment and the contribution of the Institute of Physics (in parenthesis).

- **Tip Enhanced Raman Spectrometry TERS** (with 2 other Chairs at MUL) 434 k€ (94 k€)
- **Diffractionmeter D8-Eco** (with Chair of Physical Chemistry) 182 k€ (49 k€)
- **High Performance Computing Cluster HPC** (with 7 Chairs at MUL) 198 k€ (12 k€)

2.4 Research Reports

The research activities during the reporting period are compiled and comprehensively presented in the following short research reports. They are structured according to the four independent research groups, each coordinated by one of the four Professors of the Institute. It should be mentioned, however that the Senior Lecturers Markus Kratzer, Rainer T. Lechner and Gerhard Popovski work to a large extend independently.

- **Nanomaterials and Scattering** *Oskar Paris*
- **Surface Physics and Scanning Probe Microscopy** *Christian Teichert*
- **Photonics and Nanoelectronics** *Ronald Meisels*
- **Simulation Electric Transport** *Josef Oswald*

Nanomaterials & Scattering

Ion charge storage in disordered nanoporous carbons

Christian Prehal, Christian Koczwara, Oskar Paris
christian.prehal@tugraz.at
oskar.paris@unileoben.ac.at

Storage and release of electric energy on a wide range of timescales are crucial for a sustainable energy management when implementing green technologies. This applies in particular to electric cars, microelectronics, or new forms of energy conversion. Today electric buses, aircraft doors, or systems that recover braking energy from vehicles already utilize an ultrafast energy storage technology called electrical double-layer capacitors or supercapacitors. These systems reveal higher power densities and much longer cycle lifetimes (>1 Million) than batteries. Although the design is like a conventional electrochemical cell, the charge storage mechanism in supercapacitors is completely different. If the supercapacitor is charged electrons (or holes) attract cations (or anions) at the electrode-electrolyte interface forming an electric double-layer and thereby provide the capacitive behavior. In order to store as many ions as possible, the electrodes are highly porous with typical specific surface area of several thousand square meters per Gram of the material.

The pores in such nanoporous carbon electrodes are not much larger than the (hydrated) ions themselves. Within the cross-linked network of pores, the ions have to share space with water molecules and ions of opposite charge.

In this confined space large amounts of energy can be stored; yet ion transport could be hindered due to mutual blocking of ions with opposite charge, comparable to ion traffic jams. High energy densities therefore come along with low power densities. This subtle trade-off between power and energy needs to be understood on an atomistic level in order to improve the overall performance of supercapacitors.

We have recently introduced in situ small angle X-ray scattering (in situ SAXS) to study global ion fluxes and local ion rearrangements in nanopores of carbon electrodes during charging [1, 2]. In the present work we report a novel experimental and data analysis tool to increase the fundamental understanding of such phenomena. Combining in situ X-ray scattering and atomistic modeling we were able to visualize ion electrosorption on a sub-nanometer scale and to benefit from the further development of optimized electrode materials. To achieve time resolutions in the sub-second regime most in situ scattering experiments were carried out at the Austrian SAXS Beamline at the ELETTRA synchrotron radiation source (Trieste, Italy) and the ID02 Beamline at ESRF (Grenoble, France) using a custom-built in situ supercapacitor cell. Different nanoporous carbon materials were used as electrode material and concentrated aqueous CsCl solutions as electrolytes. Installing a potentiostat at the beamline, 2D SAXS patterns of the electrolyte-filled working electrode were recorded during charging and discharging. There are considerable changes of the time-dependent SAXS data, however, the complexity of the system makes their interpretation difficult. Therefore, a novel data analysis approach, as visualized in Figure 1, was introduced [2, 3]. First, a 3D pore model was generated from a simple ex situ SAXS measurement of the carbon electrode in air using the concept of Gaussian Random Fields (Figure 1a and 1b) [2, 4].

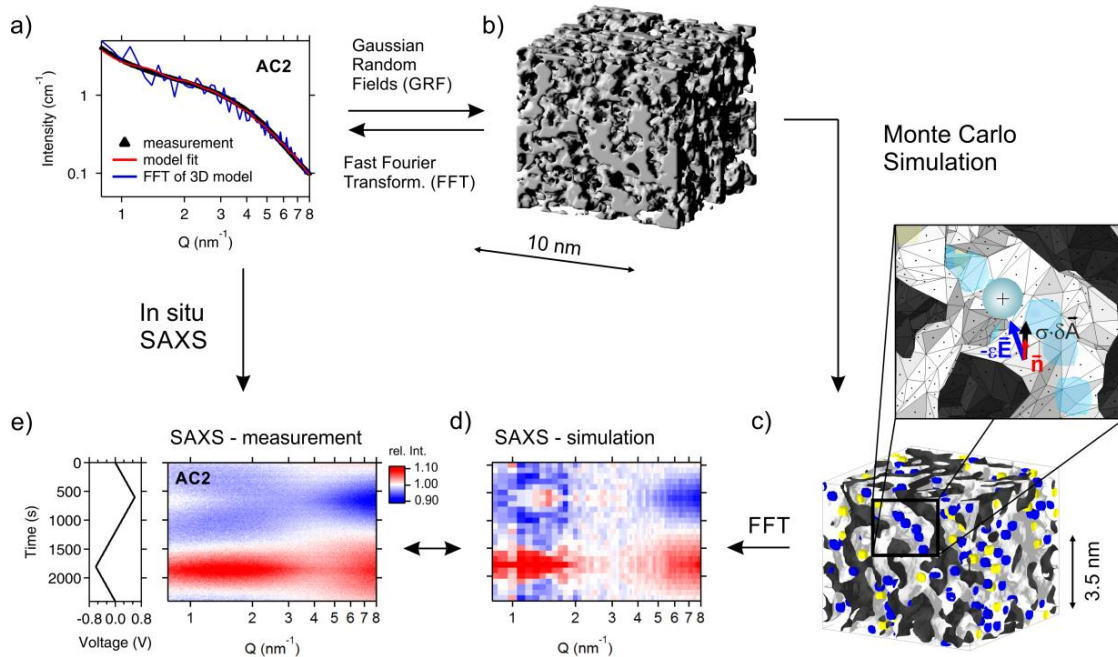


Figure 1: Scheme of the in-situ SAXS experiments and the data evaluation strategy. Reproduced and adapted from Ref. [3] with permission from Nature Publishing Group.

The pore model was then populated with a specific number of cations and anions obtained from the in situ experiment for each voltage step (c). Using a Monte Carlo simulation (Figure 1c), the equilibrium configurations of ions were determined and a subsequent Fourier Transform provided simulated scattering intensities for each cell voltage. These simulated patterns could be compared with real in-situ measurements (Figure 1d, 1e). Using this analytical tool the ion positions can be tracked within the real space pore structure as a function of the applied voltage. Interestingly, ions do not just change their concentration within the electrode upon charging, but they also change their positions within the nanopores. Defining a parameter called “degree of confinement” (DoC), the local ion re-arrangement was investigated quantitatively (Figure 2).

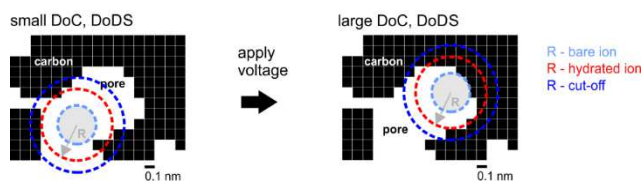


Figure 2: The sketch of a two dimensional (2D) cross section of the 3D pore structure visualizes the concept of degree of confinement (DoC). Reproduced from Ref. [3] with permission from Nature Publishing Group.

As shown in Figure 3a the mean DoC of counter-ions increases and the one of co-ions decreases for both positive and negative polarization of the electrode. This means that as the number of counter-ions is increased due to ion swapping, they also tend to occupy sites with a higher DoC. Correspondingly, the number of co-ions is decreased and sites with high DoC become more unlikely for co-ions.

In Figure 3b, the number of cations and anions assigned to a specific DoC at 0 V and at -0.6 V cell voltage are plotted in a DoC histogram. The histograms do not only change their absolute height (depending on the ion concentration) but also their overall shape. Ions on sites with high DoC can be conceptualized as ions in smaller pores. Accordingly, ions were classified in the DoC histogram into two categories, representing ions in either strong confinement or weak confinement. This permits to quantify the number of counter- and co-ions in two differing confining environments (or pore sizes) as a function of the state of charge from one single data set (Figure 3c), allowing to quantitatively separate the local rearrangement in strong and weak confinement.

This rearrangement is accompanied with a partial loss of the hydration shell each ion is carrying. Comparing three different nanoporous carbons with average pore sizes ranging from 0.65 – 1.3 nm, ion charge was found to be stored in pore systems enabling the largest change of the ions DoC (Figure 4). This way, the repulsive interaction between ions of the same charge is most effectively screened and ions can be packed most densely. In situ SAXS, therefore, allows a direct prediction of the capacitive performance of nanoporous carbon electrodes. The developed method and insights are of great relevance also for other, related technologies dealing with ion electrosorption, like for instance capacitive seawater desalination.

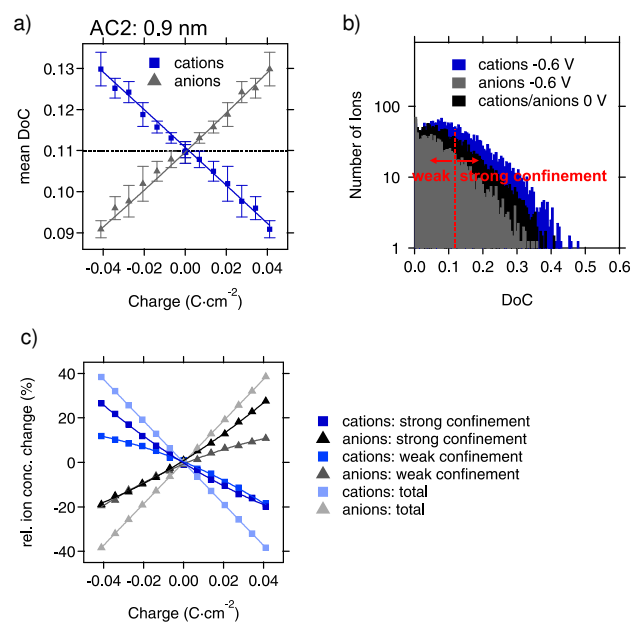


Figure 3: (a), Mean degree of confinement (i.e., mean value of DoC histogram, shown in (b) for selected voltages) for cations (Cs^+) and anions (Cl^-) as a function of the electrode charge for an activated carbon electrode. Selected DoC histograms of cations and anions are shown for 0 V and for -0.6 V in (b). The vertical dotted line separates ions into two groups corresponding to “small” and “large” DoC, representing qualitatively “large” and “small” pores as indicated. (c), the cation and anion concentration changes relative to their concentration at 0 V are given as a function of the SOC for two classes of confinement. Reproduced from Ref. [3] with permission from Nature Publishing Group.

Funding

Austrian “Klima- und Energiefonds” under the program line “Energieforschung” managed by the FFG, Project „Hybrid Supercap”; Project number 848808.

Cooperation

- Volker Presser, Nicolas Jäckel, Anna Schreiber (INM - Leibniz Institute for New Materials, Saarbrücken, Germany)
- Heinz Amenitsch, Max Burian (Austrian SAXS Beamline, Synchrotron ELETTRA, Trieste, Italy)

References

- [1] Prehal, C., et al., *Tracking the structural arrangement of ions in carbon supercapacitor nanopores using in situ small-angle X-ray scattering*. Energy Environ. Sci., 2015. **8**(6): p. 1725-1735.
- [2] Prehal, C., *Ion electrosorption in nanoporous carbons*, Dissertation, Montanuniv. Leoben 2017.
- [3] Prehal, C., et al., *Quantification of ion confinement and desolvation in nanoporous carbon supercapacitors with modelling and in situ X-ray scattering*. Nat. Energy, 2017. **2**: p. 16215.
- [4] Prehal, C., et al., *A carbon nanopore model to quantify structure and kinetics of ion electrosorption with in situ small angle X-ray scattering*. Phys. Chem. Chem. Phys., 2017. **19**: p. 15549.

Nanomaterials & Scattering

Carbons with hierarchical porosity: structural and electrochemical characterisation & electrosorption induced swelling

Christian Koczwar, Christian Prehal, Oskar Paris
christian.koczwar@unileoben.ac.at
oskar.paris@unileoben.ac.at

1) Introduction

With their high power densities and long cycle lifetimes supercapacitors play an important role in energy storage devices that require short charging and discharging times. They typically consist of two nanoporous carbon electrodes with their interparticle and intraparticle pore volume filled with a liquid electrolyte. Once a voltage is applied, an electrical double-layer will form at each electrode-electrolyte interface causing the capacitive behaviour.

During the last few years, we used in situ small-angle X-ray scattering to study ions in supercapacitor electrodes made of commercially available activated carbons. In addition to these disordered microporous materials, we started the investigation of hierarchical carbons synthesized by Nicola Hüsing's group (Paris Lodron University of Salzburg), with disordered micro- and macroporosity, but ordered mesoporosity. This type of materials enabled us to analyse new effects like electrode swelling on the nanometer scale, which is not be accessed in disordered materials. Additional activation allowed us to investigate the influence of micropore content on these effects. In addition we also started investigating the ion kinetics, which is an important parameter for the performance of supercapacitor devices.

2) Material synthesis

Two types of hierarchically ordered carbons synthesized via different processing routes were investigated. The first material was synthesized via a nanocasting route. A monolithic macro-/meso-/microporous silica template with ordered cylindrical mesopores on a 2D hexagonal lattice was infiltrated with a polymeric carbon precursor and carbonized. In a last step, the silica precursor is then removed by HF etching. The resulting material represents a positive replica of the macropore- and a negative replica of mesopore structure of the original silica, i.e. cylindrical carbon nanorods ordered on a 2D hexagonal lattice (Figure 1). We refer to this material as **Nano-Casted Carbon (NCC)**. The second material was produced via a soft-templating route, resulting in carbon structures with cylindrical mesopores ordered on a 2D hexagonal lattice, thus representing the negative mesopore structure as compared to the nano-casted carbon. Based on the synthesis process for this material, we refer it as **Soft-Templated Carbon (STC)**.

Due to the carbonisation process, the materials contain already some amount of micropores. Microporosity can be enhanced by additional CO₂ activation. This activation

process has only minor influence on the mesopore structure, but drastically increases the amount of micropores, and thus, the specific surface area in the material.

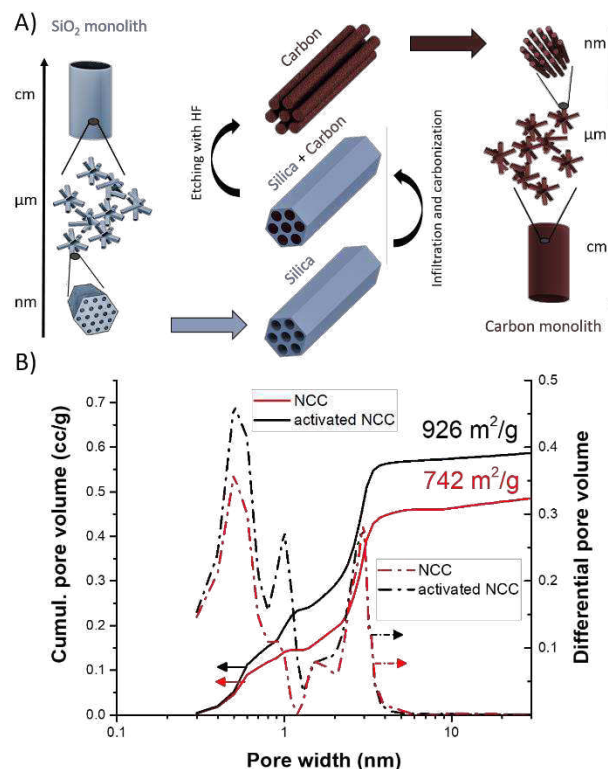


Figure 1: A) schematic representation of the synthesis of an ordered mesoporous carbon (NCC); B) Cumulative specific pore volume and differential pore size distribution of the untreated and the activated NCC carbon electrodes containing 10 mass% PTFE binder, determined from CO₂ and N₂ sorption isotherms (Reprinted with permission from [1]. Copyright (2017) American Chemical Society).

3) Characterisation

Gas sorption analysis, electrochemical testing and ex situ small-angle X-ray scattering (SAXS) are part of the standard characterisation protocol.

In Figure 1b the pore size distribution of an activated and an untreated NCC sample derived from N₂ and CO₂ gas sorption are shown. The amount of pores larger than 2 nm (mesopores) is nearly unchanged, while the amount of very small pores (micropores) is increased after activation. Gas sorption analysis was performed by our partners at the INM Saarbrücken.

The rectangular shape of the cyclic voltammetry (CV) curves (Figure 2a) confirms that electrodes made from these materials behave nearly as ideal electrical double-layer capacitor electrodes. The specific capacitance increases upon activation as expected. Fig 2b shows the relative change of the capacitance for scan rates from 0.5 mV/s to 50 mV/s for NCC and STC, compared to a commercially available activated carbon (YP-80). Both, the NCC and STC increase their performance upon activation. For the STC sample this increase is substantial. This demonstrates that the activated ordered mesoporous carbons outperform the commercially available reference material in terms of rate handling capability. A tentative explanation is that the mesopores

in the STC and NCC samples serve as additional ion/electrolyte reservoir or “ion highways”.

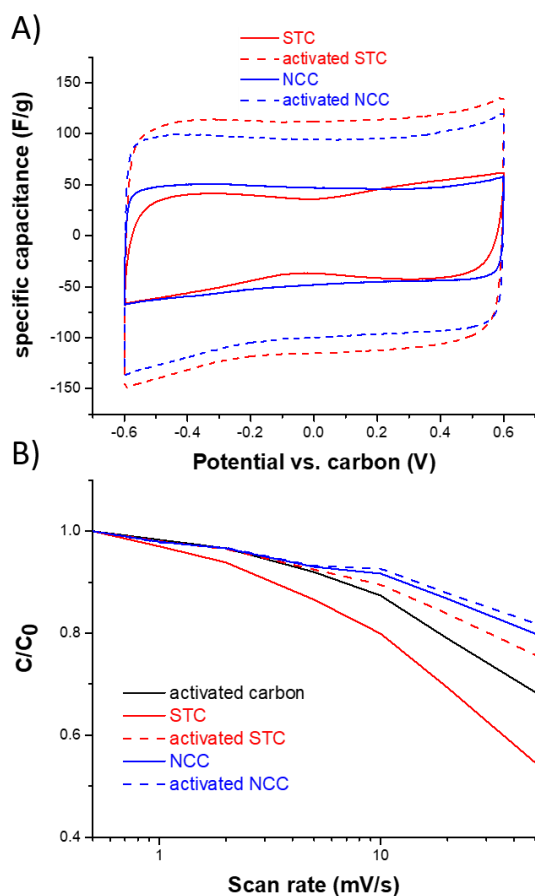


Figure 2: A) CV curves for activated and untreated NCC and STC electrodes, measured at 10 mV/s; B) relative capacitance for different scan rates.

SAXS measurements on these ordered hierarchical carbons show Bragg reflections originating from the ordered pore lattice (Figure 3). Even though the materials show similar peaks, it is clear that their mesopore structure is very different. NCC are built of carbon nanorods on a hexagonal lattice while STC have hexagonally ordered cylindrical pores in a carbon matrix. The quite different behaviour of the diffuse scattering gives also some hints to different micropore structures in the two materials. The elaboration of a detailed structural picture from SAXS with the help of TEM is currently in progress.

4) Electrosorption induced electrode swelling

With the hexagonally ordered materials at the mesopore level, we have a perfect model material to study electrosorption-induced deformation of the electrodes, during CV scans by simply measuring the shift of the Bragg reflections. In situ experiments were done at the Austrian SAXS beamline located at the synchrotron radiation facility Elettra in Trieste, Italy. All in situ SAXS measurements were made in specifically designed custom built housing. The actual supercapacitor cell built inside the housing is a sandwich-like design with holes in every component except the working electrode, which should be analysed.

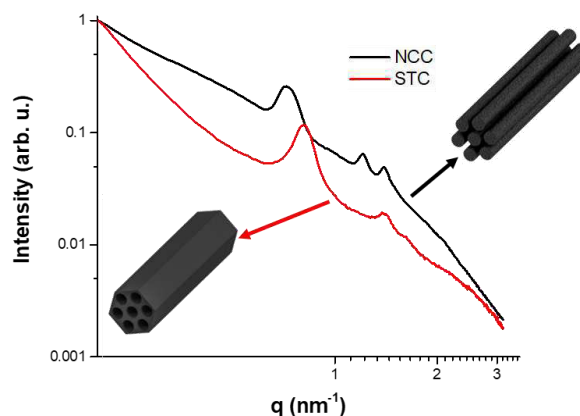


Figure 3: SAXS curves for untreated NCC and STC samples

To analyse the dimensional changes of the carbon electrode, the strongest Bragg peak has been tracked during in-situ CV scans on supercapacitor devices with NCC based working electrodes. The peak position for each frame was determined from the maximum of a fitted log-normal function. From the measured peak shifts, it is possible to calculate the occurring strain by using $\varepsilon = \frac{q_0}{q} - 1$, where q_0 represents the peak position at 0 V. As a result, we obtain the pore lattice strain of the electrode as a function applied potential. To compare the strain from SAXS with the macroscopic deformation of the bulk electrode, our partners from INM Saarbrücken carried out in situ electrochemical dilatometry. Figure 5 shows the strains measured with SAXS and with dilatometry for an untreated and an activated NCC material. The results are similar for both measurement techniques, indicating that the macroscopic electrode swelling originates from the deformation of the carbon material at the meso-/micropore level.

Apparently, the result for the activated NCC deviates from the untreated one. In particular it is found that the strain is asymmetric with respect to the sign of the applied voltage, the effect becoming more pronounced with activation. Since the asymmetry of the strain depends on the amount of micropores within the otherwise similar carbon nanorods, ion size effects can be rejected to be solely responsible for the asymmetry. There have to be at least two separate physical contributions of the same order of magnitude to explain these findings. A positive strain for both, positive and negative applied potential would be resulting from a steric effect caused by the local concentration change of the (similarly sized) ions. A mechanism depending on the sign of the applied potential is electron/hole doping, leading to a variation of the C-C bond length. A negative applied potential leads to an elongation of the C-C bond causing a positive strain, a positive potential leads to a shortening of the bond length causing negative strain. The combination of the two effects is shown in a simple scheme in Figure 6, explaining qualitatively the experimentally observed behaviour.

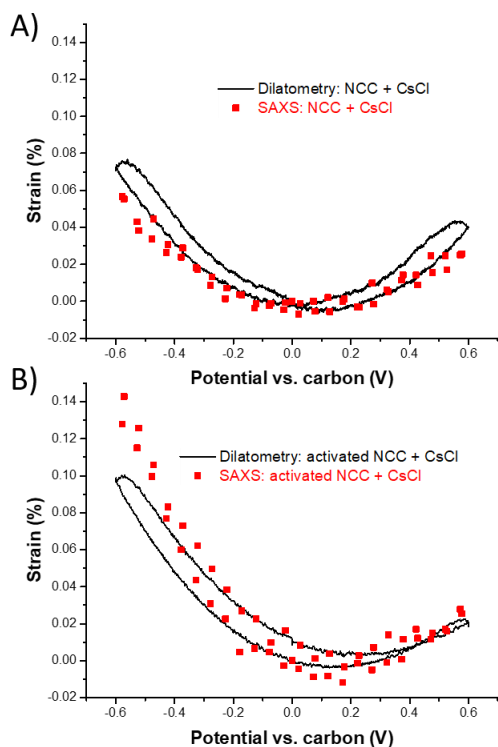


Figure 4: Strain versus electrical potential from in situ SAXS (red) and in situ dilatometry (black) for (A) NCC and (B) activated NCC, both recorded at 1 mV/s with the same electrolyte (1 M CsCl). (Reprinted with permission from [1]. Copyright (2017) American Chemical Society).

5) Outlook

Additional experiments are necessary to better understand the basic mechanisms of electrode swelling. The above-mentioned STC materials have so far been characterized electrochemically, but not in terms of electrode swelling behaviour. Since the pore space at the mesopore level is completely different for the NCC and the STC materials (negative vs. positive curvature, simple cylindrical pores vs. complex pore geometry, etc.) makes a comparison between these two material types a promising attempt. The corresponding in situ experiments are currently in progress. In order to separate the effects of SAXS contrast changes due to ion concentration changes and the pure strain effects, it is planned to perform contrast variation experiments by using anomalous SAXS (ASAXS).

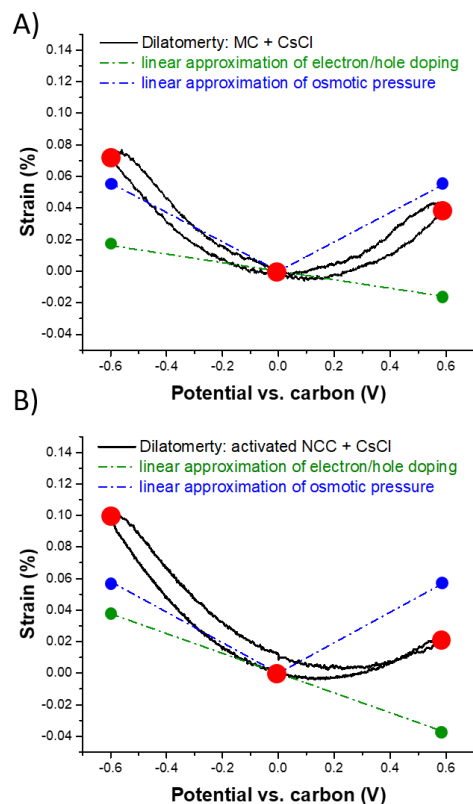


Figure 5: Linear strain approximation of the two proposed contributions electron/hole (green dots) doping and osmotic pressure (blue dots) for the NCC (A) and the activated NCC (B) sample. The red dots show the sum of the two contributions. The dashed lines serve as guides to the eye.

Funding

- Austrian “Klima- und Energiefonds” under the program line “Energieforschung” managed by the FFG, Project „Hybrid Supercap“; Project number 848808.

Cooperation

- Volker Presser, Institut für Neue Materialien (INM) Saarbrücken GERMANY.
- Nicola Hüsing, Univ. Salzburg, AUSTRIA.
- Heinz Amenitsch, TU Graz, AUSTRIA and ELETTRA Trieste, ITALY.

References

- [1] C. Koczwar, S. Rumswinkel, C. Prehal, N. Jäckel, M. S. Elsässer, H. Amenitsch, V. Presser, N. Hüsing and O. Paris, *ACS Appl. Mater. Interfaces*. **9** (2017), 23319-23324.

Nanomaterials & Scattering

Activated Carbon Cloth: a versatile material for energy storage applications

Christian Koczwar, Christian Prehal, Oskar Paris
christian.koczwar@unileoben.ac.at
oskar.paris@unileoben.ac.at

Using hydrogen in internal combustion engines or fuel cell vehicles demands highly reliable and efficient storage systems. A very promising method of storing H₂ is physically adsorbing the gas in highly porous materials with large specific surface areas. Hereby the occupied volume of H₂ is drastically reduced compared to gaseous hydrogen. Additionally, the process of physically adsorbing and desorbing is fully reversible. Activated carbon (AC) materials are suitable for the use in hydrogen storage systems, because of their high surface area, cheap production and good stability.

In this context, two research groups at Montanuniversität Leoben, represented by Christian Mitterer (Chair of Functional Materials and Materials Systems) and Oskar Paris (Institute of Physics), in close collaboration with an international and interdisciplinary team from Serbia, Cyprus, Greece and UK have successfully developed a mechanically stable and flexible nanoporous activated carbon cloth (ACC) material. The fabric-like structure with a large specific surface area (~1200 m²/g) and specific pore volume (~0.5 cm³/g) has been realized via a combination of carbonization and CO₂ activation of a low-cost cellulose-based fabric (viscose rayon cloth), see Fig. 1.

By using small-angle X-ray scattering in combination with the concept of Gaussian random fields, a 3D real space model of the ACC micropore structure has been created (Fig. 2). The 3D visualization shows that the nanopores are rather randomly shaped, and the parameters allow

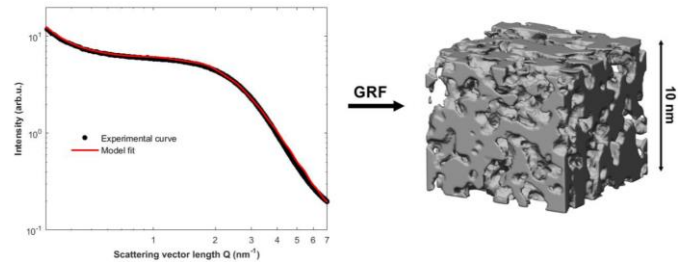


Figure 6: SAXS curve of the ACC (left) and real space model pore structure created via Gaussian Random Fields (right). Reprinted [1], Copyright (2017), with permission from Elsevier.

deducing structural parameters such as a pore size distribution, specific surface area or pore volume fraction. As compared to commercially available activated carbon materials, the carbon cloth ACC shows a superior H₂ cryo storage performance. A gravimetric H₂ uptake of 3.1 wt.% at 77 K and 70 bar could be achieved. This exceeds other AC materials, with similar specific area and pore volume by about 25 %.

In addition to the use in hydrogen storage devices, the ACC is also a suitable material for supercapacitor electrodes. Because of its mechanical stability no additional binder is necessary which increases the amount of active material compared to electrodes produced from powder materials. The electrochemical performance of this ACC is comparable to commercially available AC materials. Long-term stability tests revealed that after 10000 charging/discharging cycles about 97% of the initial capacitance was maintained. The fact that this material can be used as a stand-alone and binder-free electrode widens its possible applications.

Finally, the same material also proved to be very efficient as a membrane for selective gas separation in CO₂/CH₄ mixtures towards natural gas purification as well. The versatile character of the ACC material as a gas and ion adsorbent in combination with its fabric-like nature make it an attractive option for practical and large-scale green energy-related applications [1].

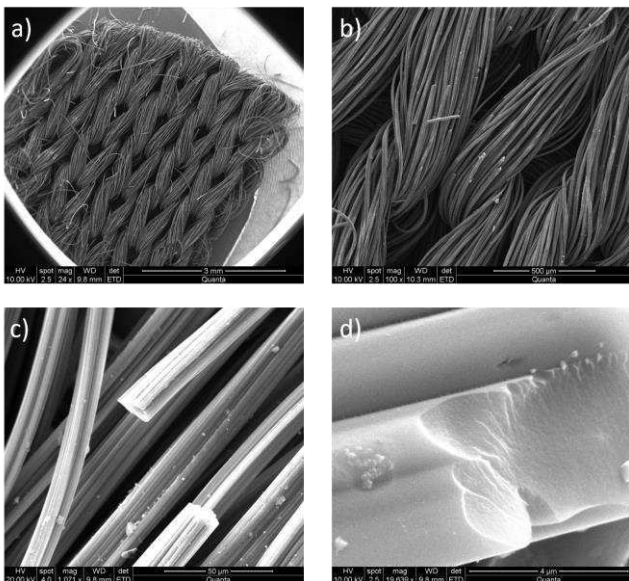


Figure 7: SEM images of ACC at different magnifications. (a) ACC cloth, (b) woven yarns, (c) carbon fibers, (d) fractured fiber surface. Reprinted [1], Copyright (2017), with permission from Elsevier.

Cooperation

- Christian Mitterer and Nikolaos Kostoglou, Chair of Functional Materials and Materials Systems, MU Leoben, AUSTRIA
- Claus Reholz, University of Cyprus, Nicosia, CYPRUS

References

[1] N. Kostoglou, C. Koczwar, C. Prehal, V. Terziyska, B. Babic, B. Matovic, G. Constantinides, C. Tampaxis, G. Charalambopoulou, T. Steriotis, S. Hinder, M. Baker, K. Polychronopoulou, C. Doumanidis, O. Paris, C. Mitterer and C. Reholz, *Nano Energy* **40** (2017) 49-6.

Nanomaterials & Scattering

Gas adsorption in carbons with hierarchical porosity

Lukas Ludescher, Oskar Paris
 lukas.ludescher@unileoben.ac.at
 oskar.paris@unileoben.ac.at

Adsorption of n-pentane and nitrogen in nanocasted, hierarchical macro-, meso- and microporous carbon materials is investigated. First, in-situ experiments during adsorption with small angle neutron scattering are presented. Then a theoretical framework is developed to model adsorption and condensation in these materials. From this model some preliminary conclusions are drawn to qualitatively understand experimental data of adsorption induced deformation.

1) Experimental Data

CMK-3 and CMK-3-type materials are a class of micro- / mesoporous carbon materials with 2D hexagonally ordered mesopores [1]. Structurally, they are a true negative of SBA-15 silica which consists of cylindrical pores arranged on a 2D hexagonal lattice. Therefore, CMK-3 materials exhibit a much more complex open mesopore space as compared to SBA-15. In addition to nitrogen adsorption, we used small angle x-ray (SAXS) and n-pentane adsorption combined with in-situ small-angle neutron scattering (SANS) for characterization.

The material under investigation was a monolithic, hierarchically ordered CMK-3 type material, synthesized by our partners from the Paris Lodron University, Salzburg. The characterization by nitrogen and n-pentane adsorption was conducted by our partners from the ZAE Bayern. The SAXS measurements were performed in-house on a Bruker Nanostar SAXS instrument. In-situ SANS data were recorded at the SANS instrument at the MLZ in Garching, Germany. The overall design of the in-situ measurements is similar to previous work on monolithic, hierarchically porous silica performed by our group [2].

The overall mesostructure of the material consists of 2D hexagonally ordered, parallel carbon nanowires. The actual mesopore-space is of concave nature and the adsorption behavior is markedly different from other prominent, highly ordered mesoporous materials like SBA-15. Because the carbon material is a negative replica of the aforementioned silica materials, however, the same data evaluation techniques can be applied for the SAXS and SANS data. The nanowire distance D is determined from the Bragg peak positions by applying Bragg's law, and the mean nanowire radius is determined from the height of the Bragg reflections via a Formfactor fit. The values for the nanowire distance D and their radius r were determined to be 10.1 nm and 3.9 nm, respectively. Adsorption induced deformation in these ordered materials can easily be determined by using in-situ X-ray or neutron scattering. To avoid so-called contrast effects, we used neutron scattering with the approach to tune the effective scattering length density of the adsorptive to zero [2]. This was achieved by a proper mixture of non-deuterated and deuterated n-pentane.

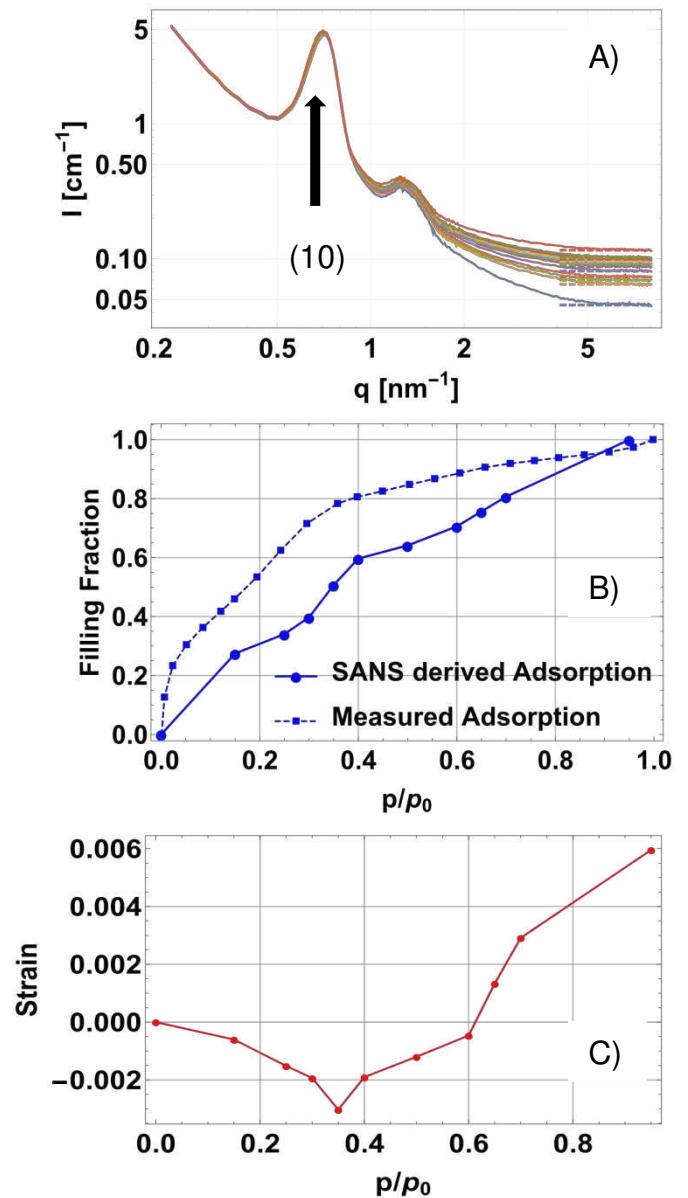


Figure 1: (A) SANS profiles from monolithic CMK-3 type material at distinct relative pressures of n-pentane. The incoherent background is highlighted by the dashed lines. (B) The filling fraction derived from SANS (thick line) and from a dedicated measurement (dashed). (C) Resulting strain isotherm derived by the relative peak shift of the (10) peak highlighted in A.

Scattering patterns were collected at 11 distinct relative pressures in adsorption (Fig. 1A). Quantitative information on the filling of the sample can – besides the usual sorption isotherms measured volumetrically with commercial instruments - also be obtained from the incoherent background (dashed lines in Fig. 1A), which is for our system practically determined by the amount of hydrogen in the sample. This information can be transformed into an adsorption isotherm [2], and compared with a volumetrically determined isotherm (Fig. 1B). Overall, the small angle neutron scattering derived filling data represents the general trend from the n-pentane adsorption measurement. Information on the adsorption induced deformation is obtained from the shift of the (10) peak at different pressures in relation to the first recorded pattern. In Fig. 1C the resulting strain

isotherm is presented, showing a qualitatively different behavior than deformation data from the original silica structure [2].

Of note are the two discontinuous, step-like features in the adsorption isotherm (Fig. 1B), which seem to be also presented in the strain-isotherm (Fig. 1C). This suggests two separate filling events which have not been discussed so far in literature for materials exhibiting similar mesostructure.

2) Modelling of Adsorption in CMK-3-type Materials

To describe the adsorption and condensation processes in the hierarchically porous carbon material, a theoretical model from literature was adopted [3]. We assume three different phases which are labelled as “separated”, “bridged” and “filled”. The separated phase describes the simple layer growth of adsorbate on the individual nanowires, whereas the filled phase denotes the completely filled void space. The bridged phase describes the existence of liquid bridges, spanning the void space between neighboring carbon nanowires. For all three phases, the grand potential was formulated as a function of the liquid-vapor profile and then minimized via the Euler-Lagrange equation.

The resulting non-linear, ordinary differential equations were then solved and the grand potential determined for all three phases. This was executed for a set relative pressures between 0 and 0.95 and for varying nanowire radii between 3.2 nm and 4.4 nm. The nanowire distance was kept constant at the experimentally determined value of D . For every single configuration of geometry and pressure, the phase with the lowest grand potential was determined and a phase diagram was drawn (Fig. 2). Fig. 2 also shows the experimentally determined transition pressures from the shoulders in the adsorption isotherm (Fig. 1B) (vertical green bars) and the ratio $D/r = 2.6$ determined from SAXS (horizontal blue bar). Phase diagrams were calculated for both nitrogen (Fig. 2A) and *n*-pentane (Fig. 2B) using corresponding reference isotherms for the quantification of the liquid-solid interaction potential. In both cases the agreement between calculation and experiment is excellent. The fact that equilibrium calculations describe the pressures of existence of the phases so well points to heterogeneities forming nucleation sites between neighboring nanorods.

3) Adsorption induced deformation

In Fig. 1C the sample contracts at low relative pressures with a minimum at $p/p_0 \approx 0.35$, and shows a second discontinuity at $p/p_0 \approx 0.6$. This second discontinuity corresponds well to the bridged-filled transition (Fig. 2B). The minimum at 0.35 on the other hand corresponds well to the end of the separated-bridged transition, which can be expected to be somewhat smeared due to a rough surface of the carbon nanowires. Therefore, we tentatively relate the discontinuities in the strain isotherms to the two phase transitions. Both of them create a negative Laplace pressure causing the sample to contract, while overall the strain increases with relative pressure due to the decrease of the liquid-solid interfacial energy (Bangham effect).

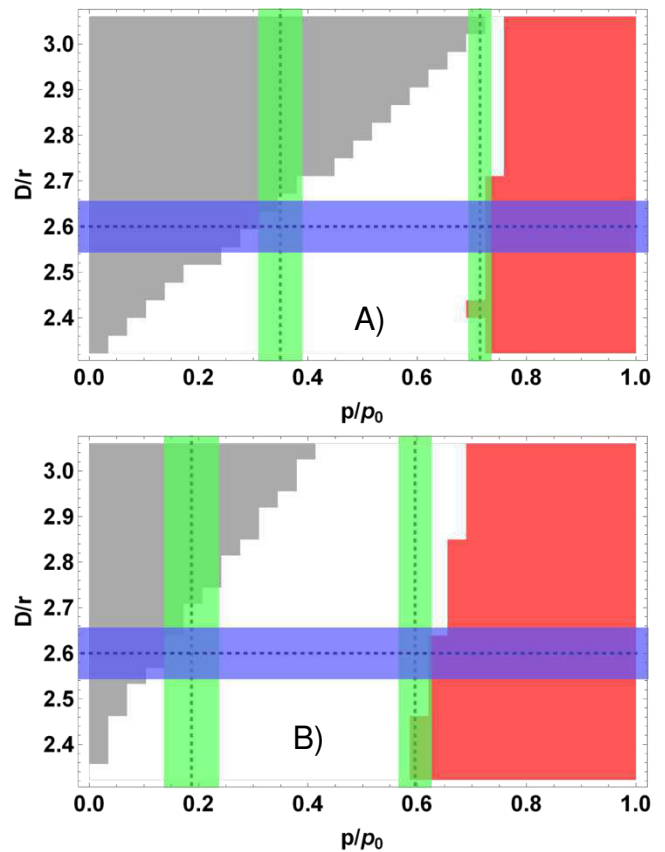


Figure 2: Calculated phase diagrams for nitrogen (A) and *n*-pentane (B) in hierarchical, monolithic CMK-3 type carbon material. The grey, white and red areas denote the separated, bridged and filled phase, respectively. Dashed vertical lines denote the mean relative pressure at which a phase transition occurs experimentally, with the green bars denoting the error of measurement. Horizontal dashed lines indicate the ratio $D/r = 2.6$ as determined by SAXS, with the blue bar again denoting the error of measurement.

Funding

Austrian Science Foundation FWF (project I 1605-N20) in the framework of the DACH agreement.

Cooperation:

- Gudrun Reichenauer, Center for Applied Energy Research Bavaria (GERMANY)
- Nicola Hüsing, Chemistry and Physics of Materials, Paris-Lodron University Salzburg (AUSTRIA)
- Gennady Gor, New Jersey Institute of Technology (USA)

References:

- [1] Jun, Shinae, et al. Synthesis of new, nanoporous carbon with hexagonally ordered mesostructure. *J. Am. Chem.Soc.*, 2000, 122, 10712-10713.
- [2] Morak, Roland, et al. Quantifying adsorption-induced deformation of nanoporous materials on different length scales. *J. Appl. Crystall.*, 2017, 50, 1404-1410.
- [3] Dobbs, H. T.; Yeomans, J. M. Capillary condensation within an array of cylinders. *Molecular Physics*, 1993, 80, 877-884.

Nanomaterials & Scattering

Silica with hierarchical porosity: Water adsorption-induced deformation

Roland Morak, Lukas Ludescher, Oskar Paris
 lukas.ludescher@unileoben.ac.at
 oskar.paris@unileoben.ac.at

1) In-situ neutron scattering

Ordered porous systems are used as catalyst (support), or as actuators and sensors for diverse applications [1]. In particular with respect to actuation or sensing the sorption-induced deformation of porous systems as a result of their interaction with fluids is of interest. We use silica monoliths with hierarchical porosity as a model system to investigate sorption induced deformation at the macroscopic scale as well as at the mesopore scale in-situ during adsorption and desorption of fluids. On the macroscopic scale, length changes of the monolithic samples are measured by high resolution dilatometry (DIL). On the mesoscopic scale, the highly ordered arrangement of pores in a two dimensional, hexagonal lattice (Fig. 1A) is utilised to monitor the shift of Bragg peaks by using X-ray (SAXS) or neutron small-angle scattering (SANS). We combined DIL and SANS at the SANS I instrument at the MLZ (Munich, Germany) using a custom built sample holder (Figure 1B) accommodating a thin section (< 1mm) of the silica monolith.

SANS and DIL was measured as a function of relative water pressure and at the same time the macroscopic sample extension was monitored by the pushing rod of the dilatometer [1]. The relative water pressure in the sample cell was stepwise increased by a connected vapour dosing system. The water used for the adsorption was partially deuterated to enable zero scattering length density (zero-SLD) of the adsorbent. Therefore, only the change of the lattice parameter of the mesopore lattice was measured, without the influence of contrast effects due to the change in the scattering length density in the pores, usually experienced in X-ray scattering [2,3]. Prior to the in-situ experiments, water isotherms were recorded to determine the relative pressure regimes of interest for which in-situ SANS experiments were performed.

Three different samples, synthesised by our partners from University of Salzburg were investigated: the first sample was supercritically dried after synthesis and subsequently aged, which means it contained still some organic residues inside the pore walls, at least partially clogging the micropores. The second sample was in addition calcined at 310°C and then aged again, with the aim to remove the organics and create accessibility to the microporosity. The third sample was sintered at 750°C for 15 minutes after the calcination step in order to remove the micropores without affecting the hexagonal arrangement of the mesopores. SAXS and N₂ sorption showed that the structural changes due to the post-treatments were minor at the levels of the macro and mesopores, but severely influenced the microporosity.

We found that the maximum values of the sorption induced deformation differed by almost an order of

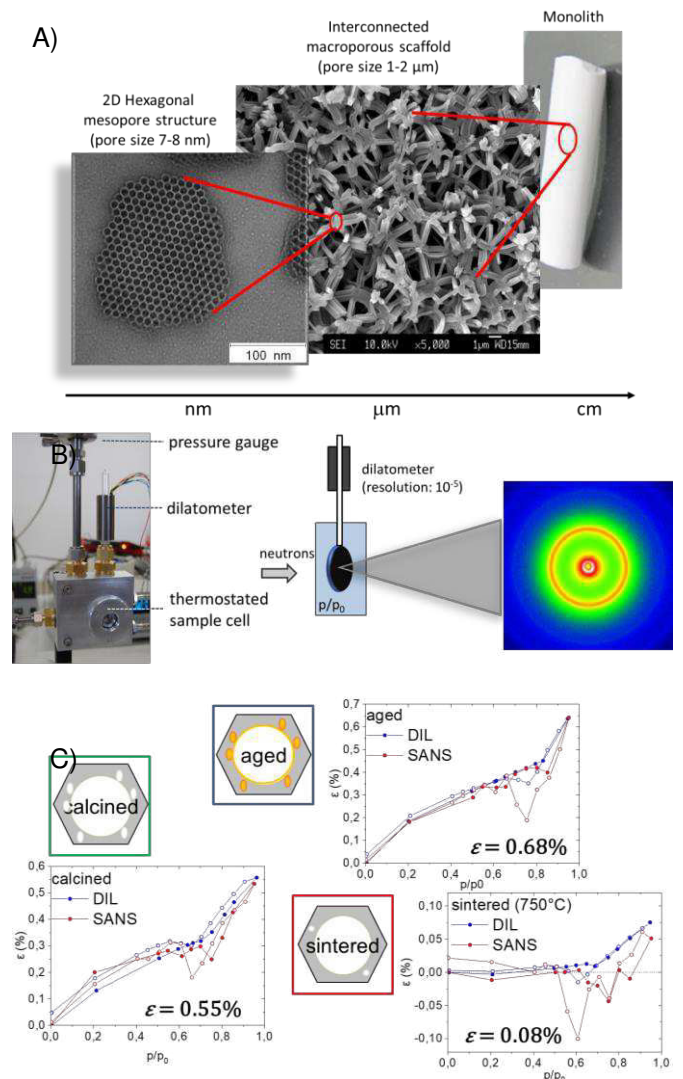


Figure 1: A) Hierarchical structure of the silica monolith. B) Set-up of the in-situ SANS-DIL measurement. C) DIL and SANS derived strain-isotherms for the 3 samples

magnitude (Figure 1C), being largest for the aged sample and smallest for the sintered sample. The overall magnitude of the strain is similar for the aged and calcined samples, more or less irrespective of the organics. For every sample investigated, we could show that the overall strain measured by dilatometry and small angle neutron scattering with a zero scattering length density adsorbate was essentially the same, except the region of capillary condensation, as predicted by theory [4]. This indicates that the largest effect of the sorption induced deformation must be attributed to effects taking place within the mesopore walls, i.e., in the micropores in the calcined sample and the additional organic residues in the aged sample.

2) Apparent Lattice Deformation in SAXS

Employing SANS with zero-SLD proved to be essential to obtain reliable strain data from scattering. Earlier work [3] has already shown that artifacts observed in in-situ sorption strain measurements by SAXSA are based on the change of contrast of the pore space upon filling. Figure 2A compares the SANS strain isotherm to the one measured using SAXS for the identical sample and adsorptive. In contrast to the SANS experiment, the

scattering length density of the adsorptive is not zero for the SAXS experiment, and the strain isotherm is influenced by so called pseudo-strain or apparent strain arising from the change in scattering length density within the mesopore space. Assuming that SANS with zero-SLD water delivers the “true” strain isotherm. Hence, we define the apparent strain $\varepsilon_{\text{apparent}} = \varepsilon_{\text{SAXS}} - \varepsilon_{\text{SANS}}$ as the difference between the two contrast scenarios (Fig. 2A, green curve).

To model this apparent strain, we use a similar approach as introduced in [3], but we also consider the adsorbed film and its growth [5] with increasing relative pressure. In contrast to [3] we calculate the Fourier transform of a model mesoporous strut (see Fig. 1A) by using the Debye equation. We model a hexagonal lattice of cylinders with a spacing of 11.3 nm, with their radius normal distributed around a mean of 3.6 nm and a standard deviation of 0.03 as estimated from SAXS. For each individual pore, the layer growth and filling is calculated at discrete relative pressures ranging from 0 to 0.99. The pressure of capillary condensation is also calculated via the adsorption condition [5] and considered in the form factor.

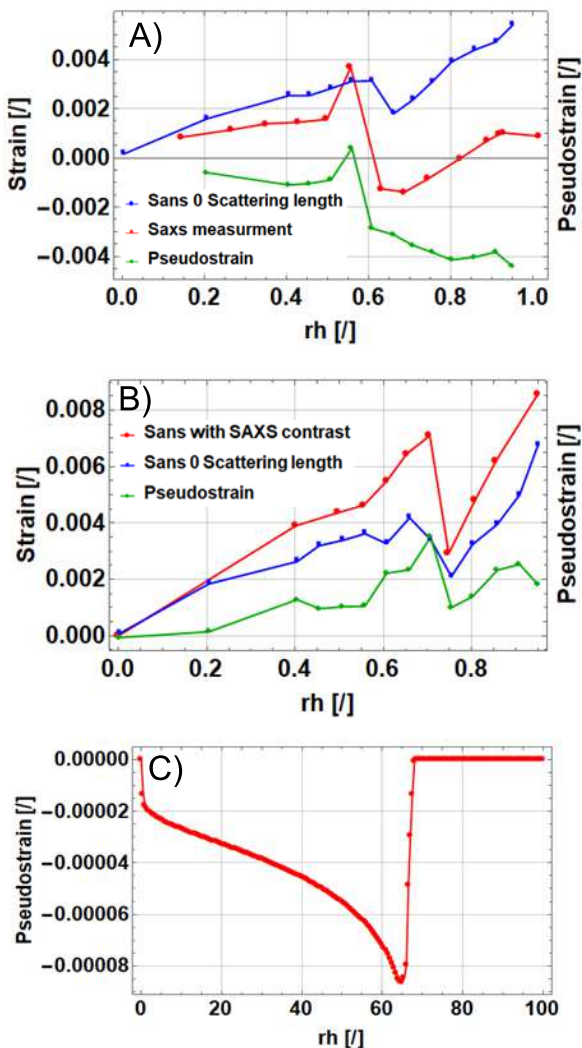


Figure 2: Strain isotherms for A) the calcined sample measured with SAXS and SANS (zero SLD) and B) the aged sample measured with SANS with 2 different contrasts. C) Calculated apparent strain for pure film growth in the mesopores.

For each pore, the scattering is determined by the analytically given form factor, and then summed via the

Debye equation. At each relative pressure, the center of mass of the resulting first order Bragg peak is determined and strain is calculated from its relative shift with respect to the empty pore. Because in this case there is no actual deformation, we basically evaluate the apparent strain. Figure 2C shows that the calculated apparent strain is always negative below capillary condensation, and jumps back to zero after all pores are completely filled. Qualitatively the experimental data in Fig. 2A show a similar trend, but the absolute values are far off from the calculated ones. Additionally, the apparent strain does not go back to zero for completely filled pores. We attribute this to a strong influence of the micropores, a scenario which has not yet been included in the model.

We also performed SAXS and SANS of the aged sample with two SLD'S of the water vapor for SANS: i) zero-SLD, and ii) SLD chosen to match the electron density from SAXS (Fig. 2B). Interestingly, while SAXS shows qualitatively the same behavior as in Fig. 2A (not shown) resulting in a negative apparent strain, the corresponding SANS data lead to a positive apparent strain (Fig. 2B). From the simulation we know, that film growth inside the mesopore alone can only attribute for negative apparent strains of lower magnitude. Consequently, the apparent strains observed in these experiments need to be related to changes in the pore walls, which are not yet considered in the simulation. In particular, the difference between SAXS and SANS with nominally the same SLD of the adsorbing fluid must be attributed to the different scattering length density of the organics situated in the micropores in the pore wall. Hence, these experiments allow, in principle, to deduce additional information on the role of the residual organic phase in adsorption induced deformation.

Funding

Austrian Science Foundation FWF (project I 1605-N20) in the framework of the DACH agreement.

Cooperation:

- Center for Applied Energy Research Bavaria (GERMANY)
- Department Chemistry and Physics of Materials, Paris-Lodron University Salzburg (AUSTRIA)

References:

- [1] Morak, R., Braxmeier, S., Ludescher, L., Putz, F., Busch, S., Hüsing, N., Reichenauer, G., Paris, O., *J. Appl. Crystall.*, 2017, 50, 1404-1410.
- [2] Balzer, C., Morak, R., Erko, M., Triantafillidis, C., Hüsing, N., Reichenauer, G., Paris, O., *Z. Phys. Chem.* 2015; 229, 1189–1209.
- [3] Prass J., Müter D., Erko M., Paris O., *J. Appl. Crystall.* 2012, 45, 798-806.
- [4] Balzer, C., Waag, A., Gehret, S., Reichenauer, G., Putz, F., Hüsing, N., Paris, O., Bernstein, N., Gor, G.G., Neimar, A.A., *Langmuir*, 2017, 33, 5592-5602.
- [5] Broekhoff, J.; De Boer, J., *J. Catal.*, 1967, 9, 8-14.

Nanomaterials & Scattering

Colloidal Nanocrystals

Rainer T. Lechner, Lukas Ludescher
rainer.lechner@unileoben.ac.at

1) Atomistic reconstruction of non-spherical graded core/shell nanocrystals

The wet chemical synthesis of core/shell colloidal nanocrystals (NCs) has led to a pronounced improvement in the optical properties and the chemical stability of semiconducting NCs [1, 2]. Engineering the compositional gradient for core/shell semiconductor nanocrystals improves their optical properties. To date, however, the structure of graded core/shell nanocrystal emitters has only been qualitatively described. In this report, we demonstrate an approach to quantify nanocrystal structure, selecting graded Ag-In-Se/ZnSe core/shell nanocrystals as a proof-of-concept material.

Our approach is illustrated in Figure 1: A combination of anomalous small angle x-ray scattering (ASAXS), wide angle x-ray scattering (WAXS) and electron microscopy techniques enables us to establish the radial distribution of ZnSe with sub-nanometer resolution, even for non-spherical particle shapes (see Figure1).

As a model system, we choose the case of Ag-In-Se/ZnSe core/shell NCs. Upon growth of a ZnSe shell, the luminescence efficiency increases, with current reports of up to 70% quantum yield (QY) for this system [3]. Owing to high miscibility between I-III-VI and II-VI semiconductors and to a large number of cationic defects, which facilitate diffusion, this system yields graded core/shell structures.

Anomalous small-angle X-ray scattering (or ASAXS) is sensitive to element-specific variations in a material. This is achieved by measuring at energies around the absorption edge of the element of interest.

In the case of graded Ag-In-Se/ZnSe core/shell NCs, Zn is chosen as the anomalous scatterer.

For spherical core/shell NCs with an abrupt core/shell interface, the electronic density contrast between core and shell material (both total and element-specific) as well as geometrical variables (shell and core thickness) are the fitting parameters. Indeed, this has been demonstrated for PbS/CdS core/shell NCs, systematically varying core size and shell thickness [2].

Core/shell NCs with gradient-shell morphology represent an even more complex object for ASAXS analysis, requiring a large number of parameters in the fitting model (e.g., more than 20 fitting parameters for 5-shell ASAXS model) [3]. To reduce the number of fitting parameters in an equispaced multi-shell ASAXS model, we include information of several electron microscopy techniques, like energy-dispersive X-ray (EDX) spectroscopy. Additionally, the elliptical particle shape is derived by combining 2D TEM analysis with 3D shape retrieval from SAXS data [3, 4].

To determine the crystal structure of Ag-In-Se/ZnSe core/shell NCs, we analyze the WAXS spectra. The crystal structure of Ag-In-Se/ZnSe core/shell NCs belongs to the hexagonal wurtzite-type structure. The core-only Ag-In-Se NCs exhibit same crystal structure, which confirms that the cation-exchange shell growth process does not substantially affect the anionic sublattice [3].

Combining the averaged structural parameters derived from a large NC ensemble using ASAXS, SAXS, and WAXS with the local sensitive electron microscopy and spectroscopy techniques, we can obtain atomic reconstructions of Ag-In-Se/ZnSe core/shell NCs. Such accurate atomic reconstructions of NCs provide not only convenient visualization, but are necessary for theoretical studies using tight binding simulations, density functional theory, ab initio molecular dynamics.

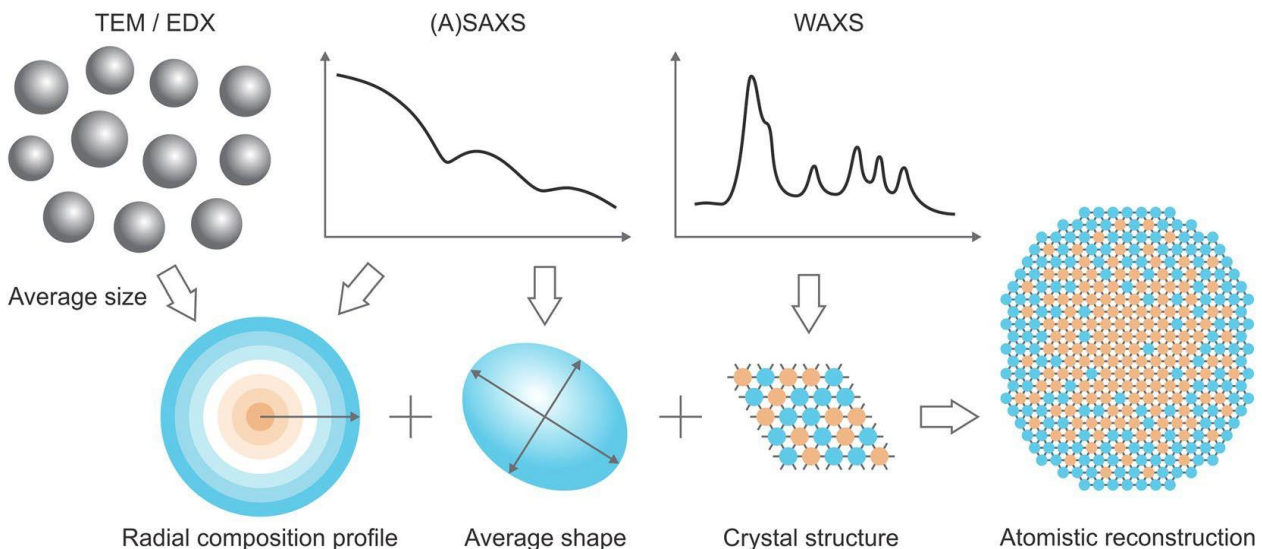


Figure 1: Approach for atomistic reconstructions. The structure of graded core/shell nanocrystals can be resolved on atomic level, using a combination of electron microscopy and X-ray scattering methods. TEM denotes transmission electron microscopy; EDX – energy-dispersive X-ray spectroscopy; (A)SAXS – (anomalous) small-angle X-ray scattering; WAXS – wide-angle X-ray scattering.

2) Quasi-epitaxial inorganic ligand shells on PbS nanocrystals

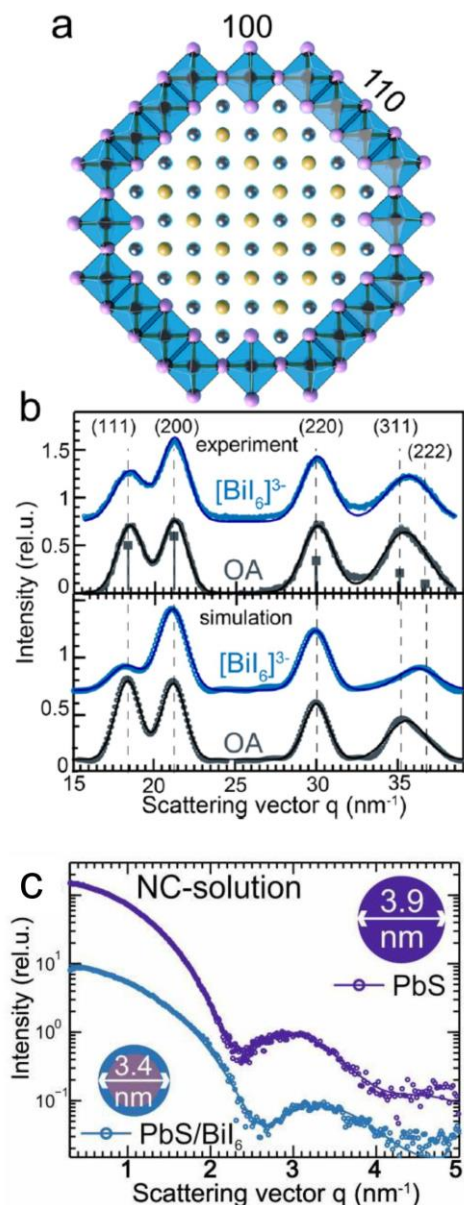


Figure 2: (a) Stick and ball model of a PbS nanocrystal with an epitaxial octahedral methylammonium metal halide cluster shell ([001] projection). (b) Comparison between simulated and measured (symbols) XRD of oleate (OA) covered and methylammonium bismuth iodide covered PbS nanocrystals. The full lines are the fits to the data using Gaussian peaks. (c) SAXS data from the pure PbS NCs (dark blue) and the PbS/Bil₆ core/shell NCs (light blue): The intensity is plotted vs. the scattering vector q . The data (symbol) are fitted (lines) with a sphere model for the case of the PbS NCs and with a spherical core/shell model for the PbS/Bil₆ NCs.

Epitaxial growth techniques enable nearly defect free heterostructures with coherent interfaces, which are of utmost importance for high performance electronic devices. Here we pursue a purely solution processed approach to obtain nanocrystals with epitaxially coherent and quasi-lattice matched inorganic ligand shells.

Octahedral metal-halide clusters, respectively 0-dimensional perovskites, were employed as ligands to match the coordination geometry of the PbS cubic rock-

salt lattice as shown in Figure 2 and Ref. [5]. The inorganic ligand shell is realized by a ligand exchange reaction, where the organic oleic acid shell is replaced by different metal-halide clusters [5].

The ligand attachment and coherence of the formed PbS/ligand core/shell interface was confirmed by combining the results from TEM, SAXS, nuclear magnetic resonance spectroscopy and powder X-ray diffraction (XRD, WAXS). For simulating the XRD patterns (see Figure 2b) assuming a perfect epitaxial perovskite shell the structural parameter derived from core/shell fits of the SAXS data (see Figure 2c) are used: The simulated reductions of the (111) and (311) peak intensities are observed in the experimental data (Figure 2b, top curve) as well, but are less pronounced.

This could be attributed to a slight change of the nanocrystals shape during ligand exchange. Thus, we performed an additional shape retrieval analysis of the SAXS data [4], which reveals a slightly elliptical and faceted mean shape for the PbS/Bil₆ core/ligand-shell nanocrystals [5]. This nonspherical shape is not only visible in SAXS, but also from a detailed analysis of the XRD spectrum in Figure 2b: a narrower width of the (200) Bragg peak of the PbS/Bil₆ NCs as compared to the other crystal directions suggests NCs with more pronounced (100) facets. These facets might be caused by a preferential shell growth in the [100] direction.

The lattice mismatch between ligand shell and nanocrystal core plays a key role in performance. In photoconducting devices the best performance was obtained with Bil₆ ligands, providing the smallest relative lattice mismatch to the PbS core of ca. -1%. Thus, by selection of ligands with appropriate geometry and bond lengths optimized quasi-epitaxial ligand shells were formed on nanocrystals, which are beneficial for applications in optoelectronics.

Cooperation

- W. Heiss, M. Sytnyk (FAU Erlangen-Nürnberg)
- M. Kovalenko (ETH Zürich & EMPA Dübendorf)
- M. Yarema, V. Wood (ETH Zürich)
- H. Amenitsch, M. Burian (TU Graz @ ELETTRA)
- C. Karner, C. Dellago (Univ. Wien)

References

- [1] M.V. Kovalenko et al., ACS Nano **9**, 1012-1057 (2015)
- [2] R.T. Lechner, G. Fritz-Popovski, M. Yarema, W. Heiss, A. Hoell, T.U. Schüllli, D. Primetzhofer, M. Eibelhuber and O. Paris, Chem. Mater. **26**, 5914-5922 (2014)
- [3] M. Yarema, Y. Xing, R.T. Lechner, L. Ludescher, N. Dordevic, W. M. M. Lin, O. Yarema and V. Wood, Mapping the Atomistic Structure of Graded Core/Shell Colloidal Nanocrystals, Sci. Rep. **7**, 11781 (2017)
- [4] M. Burian, G. Fritz-Popovski, M. He, M.V. Kovalenko, O. Paris and R.T. Lechner, J. Appl. Cryst. **48**, 857-868 (2015)
- [5] M. Sytnyk, S. Yakunin, W. Schöfberger, R.T. Lechner, M. Burian, L. Ludescher, et al., and W. Heiss, Quasi-Epitaxial Metal-Halide Perovskite Ligand Shells on PbS Nanocrystals, ACS Nano **11**, 1246-1256 (2017)

Nanomaterials & Scattering

Semiconductor Multilayers

Rainer T. Lechner
 rainer.lechner@unileoben.ac.at

This study was enabled by a collaboration of the Material Physics Department and Erich Schmidt Institute (ESI) with the Institute of Physics: We have performed the characterization of an high-electron-mobility transistor (HEMT) $Al_xGa_{1-x}N$ heterostructure via X-ray diffraction (XRD) combined with ion beam layer removal method (ILR) and TEM analyses.

Additionally, the decreasing dislocation-densities within the individual sublayers are visualized by scanning transmission electron microscopy (STEM). The documented stepwise improved crystal quality enables the formation of a highly tensile stressed 20 nm thick $Al_{0.17}Ga_{0.83}N$ top barrier-layer resulting in a pseudomorphic GaN/ $Al_{0.17}Ga_{0.83}N$ interface.

Cooperation

- J. Keckes, M. Reisinger (ESI, MU Leoben)

References

[1] M. Reisinger, M. Tomberger, J. Zechner, I. Daumiller, B. Sartory, W. Ecker, J. Keckes, and R.T. Lechner, *Resolving Alternating Stress Gradients and Dislocation Densities Across $Al_xGa_{1-x}N$ Multilayer Structures on Si(111)*, Appl. Phys. Lett. 111, 162103 (2017)

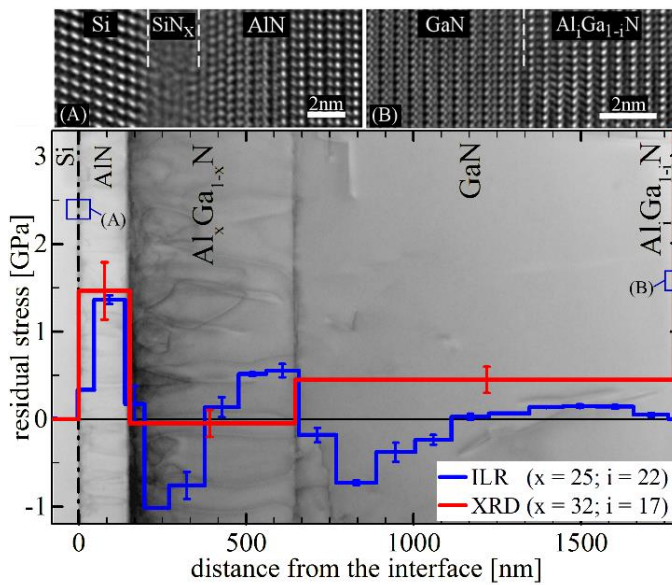


Figure 1: A comparison of average sublayer stresses (obtained using XRD) and individual sublayer stress gradients (evaluated using ILR) of two very similar HEMT structures, which vary in their composition of the $Al_xGa_{1-x}N$ transition and the $Al_iGa_{1-i}N$ barrier layer. The ILR data were obtained with a spatial resolution of 100 nm. The stress data correlate well with the microstructural features of the STEM cross-section image in the background. Filtered HRTEM images show the Si/AlN (inset A) and GaN/ $Al_iGa_{1-i}N$ (inset B) interfaces of the heterostructure.

Gradients of residual stresses and crystal qualities across a 2 μm thick $AlN/Al_{0.32}Ga_{0.68}N/GaN/Al_{0.17}Ga_{0.83}N$ multilayer stack deposited on Si (111) were evaluated by combining the above mentioned techniques (see Figure 1) and Ref. [1].

ILR with 100 nm depth resolution reveals the alternating stress profiles, which are related to sublayer dislocation-density gradients. The laboratory XRD confirms the derived mean stress values, the presence of stress gradients within the sublayers and decreasing average sublayer threading dislocations-densities across the heterostructure.

Nanomaterials & Scattering

Biological Materials

Gerhard Fritz-Popovski, Lukas Ludescher, Oskar Paris
 gerhard.popovski@unileoben.ac.at
 oskar.paris@unileoben.ac.at

Research on biological materials focused on the crystals within cotton fibers and their arrangement and on teeth.

1) Microfibril angle in cotton

Cotton fibers consist of elongated plant cells, which are attached to the seeds. The secondary cell wall of these fibers contains cellulose microfibrils, which wind helically around the interior of the cell. The angle between the orientation of the cellulose microfibrils and the axis of the cell is called microfibril angle (MFA). Its value determines the mechanical properties of the fiber, since a small MFA is linked to stiff, but brittle behavior while a large MFA results in a less stiff, but tougher material.

Our cooperation partner, Filipe Natalio, has developed a technique to grow cotton *Gossypium hirsutum* L. fibers in greenhouse and hydroponic conditions. This could lead to faster growth, better management of natural resources and better control of fiber quality. Therefore, the determination of the MFA of the thus grown fibers is of great interest to check the quality of the product.

It is rather straightforward to measure the MFA of straight softwood cells by means of small angle scattering. In this case, the azimuthal distribution of the scattering signal can be related directly to the MFA. Cotton fibers are, however, coiled, which would lead to a spread of the distribution, even if the MFA were zero.

A new evaluation technique was developed [1], which allows for the determination of the MFA of such helical plant cells. It combines the azimuthal intensity distribution of small angle (SAXS) and wide angle (WAXS) x-ray scattering (Figure 1). The cellulose (002) peak, which is found at scattering angles close to 23°, is linked to the orientation of the cellulose crystals and therefore to the orientation of the microfibrils relative to the scattering instrument. The small angle signal shows little signature of nanostructures, since the electron densities of the various biopolymers within the dried material are rather similar to each other. Therefore, the dominating contrast is the one between the fiber and the surrounding air and the distribution of fiber orientations can be obtained from these data. The deconvolution of these two distributions then leads to the distribution of microfibril orientation relative to the fiber orientation, *i.e.* the microfibril angle.

2) Chemically modified cotton

Functional fibers include additional functionalities that would not be present in the natural fiber, similar to conventional dyes. However, the necessary and relatively complex modifications of the product should not be removed by washing or wear. Therefore, Filipe Natalio has developed modified sugars that contain a residue introducing the new functionality [2]. If such sugars are offered in the nutrition medium to a cotton ovule, the growing fibers will incorporate the sugars and thereby the

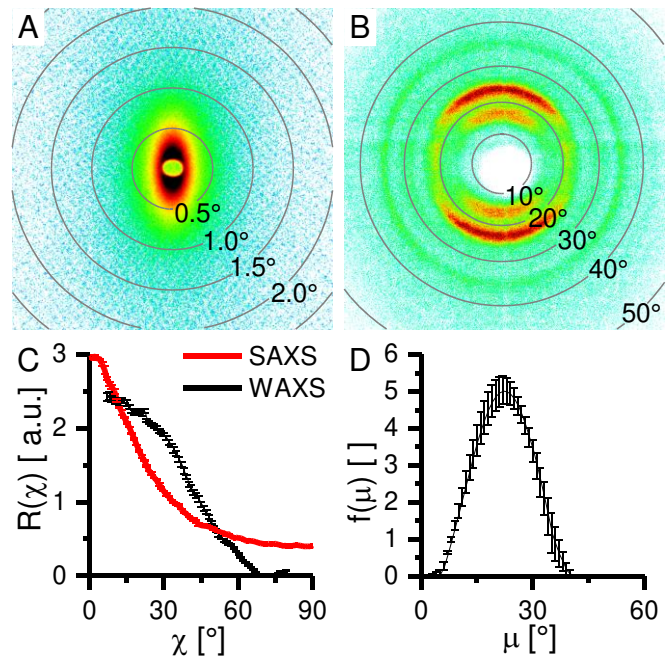


Figure 1: (A) SAXS and (B) WAXS patterns of cotton fibers. (C) Half of azimuthal peaks determined at scattering angles of 0.56° and at 23. (D) Microfibril angle distribution.

functional residues within their structure and not only at their surface.

The modified cotton fibers had clearly fluorescent (sample FGIO) and magnetic (sample Glc-DOTA-Dy(III)) properties. However, nanostructural properties of the original cotton fiber may be lost due to the different structure of the molecules used for building the cellulose. The molecular structure of the modified cellulose molecules was investigated by wide angle x-ray scattering. The control sample grown without modified sugars shows the typical (011̄), (011), (002), and (004) peaks of crystalline cellulose (Figure 2A). The fluorescent sample, however, shows only one broad peak centered

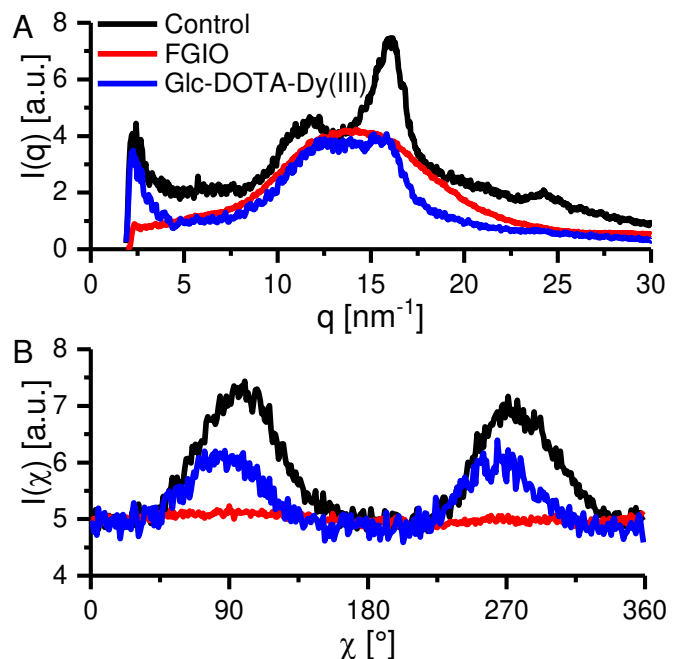


Figure 2: Radial profiles of cotton fibers (A) and azimuthal profiles (B) of native and functionalized cotton.

at $q \approx 13 \text{ nm}^{-1}$. This proves that the crystalline structure is largely lost for this sample and that the fiber consists of amorphous modified cellulose. The magnetic sample, on the other hand, does show some weak crystalline peaks, albeit much weaker than in the control sample and obviously on top of a strong amorphous peak.

Similar observations can be made for the azimuthal intensity distribution (Figure 2B). The control sample shows a strong preferred orientation of the molecules, whereas much less orientation is seen for the magnetic fibers. The fluorescent amorphous fibers show not only no crystalline peaks but also no preferred orientation of the amorphous molecules.

3) Teeth

As most biological tissues, teeth are a multicomponent, hierarchically ordered composite material. We investigated the root dentin being part of human teeth which on the nanometer level is built up from densely packed parallel collagen molecules aligned along their long axis in a staggered manner. Due to the staggered alignment, periodic gaps form between longitudinally adjoining collagen molecules, in which hydroxyapatite platelets are situated. These collagen molecules are then packed into fibrils, forming sheet like structures that are aligned perpendicularly to the microtubule, which are micrometer sized channels running from the root of a tooth to its surface [3]. As a large part of the dentine consists of collagen, humidity changes will affect the water content and therefore the lateral packing of the individual collagen fibrils.

To investigate the effect of varying water content on the human root dentine, a custom water vapor dosing system was attached to a Nanostar SAXS instrument to conduct in-situ measurements. The root dentine sample was supplied as a 200 to 400 μm thick slice by our partner Paul Zaslansky from Charite Berlin. The relative humidity was set at ten distinct values in ad- and desorption with a higher density of measuring points at very low humidity. Because of the anisotropy of the collected SAXS patterns, we analyzed the data accordingly. Integral parameters along the two main axes of the scattering pattern (Figure 4C) were determined to calculate the mean thickness (T-parameter) of the present structures as a function of humidity. Interestingly the T-parameter shows a closed hysteresis loop with a total size change of about 15 % (Figure 3). The reason for this big difference is mostly likely due to the changes in the distance between the collagen sheets. An indication of this fact is the clearly visible, peak-like feature at low q (~ 0.1 to 0.15 nm^{-1}) which shifts its position in the magnitude of up to 15% (Fig. 4A). This peak like feature is most dominant in directions along the long axis of the micro tubuli, indicating that in fact the distance between the sheet like collagen structures changes upon water ad- and desorption. As expected, most of the changes occur at low relative humidities, as indicated in Figure 4B and 4C.

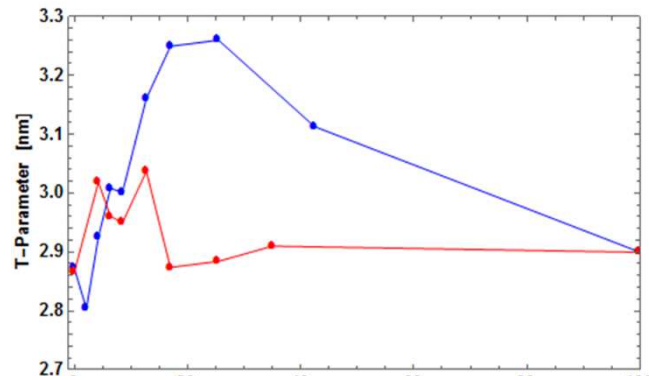


Figure 3: Red shows the desorption branch of the size parameter, blue the adsorption branch. Of note is the fact, that the hysteresis loop is closed.

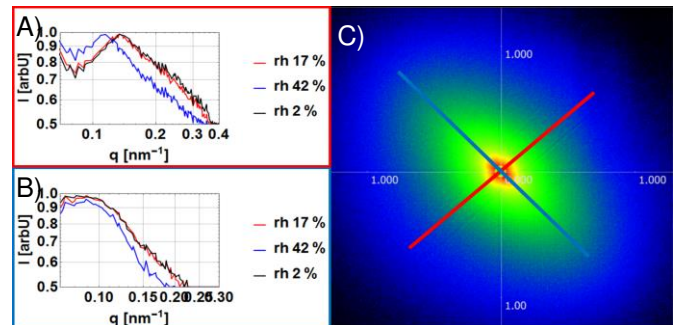


Figure 4: A) The peak like feature along the tubuli axis is shown for three relative humidities. B) The scattering perpendicular to the tubuli axis is depicted. C) The measured 2-D scattering pattern of a specific position on the tooth is shown. The red bar indicates the direction of the tubuli axis, the blue bar shows the direction perpendicular to it.

Cooperation:

- F. Natalio (Martin-Luther Universität Halle-Wittenberg, Germany and Weizmann Institute of Science, Israel)
- P. Zaslansky (Julius Wolff Institut für Biomechanik und Muskuloskeletale Regeneration, Charité Berlin, Germany)

References:

- [1] F. Natalio, M. Nawaz Tahir, N. Friedrich, M. Köck, G. Fritz-Popovski, O. Paris & R. Paschke: *Structural analysis of Gossypium hirsutum fibers grown under greenhouse and hydroponic conditions*, J. Struct. Biol. **194**, 292–302 (2016)
- [2] F. Natalio, R. Fuchs, S. R. Cohen, G. Leitus, G. Fritz-Popovski, O. Paris, M. Kappl & H.-J. Butt: *Biological fabrication of cellulose fibers with tailored properties*, Science **357**, 1118–1122 (2017)
- [3] Forien, Jean-Baptiste, et al. In situ compressibility of carbonated hydroxyapatite in tooth dentine measured under hydrostatic pressure by high energy X-ray diffraction. *Journal of the mechanical behavior of biomedical materials*, 2015, 50. Jg., S. 171-179.

Nanomaterials & Scattering

Further development of scattering techniques

Roland Morak, Gerhard Fritz-Popovski, Oskar Paris
gerhard.popovski@unileoben.ac.at
oskar.paris@unileoben.ac.at

1) In-situ GISAXS-Stage

Grazing incidence small angle scattering is a helpful tool to investigate processes that change structures in on the scale of nanometers close to surfaces *in-situ*. Many interesting processes require, however, control of the sample environment like temperature or chemical composition of the space at and above the surface. Consequently a commercial heating stage (TC-Dome, Bruker AXS), which was originally designed for diffraction experiments was adapted to be used within the sample chamber of a Nanostar SAXS instrument. The sample is heated from below with a strip heater and kept in place by two corundum bars from the top (Figure 1a). This should allow for temperatures up to 1100°C and has been tested up to 900°C [1].

A separation of the heating stage and sample from the sample chamber of the instrument was necessary in order to provide an atmosphere for the reaction without flooding the whole instrument with the desired gas. This was achieved by means of a dome. Kapton windows allow the x-ray beam to enter and the scattered radiation to reach the detector. The energy introduced into the set-up by means of the heating strip would lead to considerable heating of the dome and of the windows, which might harm the structure. Therefore, the dome is double shelled with cooling water flowing between the two shells.

The instrument was tested by heating a film of mesoporous silica/polymer hybrid material obtained from a block copolymer solution containing tetraethyl

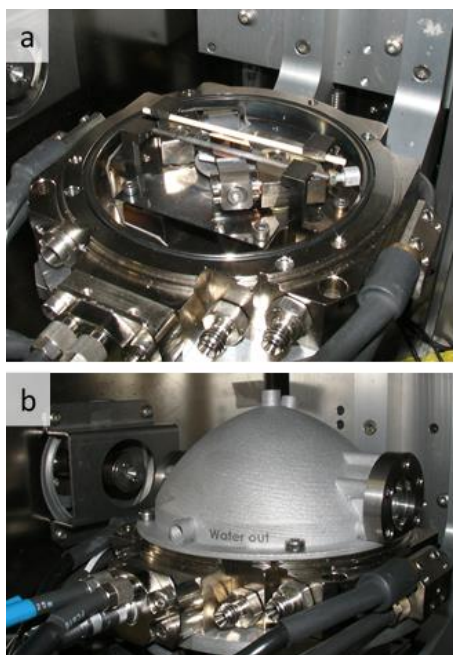


Figure 1: GISAXS heating stage (a) without dome and (b) with atmosphere control dome.

orthosilicate after evaporation induced self-assembly. Heating such a film leads to the removal of the organic material and to the formation of a nanoporous silica film containing oriented cylindrical pores with elliptical cross section [2,3].

Figure 2 shows the GISAXS patterns obtained at low and at high temperatures. One clearly observes a vertical shift of the Bragg peaks, which corresponds to a vertical shrinkage of the pore lattice. This change takes place mainly from 400°C to 600°C. A detailed analysis of the peak intensities with a newly developed model [2] shows that the cross section of the pores is also deformed to increasingly more elliptical shape. The temperatures, where one can observe this change are identical to the ones of the lattice shrinkage.

2) In-situ sorption set-up

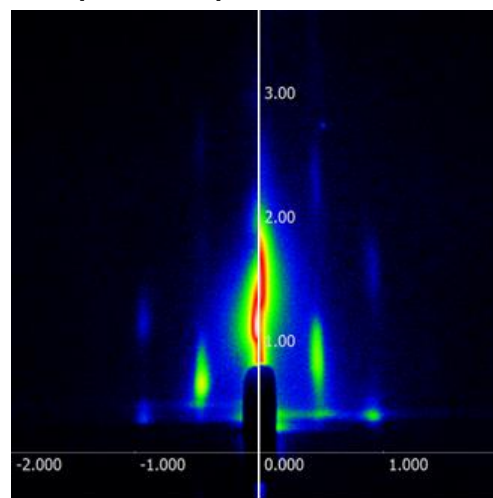


Figure 2: GISAXS patterns of a film silica templated by blockcopolymers at 150°C (left half of the image), and at 750°C (right half of the image)

Porous materials are usually characterized by sorption of nitrogen or other inert gases at low temperatures. Therefore, either gravimetric or volumetric set-ups are commonly used. Structural changes such as sorption induced deformation of ordered mesoporous materials can be investigated by a combination of small angle scattering using (synchrotron radiation) X-rays or neutrons during sorption of n-pentane or water at room temperature. So far however, only very rarely in-situ sorption with SAXS or SANS at low temperatures has been reported, and to our knowledge no system connected to a laboratory SAXS instrument is available. We developed a new instrument to enable in-situ scattering and adsorption (ISSU, see Fig. 3 and 4) with a laboratory SAXS instrument (Bruker N8-Horizon). The instrument consists of a gas dosing system and either a circulating cooling set-up with different cooling liquids or a closed cycle cryostat. Depending on the cooling system, sample temperatures between < 12 K and 500 K can in principle be realized.

Dosing of the adsorptive toward the sample can be executed either continuously with a very slow dosing rate, or stepwise. The stepwise mode allows equilibrium states of adsorbent and adsorbate to be measured. The pressure inside the sample cell can be controlled between 10^{-6} bar and 2 bar and the amount of adsorbate can be calculated for each sorption step after precise calibration of all volumes in the system.

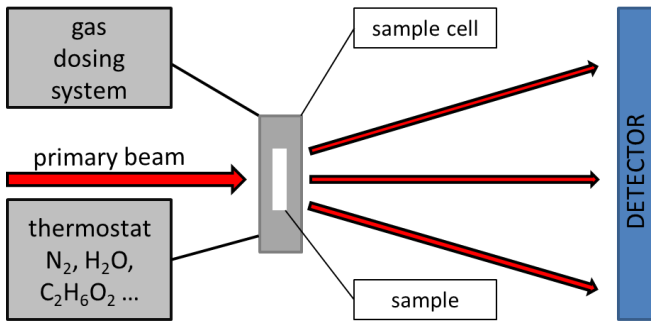


Figure 3: In-situ scattering and sorption unit (ISSU)

A special sample holder was designed to provide on the one hand room for the circulating cooling liquid, and on the other hand a vacuum cover for the cold-finger of the closed cycle cryostat (see Figure 5). First in-situ test measurements on hierarchical silica samples were performed with water at 290 K (Fig. 6). The integrated intensities of the scattering curves show a direct correlation with the sorption isotherms previously measured. Currently, the final calibration of the system and the commissioning of the low temperature option (particularly N₂ at 77 K) are in progress.



Funding:

COMET Funding Programme (Austrian Federal

Figure 4: Gas dosing system combined with the N8 Horizon instrument from Bruker AXS.

Government represented by FFG, Styrian and the Tyrolean Provincial Governments, represented by SFG and Standortagentur Tirol)

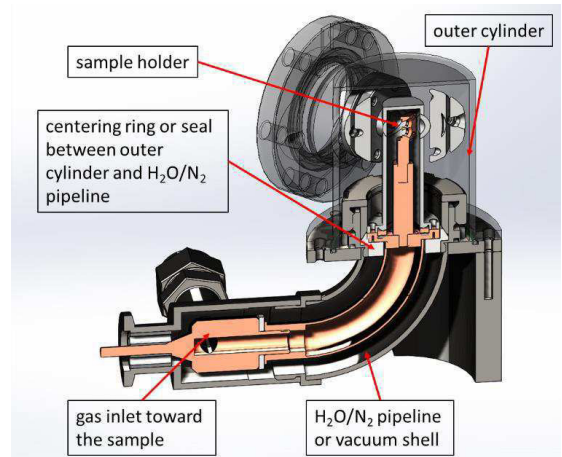


Figure 5: Sample holder with double shell construction for circulation of cooling medium or vacuum

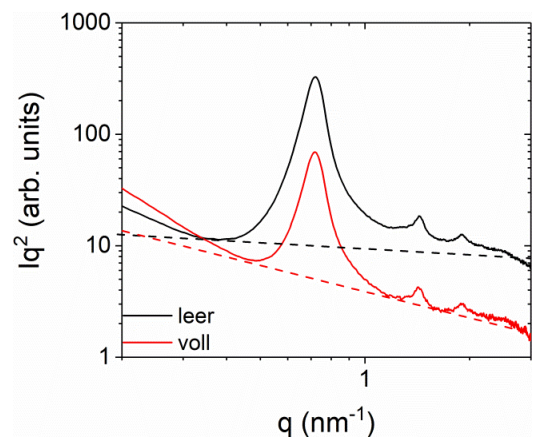


Figure 6: Kratky plot of a hierarchical porous silica sample in the full and empty state measured with ISSU

Cooperation:

- L Chitu, L. Bruegemann, J. Lange, H.G. Krane (Bruker AXS GmbH, Germany)
- G. A. Maier, F. Sosada-Ludwikowska (Materials Center Leoben)
- S. C. Bodner (Department of Materials Physics, Montanuniversität Leoben and Erich Schmid Institute for Materials Science, Austrian Academy of Science)

References:

- [1] G. Fritz-Popovski, S. C. Bodner, F. Sosada-Ludwikowska, G. A. Maier, R. Morak, L. Chitu, L. Bruegemann, J. Lange, H.-G. Krane, O. Paris *A new device for high-temperature in situ GISAXS measurements.* Rev. Sci. Instr. **89**, 35103 (2018).
- [2] G. Popovski, R. Morak, P. Sharifi, H. Amenitsch, O. Paris, *Pore shape and sorption behaviour in mesoporous ordered silica films,* J. Appl. Crystall. **49** 1713-1720 (2016).
- [3] O. Paris et al., *Complementary high spatial resolution methods in materials science and engineering,* Adv. Eng. Mater. **19**, 1600671 (2017).

Surface Physics & Scanning Probe Microscopy

Effect of TiO₂(110) surface roughness on the growth and stability of organic thin films

Markus Kratzer, Christian Teichert
 Markus.Kratzer@unileoben.ac.at

Tayloring morphology, structure and stability of organic thin films is a key issue for the design of organic based electronic devices. Here, we investigated the growth and stability of ultra-thin films of para-hexaphenyl (6P) on ion-bombardment modified TiO₂(110) surfaces. The combination 6P/TiO₂(110) serves as a model system for an organic/inorganic interface. The rutile TiO₂ plays the role of a transparent electrode and the 6P represents the active organic component. Classical ways of controlling morphology and interfacing usually include heat treatment, chemical surface activation, or introduction of interface layers. In this case, targeted surfaces modification by generating nm-size ripples has been applied in order to influence 6P's growth morphology and stability. The ripples represent stepped structures with a certain terrace width depending on the local slope of the ripple. The ripples' properties like depth, period, and local slope can be adjusted by proper selection of the ion-bombardment parameters as ion-flux, angle of incidence, projected beam direction, etc. In Figure 1 examples for long ripples with low local slope (large terrace width) and short ripples with high local slope (small terrace width) are presented. The narrower a terrace is the less molecules can fit there. Under the applied conditions molecules will preferably grow in the upright configuration. At the terrace edges molecules have to shift by the step height along their long axes which reduces the effective binding length of molecules at the step edges, thus leading to a reduced stability. For large terraces the edge contribution barely plays a role. However, on substrates with narrow terraces (high step density) a high fraction of the molecules are in edge position which significantly reduces the overall stability.

It turned out that on the highly stepped surfaces (short, steep ripples) the 6P islands could not be imaged by tapping mode atomic force microscopy (TM AFM), which was a consequence of the reduced island stability. In this case the islands could not withstand the force exerted by the tip and only the substrate was imaged. Interestingly, islands which could be imaged under very gentle imaging conditions, vanished under harder imaging conditions and reappeared almost unchanged when going back to gentle conditions. This observation was explained by a model by Butt and Franz [1] where molecules jump away under the pressure gradient under the tip. [2]

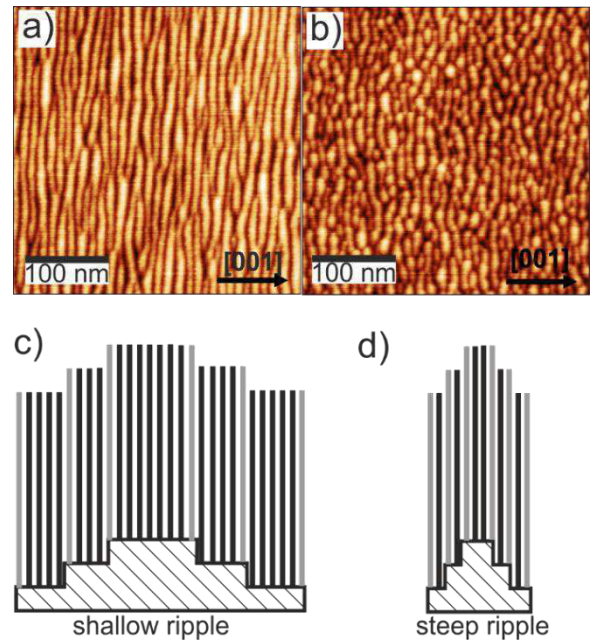


Figure 1 STM images of (a) long ripples and (b) short ripples exhibiting different side slopes. Schematic cross sections of a c) shallow ripples and d) steep ripple with molecules on top (indicated by the dark bars). The grey bars indicate molecules in edge position clearly showing the higher density of less stable edge molecules on the steeper ripple.

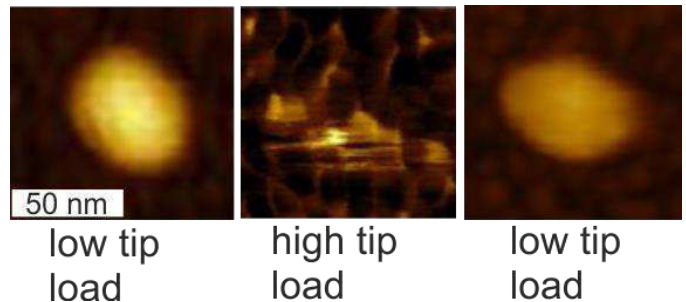


Figure 2: Sequence of tapping mode AFM images of a ~50 nm big 6P island recorded under varying tip load. At high tip load (middle image) the substrate is imaged and the island is almost invisible. After reducing the tip load (right image) the island reappears.

Cooperation:

- Prof. Franciszek Krok, D. Wrana, K. Szajna Jagiellonian University Krakow, PL., ÖAD-WTZ Project # PL 06/2016.

Selected Key References:

- [1] H.S. Butt, V. Franz, Phys. Rev. E 66, 031601 (2002).
- [2] K. Szajna, M. Kratzer, D. Wrana, C. Mennucci, B. R. Jany, F. Buatier de Mongeot, C. Teichert, F. Krok, J. Chem Phys. 145, 144703 (2016).

Surface Physics & Scanning Probe Microscopy

Micro-scale electrical analysis of surfaces using Kelvin probe force microscopy and conductive atomic force microscopy

Markus Kratzer, Caterina Czubala, Christian Teichert
christian.teichert@unileoben.ac.at
markus.kratzer@unileoben.ac.at

Atomic force microscopy based electrical characterization methods can be effectively used to reveal local electrical properties of materials which are inhomogeneous on the micro and nanoscale. A classical examples of such systems are bulk heterojunction (BHJ) solar cells which contain closely spaced, nanometer or micrometer size acceptor and donor regions. A less common example is paper that has been made conductive by incorporation of metallic nanowires. [1] Such an approach might open the way for cheap paper based materials into electronics.

In such systems, conclusions about the reasons for device failure or performance changes can often only be drawn indirectly from macroscopic measurements. In contrast, access to local information about morphology and electrical behavior reveals much more details and often enables to identify performance relevant parameters directly.

1) Characterization of CdS/Kesterite BHJ solar cells

Here, we present a study of CdS/Kesterite BHJ solar cells with micrometer size donor and acceptor domains investigated by photo assisted Kelvin probe force microscopy (PA KPFM) and photo conductive atomic force microscopy (PC-AFM) using p- and n-type probe AFM tips. [1] The character of the diode formed at the tip sample contact will change depending whether the p-type/n-type probe contacts a donor or acceptor region. Thus giving modified current images with respect to the tip-sample bias. Here, CdS is the n-type material whereas Kesterite is p-type. Kesterite ($\text{Cu}_2\text{ZnSnS}_4$) is a promising cheap replacement for $\text{CuIn}_x\text{Ga}_{1-x}\text{Se}_2$ (CIGS) which is often used in thin film solar cells.

In Figure 1 we present local current-to-voltage (IV) curves recorded with n-type and a p-type probes on a CdS grain in a CdS/Kesterite bulk heterojunction. While the p-type probe exhibits a good contact and a rather symmetric IV-characteristics the contact with the n-type probe is clearly rectifying.

Additional information can be obtained by measuring the local contact potential difference by KPFM. Comparing KPFM images in the dark and under illumination provides insight in the local photovoltage generation. In Figure 2 and b) it is clearly visible that CdS responds clearly to illumination whereas the Kesterite region is insensitive to light. This indicates that here the Kesterite material should be improved in terms of photoresponse.

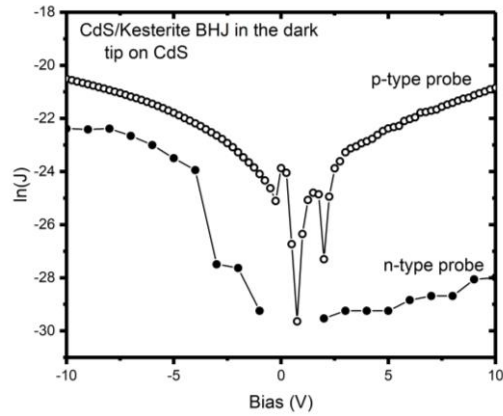


Figure 1 Comparison of local IV curves recorded with n-type (full circle) and p-type (open circles) AFM probe on a CdS grain within a CdS/Kesterite BHJ.

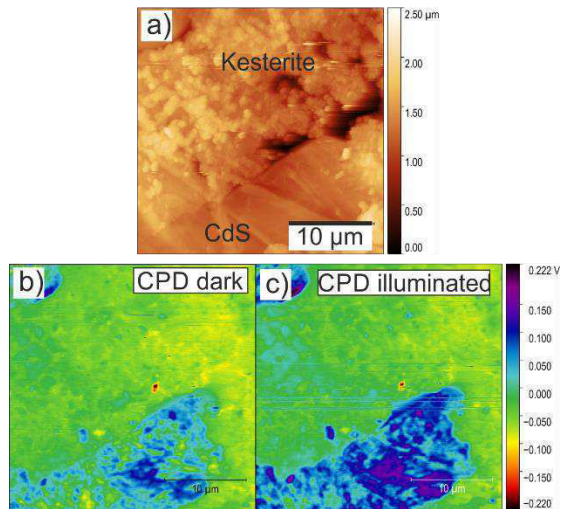


Figure 2 AFM topography image (a) together with the corresponding CPD maps in the dark (b) and under illumination (c).

2) Topographical and electrical characterization of cellulose – silver nanowires composite photo diodes

In the case of paper made conductive upon introduction of silver nanowires (AgNW) KPFM also proved to be a useful tool for characterization. The overall conductivity of the paper-metal compound depends on how well the nanowire network is interconnected. A local overview about the electrical connection can be obtained using KPFM. Metal wires which are in contact with the wire framework should essentially exhibit the same potential, whereas detached wires will in general have a different potential. In addition, local charging experiments, which can also be conducted, help to reveal locally connected parts of the AgNW network. In Figure 3 topography and KPFM images of a AgNW/cellulose fiber compound are presented. The AgNWs can be clearly identified in the cellulose fiber matrix. The AgNWs showing the same potential as the matrix are either not connected to the network and/or just covered by the cellulose. Since local charging of individual AgNWs let the potential unchanged it can be concluded that they are sufficiently well connected.

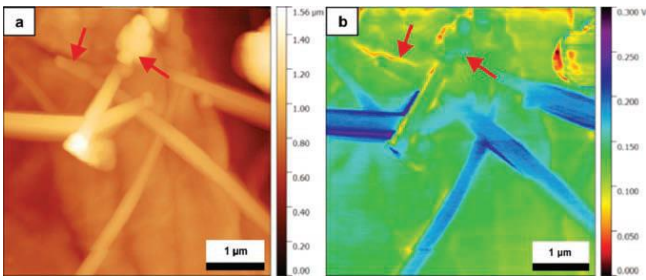


Figure 3: (a) $5 \times 5 \mu\text{m}^2$ AFM topography and (b) corresponding KPFM CPD image. (b) shows the contrast between AgNWs (blue) and the cellulose substrate (green). The red arrows indicate possible residuals from the preparation process (from [2]).

References

[1] O.P.Dimitriev, D.O.Grynko, A.M.Fedoryak T.P.Doroshenko, M. Kratzer, C. Teichert, Yu.V.Noskov, N.A.Ogurtsov, A.A.Pud, P. Balaz, M.Balaz, M.Tesinsky, Semiconductor physics, quantum electronics and optoelectronics, 20 (4), P. 418-423 (2017).

[2] C. Czibula, C. Ganser, M. Kratzer, C. Teichert, R. Schennach, M. Penn, M. Ebner, M. Pramstrahler, F. Pilat, T. Chien, B. Friedel, "Silver Nanowires: A Versatile Tool for Conductive Paper", in: "Advances in Pulp and Paper Research vol. 2", (eds. W. Batchelor, D. Söderberg), Transactions of the Fundamental Research Symposium held in Oxford 2017, pp. 723-737, ISBN 978-0-9926163-3-5.

Cooperation

- O. P. Dimitriev, D. O. Grynko, A. M. Fedoryak T. P. Doroshenko (V. Lashkaryov Institute of Semiconductor Physics of NAS of Ukraine), ÖAD-WTZ Project # UA 06/2017
- Robert Schennach, Bettina Friedel (Institute of Solid State Physics, Graz University of Technology);
- Ulrich Hirn (Institute of Paper, Pulp and Fibre Technology, Graz University of Technology) CD Labor für Faserquellung und deren Effekte auf die Papiereigenschaften

Surface Physics & Scanning Probe Microscopy

Van der Waals epitaxy: Epitaxial relation between parahexaphenyl nano-crystals and hexagonal boron nitride

Aleksandar Matković, Jakob Genser, Markus Kratzer, Christian Teichert
aleksandar.matkovic@unileoben.ac.at

Recently, two-dimensional (2D) van der Waals (vdW) materials have been proposed as substrates for the epitaxy of organic molecules. Their key advantage lies in the fact that these interfaces have vdW nature, meaning that surfaces on which organic semiconductors grow are atomically smooth with no dangling bonds and no trapped charges at the interface. This enables growth of high-quality organic crystal thin films with very large grains and low number of defects. Probably, the most important interface in organic field effect devices is the gate dielectric interface. It defines transport, since carriers accumulate at the interface only in the first few molecular layers of the organic semiconductor.

Hexagonal boron nitride (hBN) has great potential to be used as a gate material in the future flexible electronics, being an almost defect-free dielectric with a breakdown field in the order of 1 GV/m. Therefore, this study focuses on hBN as an ultra-thin vdW dielectric substrate for the epitaxial growth of highly ordered crystalline networks of the organic semiconductor parahexaphenyl (6P) [1]. Atomic force microscopy (AFM) based morphology analysis combined with density functional theory (DFT) simulations reveal their epitaxial relation. Accordingly, needle-like crystallites of para-hexaphenyl grow with their long axes oriented five degrees off the hBN zigzag directions. In addition, by tuning the deposition temperature and the thickness of hBN, ordered networks of needle-like crystallites as long as several tens of micrometers can be obtained. A deeper understanding of the organic crystallites growth and ordering at ultra-thin van der Waals dielectric substrates will lead to grain boundary-free organic field effect devices, limited only by the intrinsic properties of the organic semiconductors.

1) Growth directions of 6P needles on hBN

A major contributor to self-assembly of crystallite networks is the molecule-substrate interface. In the case of hBN and other 2D materials, on which organic crystals grow through vdW epitaxy, the substrate symmetry plays a major role since the sample and the substrate are rotationally commensurate despite the lattice constant mismatch.

To understand the mechanism behind the long-range ordering of 6P crystallites observed on hBN (e.g. see Fig 1a), preferred growth directions have been analyzed from AFM topography images. By selecting each

crystallite grown on a single hBN flake it is possible to plot their cumulative length in a given direction (with respect to the x axis of the scanner). An example of such growth direction analysis is given in Figure 1, where a histogram of the cumulative length as a function of the needle angle (Figure 1b) is obtained by analyzing an AFM topography image of the hBN flake covered by a 6P crystallite network (Figure 1a). For all of the investigated samples – considering different growth conditions and hBN flake thicknesses – the same ordering rules were observed: 6P needles grow in chiral pairs separated by $\pm 5^\circ$ from a three-fold repeating (60° repetition) separator line (high symmetry direction of the substrate).

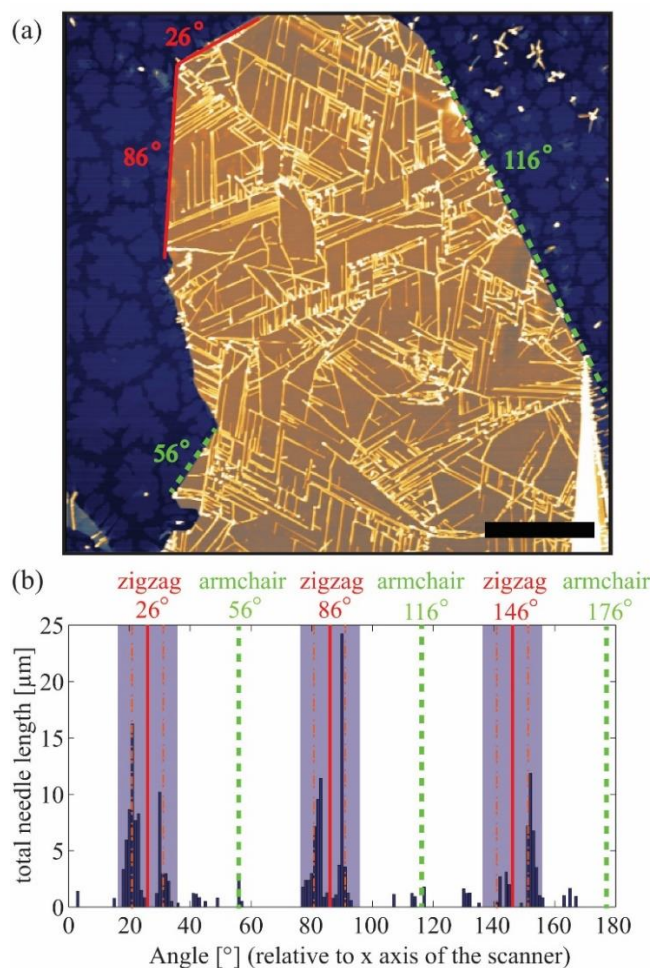


Figure 1: (a) $20 \times 20 \mu\text{m}^2$ AFM image of 18.1 nm thick bulk hBN flake covered with 6P needles ($T_D = 363 \text{ K}$, lateral scale bar $4 \mu\text{m}$, logarithmic z scale 65 nm). (b) Total needle length in a given direction with $\pm 0.5^\circ$ tolerance, considering x axis of the scanner as 0° (reprinted from [1]).

2) DFT calculation of individual 6P molecules preferred adsorption sites on hBN

We have calculated the adsorption energies of single 6P molecules on one-layer hBN substrate for nine different adsorption sites with the long axis of the 6P molecules oriented along the armchair direction of hBN, and four adsorption sites with 6P oriented along the zigzag direction. For all of them, we have optimized the internal atomic coordinates and found an average distance between 6P and the hBN substrate of about 0.33 nm. Among all these structures, the preferred adsorption site is the one with the center of the phenyl rings above the N

atom of the hBN substrate and 6P's long axis oriented along the armchair direction. The adsorption energy for this site is about 170 meV larger than the most stable site with 6P oriented along the zigzag direction. Top and side views of the most favorable structure are depicted in Figure 2(a) and (b), respectively.

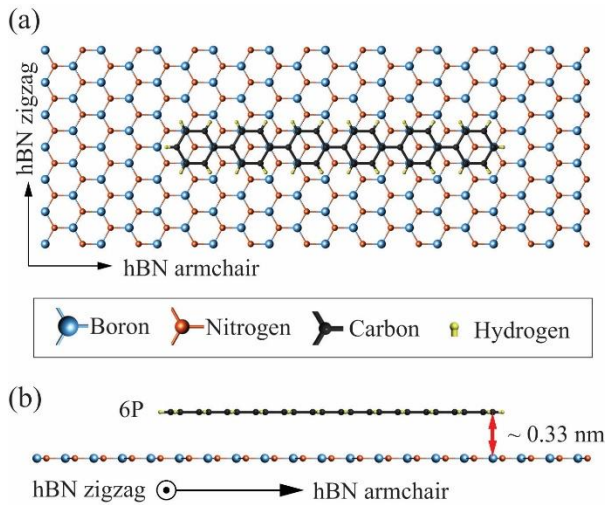


Figure 2 Scheme of the preferred adsorption site for an isolated 6P molecule on a single layer hBN as obtained by DFT calculations, (a) top view, (b) side view. (reprinted from [1].)

3) Epitaxial relation between 6P and hBN: the rule behind self-assembly of the crystallite networks

The preferred adsorption site of individual molecules provides only a starting point for the alignment of 6P crystals on hBN, during the initial stages of the growth. While the density of the molecules on the surface of hBN is small enough, substrate-molecule interaction dominates, and the molecules tend to adopt their individual equilibrium positions. However, once a critical density is reached, intermolecular interaction takes over and molecules reorganize mainly into the equilibrium bulk structure. At that point, the contact plane of the bulk molecular crystal which introduces the least amount of strain between the equilibrium adsorption sites of individual molecules and the bulk structure is chosen, being energetically most favored.

If the preferred adsorption sites of the individual molecules are taken into account, the long axis of the molecules can be fixed to an armchair direction of hBN. Then, considering all known contact planes of 6P needle-like crystallites with single crystal substrates, only the (-629) plane can describe the splitting of needle growth directions with respect to the zigzag directions of hBN. Figure 3 shows a schematic representation of the 6P β -phase with the (-629) plane in contact with the hBN (0001) plane.

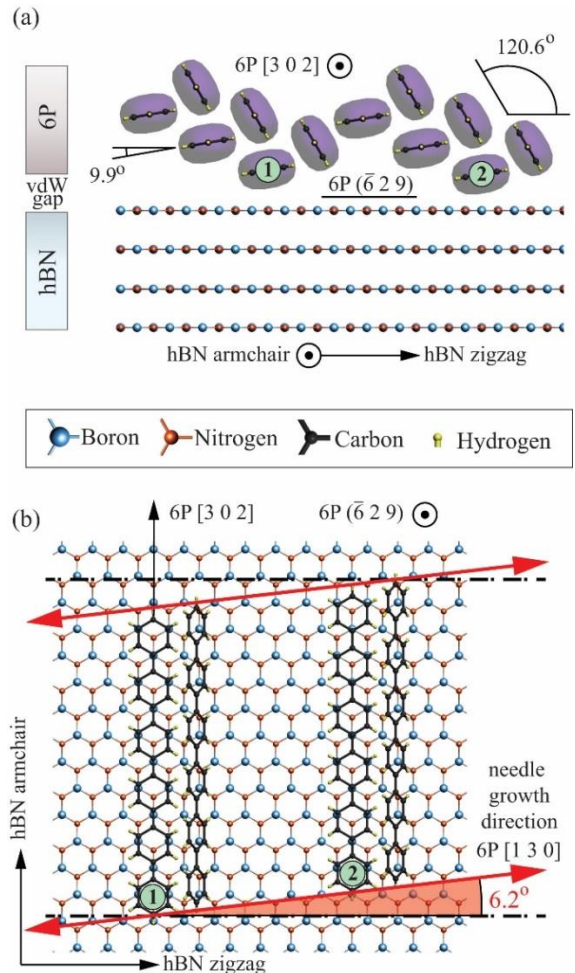


Figure 3 A schematic presentation of the (-629) 6P contact plane with hBN basal plane, (a) side view of the interface, and (b) top view. (reprinted from [1].)

Cooperations:

- P. Puschnig, D. Lüftner, Institute of Physics, KFU Graz, NAWI Graz, Austria.
- R. Gajić, B. Vasić, Institute of Physics, University of Belgrade, Serbia – ÖAD project SRB 09/2016
- Joint ANR/FWF project: I1788-N20

Selected Key References:

- [1] Matković A, Genser J, Lüftner D, Kratzer M, Gajić R, Puschnig P, Teichert C: Epitaxy of highly ordered organic semiconductor crystallite networks supported by hexagonal boron nitride. *Sci. Rep.* **6**: 38519 (2016).

Surface Physics & Scanning Probe Microscopy

Growth morphologies of higher acene derivatives on c-plane sapphire

Aleksandar Matković, Aydan Çiçek, Guanpeng Lin, Markus Kratzer, Benjamin Kaufmann, Christian Teichert
 aleksandar.matkovic@unileoben.ac.at

Dihydro-tetraaza-acenes are promising candidates for future applications in organic electronics, since these molecules form crystals through an interplay between H-bonding, dipolar, and van der Waals interactions. As a result, densely packed π - π structures – favorable for charge transport – are obtained, with exceptional stability under ambient conditions.

This study investigates growth morphologies of dihydro-tetraaza-pentacene (DHTA5) and dihydro-tetraaza-heptacene (DHTA7) on vicinal c-plane sapphire [1]. Sub-monolayers and thin films are grown using hot wall epitaxy. The resulting morphologies are investigated ex-situ by atomic force microscopy. Molecular arrangement, nucleation densities, sizes, shapes, and stability of the crystallites are analyzed as a function of the substrate temperature. The two molecular species were found to assume a different orientation of the molecules with respect to the substrate. An activation energy of (1.23 ± 0.12) eV was found for the nucleation of DHTA7 islands (composed of upright standing molecules), while (1.16 ± 0.25) eV was obtained for DHTA5 needles (composed of lying molecules).

1) Dihydro-tetraaza-acene molecules

Figure 1a,b presents the chemical structure of DHTA5 and DHTA7 molecules, respectively. The expected length of the molecules – considering van der Waals radii of the outer hydrogen atoms – is also indicated in Fig. 1a,b. The dihydropyrazine unit provides two additional electrons – compared to the parenting linear oligoacenes – that are delocalized over the entire molecule. As a result, HOMO levels are shifted lower with respect to the Fermi level (and compared to the corresponding acenes) which is correlated to better air stability of the molecules. H-donor (N-H) and H-acceptor (N=C) sites form H-bonds between the neighboring molecules. The presence of intralayer H-bonds strengthens the molecular interactions, orients neighboring molecules into a head-to-tail arrangement, and enables π - π stacking of the subsequent molecular layers. Figure 1c,d presents ball-and-stick models of DHTA5 and DHTA7 dimers confined in a plane, also indicating (NH...N) intralayer hydrogen bonding.

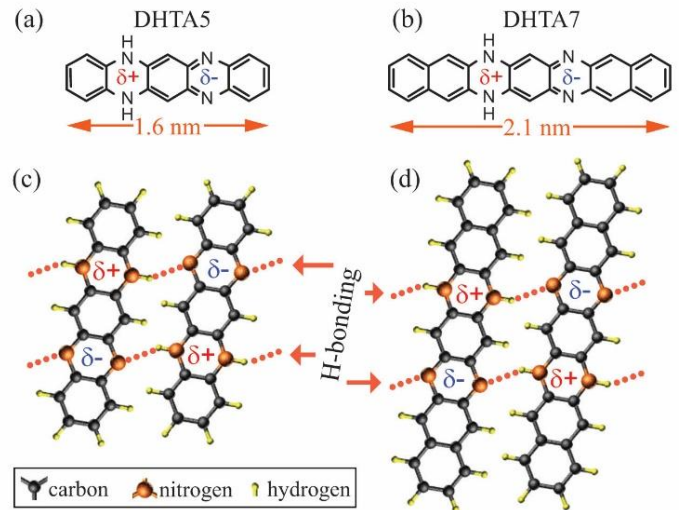


Figure 1: (a) and (b) presents the chemical structure of DHTA5 and DHTA7, also indicating the expected lengths of the molecules. (c) and (d) show ball-and-stick models of DHTA5 and DHTA7 dimers confined in a plane. (reprinted from [1]).

2) Growth morphologies of DHTA7

Growth morphologies of DHTA7 have been analyzed as a function of T_D in a range from 310 K to 440 K. By changing T_D surface diffusion of the molecules is changed, consequently giving larger crystallites and smaller number of nucleation points per unit area. An example for DHTA7 crystallite evolution with increasing T_D is presented in Figure 2. It was observed that with an increase of T_D the diffusion along the rim of the growing crystallite is also increased, resulting in a regular shape.

3) Growth morphologies of DHTA5

In a similar manner as for DHTA7, a temperature series of DHTA5 samples was examined, within a range of T_D between 340 K and 380 K. Figure 3 gives an example of one T_D series of DHTA5. Unlike DHTA7 that forms predominantly island like crystallites, DHTA5 was found

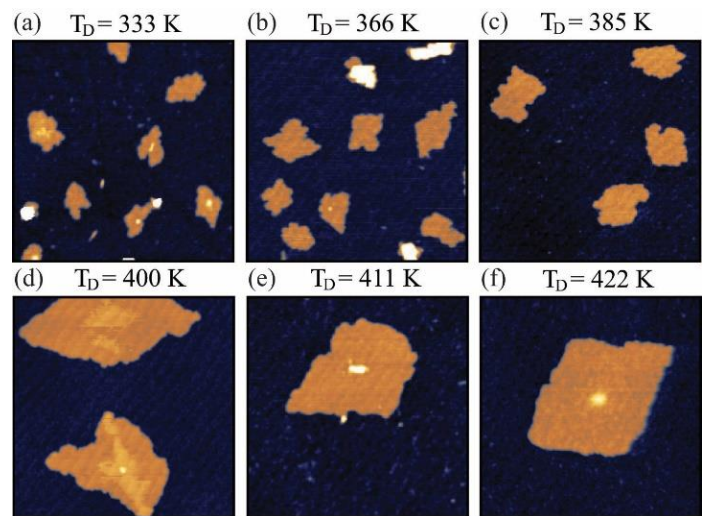


Figure 2: $1 \times 1 \mu\text{m}^2$ images of DHTA7 islands grown on sapphire (0001) in the T_D range from 333 K to 422 K, z scales 5 nm. (reprinted from [1]).

to form both three-dimensional needle-like crystallites and

islands that tend to nucleate from the needles. There was no evidence of the preferred growth directions of the DHTA5 needles. This indicates that the molecules cannot find a commensurate state on the substrate, although they assume a flat-lying orientation. Furthermore, many of the observed needles do not grow in a straight line and either have several kinks separated by straight segments or appear – to the extent of the AFM resolution – as continually curved. This morphology feature could be explained considering that the growing needle-like crystallites are not in registry with the substrate, and thus any structural defect can alter the growth direction, without being “corrected for” by the molecule-substrate interaction

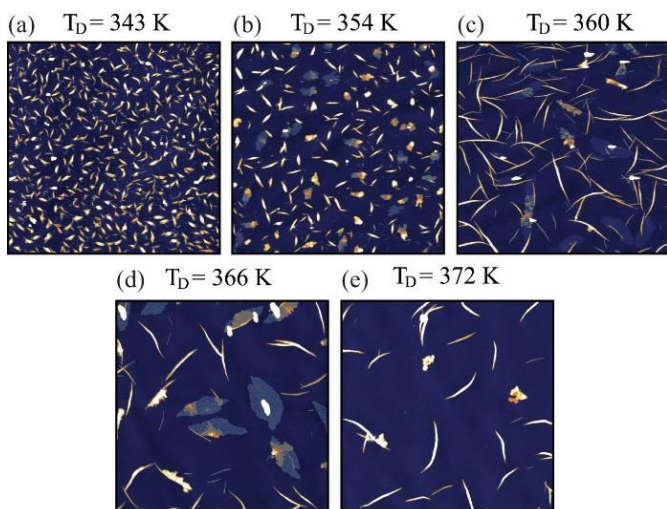


Figure 3: $5 \times 5 \mu\text{m}^2$ images of DHTA5 needles and islands grown on sapphire (0001) in the T_D range from 343 K to 372 K, z scales 10 nm. (reprinted from [1]).

4) DHTAs on other substrates

Besides (0001) sapphire, growth morphologies of DHTA5 and DHTA7 were also investigated on other substrates. Somewhat similar growth morphologies have been observed for both molecular species on amorphous SiO_2 substrates. However, on crystalline van der Waals substrates as graphene and hexagonal boron nitride (hBN), both molecular species predominantly form very elongated and straight needle-like crystallites. In particular, epitaxial relation between DHTA7 and two different 2D material substrates – graphene and hBN – has been investigated using analysis of the crystallites growth directions and considering site-specific adsorption of the individual molecules obtained from the density functional theory calculations.

Cooperation

- A. Thomas, Z. Chen, O. Siri, C. Becker, Aix Marseille Univ., CNRS, CINaM, Marseille, France.
- P. Puschnig, D. Lüftner, Institute of Physics, KFU Graz, NAWI Graz, Austria.
- Joint ANR/FWF project: I1788-N20.

Selected Key References

- [1] Matković A, Çiçek A, Kratzer M, Kaufmann B, Thomas A, Chen Z, Siri O, Becker C, Teichert C: Growth morphologies of dihydro-tetraaza-acenes on c-plane sapphire. *Surface Science*, (2018), <https://doi.org/10.1016/j.susc.2018.03.009>.

Surface Physics & Scanning Probe Microscopy

Interfacial band engineering: Charge transfer between molecular semiconductors and graphene

Aleksandar Matković, Markus Kratzer, Benjamin Kaufmann, Christian Teichert
 aleksandar.matkovic@unileoben.ac.at

The unique density of states and exceptionally low electrical noise allow graphene-based field effect devices to be utilized as extremely sensitive potentiometers for probing charge transfer with adsorbed species. On the other hand, molecular level alignment at the interface with electrodes can strongly influence the performance of organic molecule-based devices. For this reason, interfacial band engineering is crucial for potential applications of graphene in organic semiconductor technologies.

We demonstrated charge transfer between graphene and two molecular semiconductors, parahexaphenyl (6P) and buckminsterfullerene C₆₀. Through in-situ measurements, we directly probed the charge transfer as the interfacial dipoles are formed. It has been found that the adsorbed molecules do not affect electron scattering rates in graphene, indicating that charge transfer is the main mechanism governing the level alignment. From the amount of transferred charge and the molecular coverage of the grown films, the amount of charge transferred per adsorbed molecule has been estimated, indicating very weak and most likely integer charge transfer interaction [1]. The study has been supported by Austrian Science Fund (FWF) through project I1788-N20.

1) In-situ setup for the charge transfer measurements

The custom-built hot wall epitaxy (HWE) chamber used in this study has three electrical contacts attached to the sample holder, which allow to probe and tune electrical properties of the samples prior and during the growth. A layout of the growth chamber is illustrated in Figure 1a. A schematic representation of a graphene field effect transistor (FET) is shown in Figure 1b, also indicating the connections for the in-situ electrical measurement setup. From the transfer curves of graphene FETs ($I_{SD}(V_{SG})$) it is possible to recalculate the position of graphene's Fermi level, both prior and after the growth (E_{F0} and E_{F1}) as illustrated in Figure 1c. Figure 1d shows an atomic force microscopy (AFM) overview topography image of one of the devices covered with ~0.8 ML of 6P.

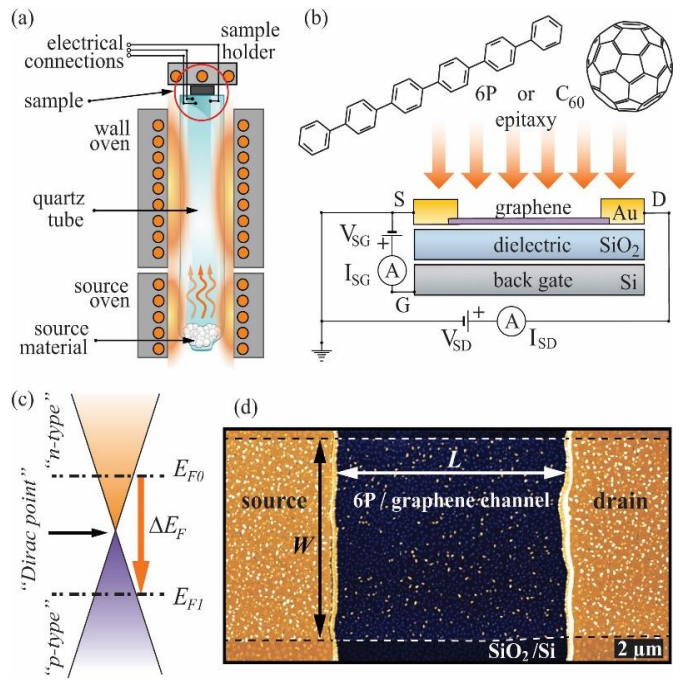


Figure 1: (a) and (b) schemes of the HWE setup and graphene FET during the growth, respectively. (c) Dispersion relation of graphene, indicating influence of charge transfer on the Fermi level position. (d) AFM topography image of one of the devices used in the study (reprinted from [1]).

2) Charge transfer / growth experiments

The following procedure was carried out for all the growth experiments and is presented in Fig. 2 for the two cases: 6P on p-type graphene and C₆₀ on an n-type graphene. Transfer curves of graphene FETs were checked in high vacuum and at room temperature moments before and after the growth (Fig. 2(a,d)). During the growth, the current across graphene channel (I_{SD}) was monitored as a function of time (Fig. 2(b,e)) and both source-drain (V_{SD}) and source-gate (V_{SG}) voltages were kept fixed. By choosing the value for V_{SG} during the growth experiment, it is possible to position the Fermi level in graphene precisely (down to few meV) having a direct control over the type of majority carriers in graphene when the growth starts.

During the growth (Figure 2(b,e)), the changes in I_{SD} are introduced by the adsorbing molecules that exchange electrons with graphene and act as an additional source of electrostatic gating. Here, band alignment between graphene and the chosen molecular species plays the most important role on the electrostatic landscape of the formed interface (Figure 2(c,f)).

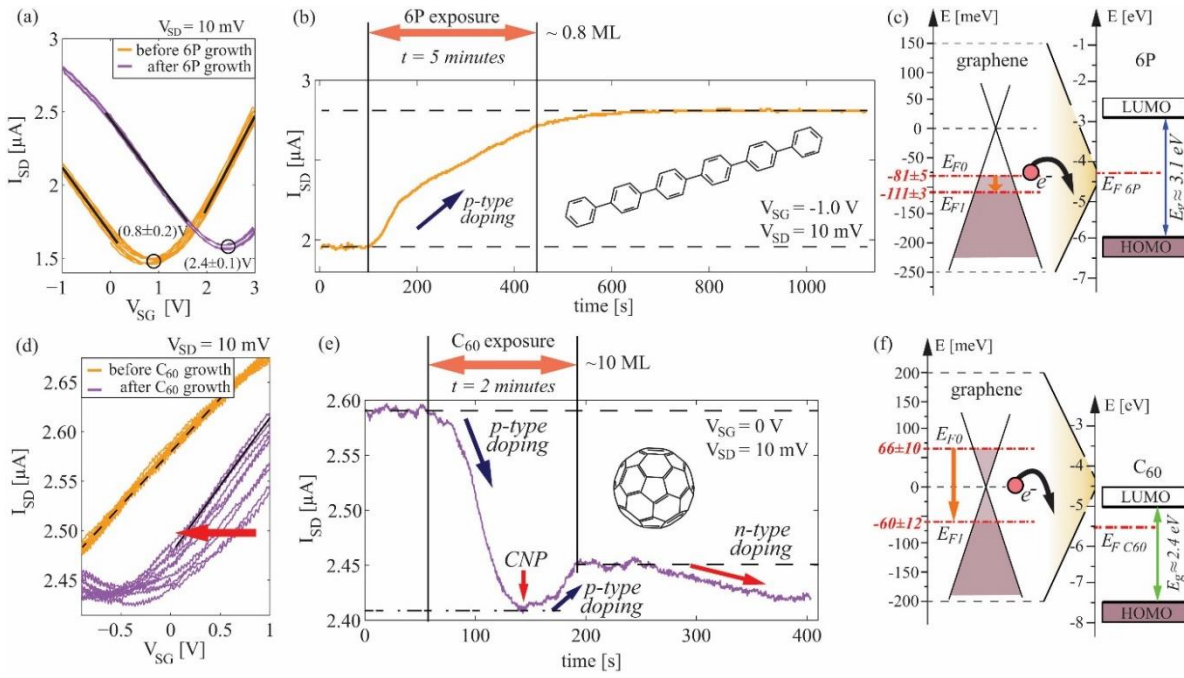


Figure 2: Charge transfer/growth experiment examples for 6P (a-c) and C_{60} (d-f). (a,d) transfer curves moments before (orange) and after (purple) the growth. (b,e) $I_{SD}(t)$ during the growth, the arrows indicate the type of doping, insets show the structures of the grown molecules. (e,f) band alignment (equal vacuum levels) indicating E_F shifts and the direction of the charge transfer (reprinted from [1].)

3) Charge transfer estimation

Since the shift of the charge neutrality point (CNP) of graphene is known from the electrical measurements, it is possible to estimate the number of transferred electrons from graphene. The detailed morphology of the grown films revealed by AFM allows an estimation of the number of deposited molecules. From these two values, the average charge transfer per adsorbed molecule can be calculated. A compilation of the estimated charge transfer per adsorbed molecule as function of the CNP position (initial Fermi level position in the top x axis) is provided in Fig. 3. The obtained charge transfer per adsorbed 6P molecule was found to be $\sim 4.7 \times 10^{-4}$ electrons/6P, and for the case of C_{60} somewhat higher values of $\sim 1.1 \times 10^{-3}$ electrons/ C_{60} were deduced. No significant change of the charge transfer was observed within the available range of the applied gate voltage (initial position of graphene's Fermi level), and the observed differences between individual devices are likely related to sample-to-sample variations.

The fact that over thousand molecules are needed to extract only one electron from graphene raises the question of the nature of the charge transfer mechanism. In this study, fractional charge transfer is less likely due to the vdW nature of the interface. Moreover, measurements of the source-drain current during the growth did not show significant changes between the first and several subsequent layers, for the case when multi-layers are grown. This observation further indicates that the charge transfer mechanism is likely an integer than a fractional one.

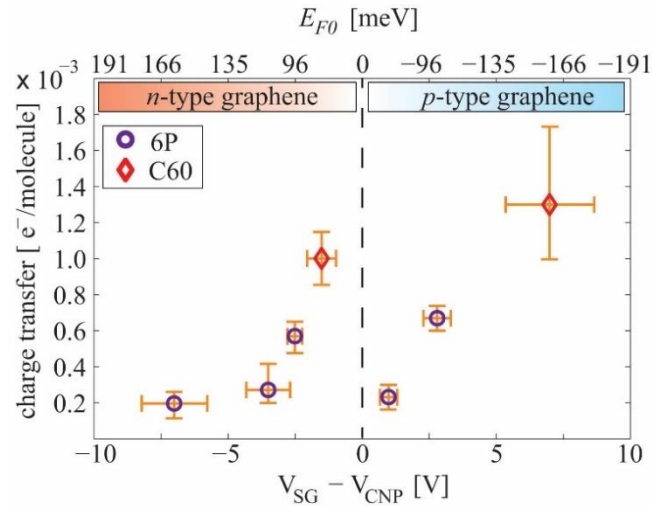


Figure 3: Charge transfer per molecule as a function of the position of the charge neutrality point (CNP) prior to the growth, for all the devices used in this study. Circles represent the data for 6P/graphene and diamonds for C_{60} /graphene interfaces. (reprinted from [1].)

Cooperation:

- R. Gajić, B. Vasić, J. Vujin, Institute of Physics, University of Belgrade, Serbia – ÖAD project SRB 09/2016
- Joint ANR/FWF project: I1788-N20

Selected Key References:

- [1] Matković A, Kratzer M, Kaufmann B, Vujin J, Gajić R, Teichert C: Probing charge transfer between molecular semiconductors and graphene. *Sci. Rep.* **7**: 9544 (2017).

Surface Physics & Scanning Probe Microscopy

Cellulose based materials

Caterina Czibula, Lisa-Marie Weniger, Christian Ganser, Christian Teichert
 teichert@unileoben.ac.at

Cellulose based materials play a crucial role in human society since ancient times and are present in a variety of forms in modern times. Everyday life would be indispensable without wood as a construction material, paper as an information carrier, and regenerated cellulose (viscose) fibers in textiles and hygiene products. Even for application in electronics, cellulose based materials have great potential and offer a renewable and sustainable alternative to other materials.

The work presented in the following was conducted within the Christian Doppler Laboratory for “Fiber Swelling and Paper Performance”, coordinated by Prof. Ulrich Hirn (Graz University of Technology) and the Christian Doppler Laboratory for “Surface Chemical and Physical Fundamentals of Paper Strength”, coordinated by Prof. Robert Schennach (Graz University of Technology).

1) Validation of an AFM based method to investigate the transverse viscoelastic properties of cellulose fibers

In the past, AFM based nanoindentation (AFM-NI) has already been successfully employed to measure elastic and plastic properties of cellulosic materials, in water, in air, and in an environment with controlled humidity [1]. Cellulosic fibers have not only anisotropic properties, but also a very rough surface which can cause uncertainties in measurements due to not well-established contact between the AFM tip and the fiber surface. For this reason, an AFM method [2] was developed to overcome the surface roughness of the pulp fibers and to determine the viscoelastic properties of single fibers in the transverse direction. The evaluation of the experimental data combines contact mechanics and viscoelastic models. Those models consist of springs and dashpots in series or parallel describing elastic and viscous behavior. In this work, the Standard Linear Solid (SLS) model and the Generalized Maxwell model, as depicted in Figure 1, are used. To validate the method, two amorphous polymers polymethylmethacrylate (PMMA) and polycarbonate (PC) are investigated by the AFM based method and the results are compared to those obtained by nanoindentation (NI) and tensile creep tests [2].

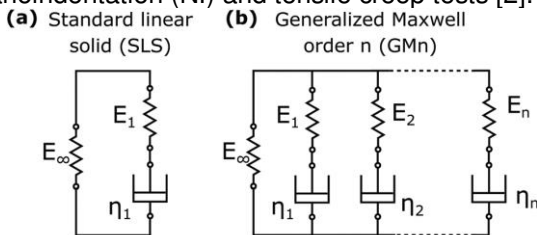


Figure 1: Linear viscoelastic models, (a) Standard Linear Solid model, (b) Generalized Maxwell model of order n (from [2]).

The results of the different tests show that the methods operating on the same scale (AFM-NI and NI) yield comparable values. However, tensile test results differ from the other two, but similarities are observed. Also, all methods show the same trend that PMMA is stiffer than PC. Furthermore, with all three methods it was possible to distinguish between PMMA and PC reliably.

2) Topography effects in AFM force mapping experiments on xylan-coated cellulose thin films

Xylan-coated cellulose thin films have been investigated by AFM phase imaging and AFM force mapping experiments with modified AFM tips (sensitive to hydrophilic OH and hydrophobic CH₃ groups) to characterize and localize the xylan on the surfaces [3, 4]. At first glance, a clear difference in the adhesion force between xylan-coated areas and cellulose has been observed, as can be seen in Figure 2. However, these different adhesion forces originate from topography effects, which prevent the identification and localization of the xylan on the cellulose thin films. It could be concluded that even for rather smooth samples, this topographical influence proves that an AFM approach based on functionalized tips cannot be easily applied to distinguish between xylan and cellulose.

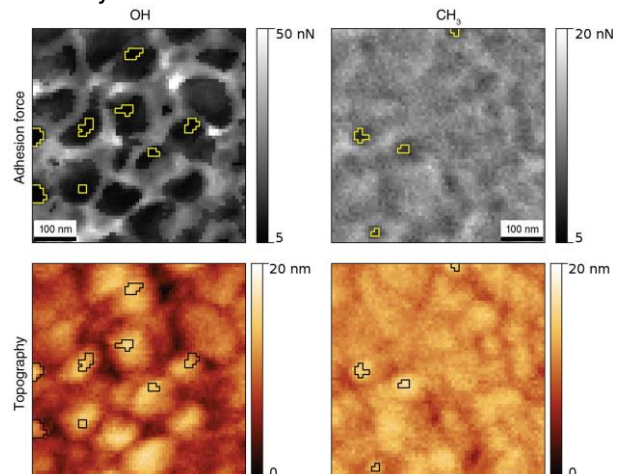


Figure 2: Adhesion force maps and the corresponding AFM topography images, recorded with OH and CH₃ functionalized tips. Regions with an adhesion force below 10 nN are marked yellow in the adhesion force maps and black in the topography maps (from [3]).

Stimuli-responsive elastomer networks

Christian Ganser, Christian Teichert
teichert@unileoben.ac.at

Recent polymer research is aiming to develop stimuli-responsive materials that change specific material properties upon an external trigger. To obtain switchable stimuli-responsive polymers which regain their original material properties by a second trigger, photo-reversible links are often used. In the last years, optically triggered cycloaddition reactions have led to the development of photo-reversible polymers, which promise spatially controlled tuning of material properties at room temperature.

The work presented in the following was conducted in collaboration with Polymer Competence Center GmbH, Leoben and chair of chemistry of polymeric materials.

A stimuli-responsive rubber with pendant anthracene groups (HXNBR, hydrogenated carboxylated nitrile butadiene rubber) was investigated for the preparation of dry adhesives with reversible adhesion strength. This has been investigated by employing AFM based adhesion mapping [5]. The results provide evidence that the non-exposed (i.e. crosslinked) area exhibits an adhesion, which is around 100 nN lower than the exposed (i.e. de-crosslinked) area. Also, variation in film thickness due to different illumination treatment has been investigated with AFM [6]. The results are shown in Figure 3. Crosslinking reactions result in volume shrinkage of the bulk material and a decrease of the film thickness (Figure 3, region III), but subsequent partial cleavage of the network induces a slight increase of the film thickness again (Figure 3, region IV).

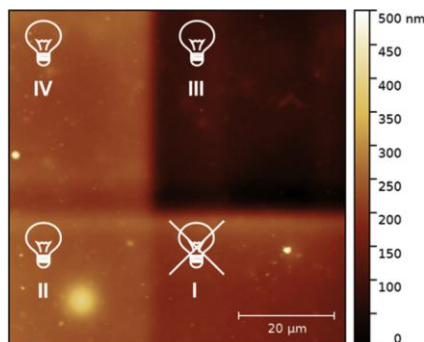


Figure 3: $70 \times 70 \mu\text{m}^2$ AFM topography image of a reversibly patterned thin rubber film prior to development in acetonitrile. The four different irradiation regions are highlighted with: (I) non-illuminated, (II) illuminated with $\lambda = 254 \text{ nm}$, (III) illuminated with $\lambda > 300 \text{ nm}$ and (IV) illuminated with $\lambda > 300 \text{ nm}$ and subsequently illuminated with $\lambda = 254 \text{ nm}$ (from [6]).

Cooperation

- Wolfgang Bauer, Ulrich Hirn, Stefan Spirk (Institute of Paper-, Pulp- and Fibre Technology, Graz University of Technology);
- Robert Schennach (Institute of Solid State Physics, Graz University of Technology);
- Wolfgang Kern, Sandra Schlögl, Simone Radl, Daniel Tscharnuter (Polymer Competence Center Leoben GmbH);
- Thomas Schöberl (Erich Schmid Institute, ÖAW Leoben);
- Leo Arpa, Gerhard Drexler, Heidemarie Reiter, Franz J. Schmied (Mondi); Richard van Hameren, Louis Saes, Ern Clevers (Océ Venlo); Michael Pohlt (Océ Poing); Ingo Bernt (Kelheim Fibres); Taoufik Mbarek (SIG Combibloc).

Selected Key References:

- [1] Ganser C, Teichert C: AFM-based Nanoindentation of Cellulosic Fibers. In: *Applied Nanoindentation of Advanced Materials*, Ed. A. Tiwari, pp. 247-267, Wiley, 2017.
- [2] Ganser C, Czibula C, Tscharnuter D, Schöberl T, Teichert C, Hirn U: Combining adhesive contact mechanics with a viscoelastic material model to probe local material properties by AFM. *Soft Matter*, **14**, 140-150 (2018).
- [3] Ganser C, Niegelhell K, Czibula C, Chemelli A, Teichert C, Schennach R, Spirk S: Topography effects in AFM force mapping experiments on xylan-decorated cellulose thin films. *Holzforschung*, **70**, 1115-1123 (2016).
- [4] Czibula C: Exploring chemical contrast on cellulosic materials with atomic force microscopy. *Diploma Thesis*, Montanuniversitaet Leoben (2016).
- [5] Kaiser S, Radl SV, Manhart J, Ayalur-Karunakaran S, Griesser T, Moser A., Ganser C, Teichert C, Kern W, Schlögl S: Switching "on" and "off" the adhesion in stimuli-responsive elastomers. *Soft Matter*, **14**, 2547-2559 (2018).
- [6] Manhart J, Ayalur-Karunakaran S, Radl S, Oesterreicher A, Moser A, Ganser C, Teichert C, Pinter G, Kern W, Griesser T, Schlögl S: Design and application of photo-reversible elastomer networks by using the $[4\pi s+4\pi s]$ cycloaddition reaction of pendant anthracene groups. *Polymer*, **12**, 10-20 (2016).

Surface Physics & Scanning Probe Microscopy

Crystal Morphology Investigation of LiFePO_4 Microparticles using AFM and First-Principles

Kevin-Peter Gradwohl, Christian Teichert
teichert@unileoben.ac.at

Olivine structure LiFePO_4 (LFP) is one of the most promising candidates for cathode materials in large scale applications such as lithium iron phosphate batteries in power storage of solar power installations and electric vehicles. The nominal output of a LFP cell is around 3.3 V, which makes a series of four cells particularly suitable for automotive applications. LFP batteries are rechargeable batteries which have a longer cycle life than common lithium cobalt nickel oxide batteries. This is due to their special crystal structure. Extracting lithium from LFP generates FePO_4 which has a similar crystal structure with a similar volume. Therefore, extracting as well as inserting lithium are very stable processes. This also leads to a higher power density over a wider temperature range than conventional lithium-ion batteries.

However, the energy needed to extract Li-ions from the LFP surface varies significantly for different facets of the crystal [1]. Therefore, the device efficiency can be increased if a cathode would consist of preferable facets only, which can be achieved by using LFP microparticles. In collaboration with the Laboratory of Nanoelectronics of the ETH Zürich and the Materials Center Leoben LFP microparticles were investigated. They were produced by modified hydrothermal synthesis with different chemical precursors [2]. Depending on type and concentration of the precursors, particle shapes ranged from flat diamonds to non-faceted ellipsoids as well as cuboids as revealed by atomic force microscopy in Figure 1 [3].

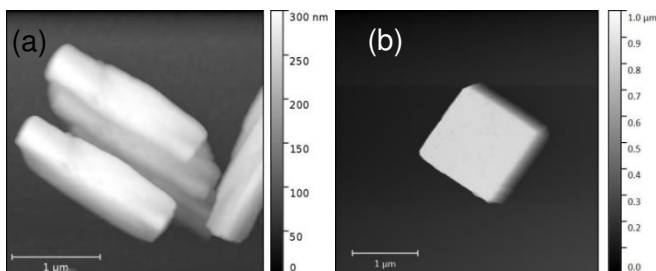


Figure 1: AFM Topographic Picture showing differently shaped LiFePO_4 microparticles (a) as the not faceted Ribbon particles and (b) the Cube particles.

1) Investigation of particle morphology

The quantitative AFM surface information (edge angles and facet tilts of the crystals, Figure 2a) was used to plot the surface normal vector distribution, referred to as facet analysis as shown in Figure 2b. By knowing all angles between facets it was possible to determine the Miller indices of each facet by an error minimization technique. This was represented in a crystallographic model such as

Figure 2c for the wide diamond particles. These results were used to obtain a better understanding of the process of synthesis as well as cleavage of the LFP [4].

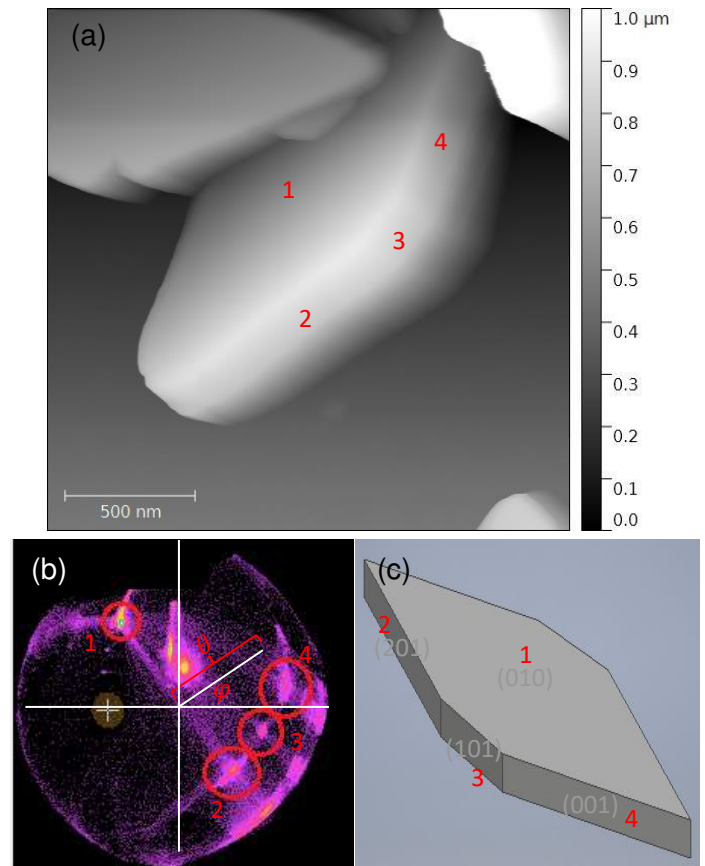


Figure 2: Analysis of LiFePO_4 wide diamond particles (a) $3 \times 3 \mu\text{m}^2$ AFM height picture, (b) polar plot representing the surface normal vector distribution of the particles and (c) crystallographic model of the particles derived from error minimization.

2) First-Principles Calculations

The experimentally observed facet orientations also have been compared to previous first-principles studies [1]. All facets observed here were low-surface energy facets previously calculated with exception of the also found (210) facet. Thus, the surface energy of (210) was calculated within density functional theory in the generalized gradient approximation (GGA) + U framework. It has been found that the missing facet contributes about 2.5 % to the total area of the Wulff plot (Figure 3).

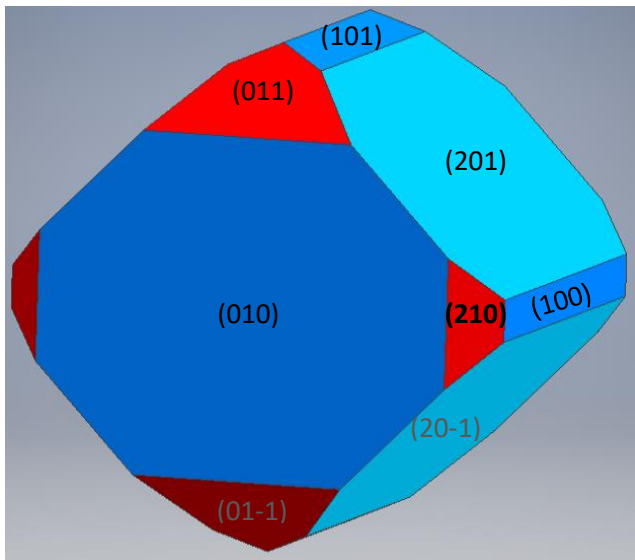


Figure 3 Wulff Plot of LiFePO₄ showing the contribution of the (210) facet, which accounts for about 2.5% of the total surface area of the polyhedron.

Cooperation:

- Peter Benedek, Maksym Yarema, Vanessa Wood (Laboratory of Nanoelectronics, ETH Zürich);
- Maxim Popov, Jürgen Spitaler (Materials Center Leoben Forschungs GmbH)

Selected Key References:

- [1] L. Wang, F. Zhou, Y. S. Meng, G. Ceder: First-principles study of surface properties of LiFePO₄ Surface energy, structure, Wulff shape, and surface redox potential, Phys. Rev. B, **2007**, 76, 165435.
- [2] X. Qin, J. Wang, J. Xie, F. Li, L. Wen, X. Wang: Hydrothermally synthesized LiFePO₄ crystals with enhanced electrochemical properties: simultaneous suppression of crystal growth along [010] and antisite defect formation, Phys. Chem. Chem. Phys., **2012**, 14, 2669.
- [3] Benedek, Peter, N. Wenzler, M. Yarema, and V. C. Wood: Low temperature hydrothermal synthesis of battery grade lithium iron phosphate, RSC Advances 7, **2017**, no. 29, 17763-17767.
- [4] K.-P. Gradwohl: Crystal Morphology of Lithium - Iron Phosphate Microparticles investigated by Atomic Force Microscopy, *Bachelor Thesis*, Montanuniversität Leoben **2016**.

Photonics & Nanoelectronics

Simulation of Complex Multilayer Structures for Extreme Ultraviolet Mirrors

Ronald Meisels, Friedemar Kuchar
 meisels@unileoben.ac.at
 kuchar@unileoben.ac.at

Motivation

Future 7 nm and sub-7nm nanolithography will require a reduction of the wavelength from deep ultraviolet radiation with 193 nm to 13.5 nm extreme ultraviolet (EUV) radiation. For this radiation lenses have to be replaced by multilayer Bragg reflection mirrors.

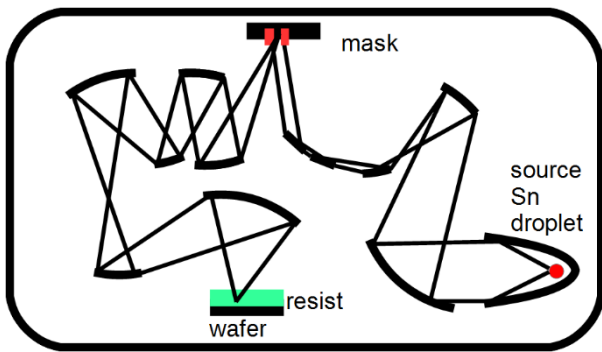


Figure 1: Schematic arrangement of the mirrors used in EUV lithography.

As shown in Fig. 1 a complex arrangement of mirrors with a wide range of incident angles is used [1]. The proposed source for the 13.5 nm radiation is a Sn plasma produced by laser pulses. In this wavelength range ordinary metallic mirrors cannot be used since the dielectric constant is no longer strongly negative, but close to unity. Here Bragg reflectors consisting of multiple layers are used to increase the reflectance by constructive interference. In this work, the influence of different design structures on the reflectance is studied.

Method

To calculate the reflectance of an array of different plane parallel layers the multiple scattering method (MSM) [2,3] is used. It yields reflectance and transmittance of the whole multilayer structure. The multilayer structure can be composed of an arbitrary arrangement of plane parallel slabs. The program MULTEM presented in Refs. 2 and 3 was modified to allow frequency dependent dielectric constants of the component slabs [4]. The dielectric constants of the slabs were calculated from the scattering factors of the atoms the slabs are made of. Their frequency dependence is available from Ref. 5. The dielectric constants are calculated using the formula [6]

$$\mathbf{n} = n + ik = 1 - \frac{r_e}{2\pi} \lambda^2 \sum_j n_j f_j$$

where $r_e = e^2 / 4\pi\epsilon_0 m_e c^2$ is the classical electron radius, n_j and f_j are atomic concentrations and complex scattering factors, respectively.

Structures

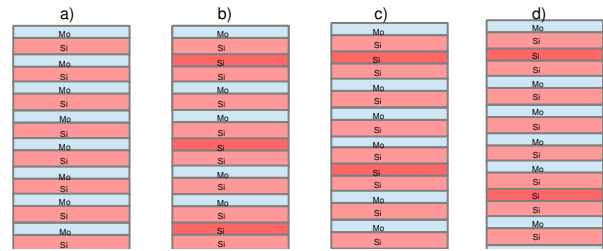


Figure 2: Top of multilayer structures. Shown from left: a) regular structure; b) superlattice with period 3 (SL-3); c) superlattice with period 4 (SL-4); d) superlattice with period 5 (SL-5); the modified layer (Si instead of Mo) is shown in darker color for emphasis. The number of Mo/Si interfaces is kept constant (40).

The regular structure has a period of $d_{dl} = 6.9$ nm. The Mo:Si ratio in a double layer is 40:60. It is used in state-of-the-art Bragg mirrors for EUV lithography. In addition to regular structures of Mo/Si double layers superlattice structures are studied. These structures are modified by replacing every n_{SL} -th, e.g. every fourth Mo layer by a Si layer of the same thickness.

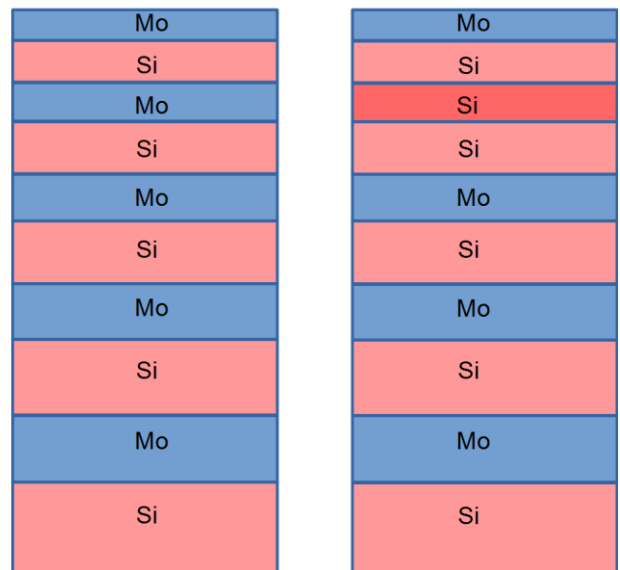


Figure 3: depth graded structure. Left: a) depth grading of regular structure; Right: superlattice imposed on graded structure.

A further modification studied is that the thicknesses of the layers are gradually increased (see Fig. 3).

Result: superlattice structures

Figure 4 shows, for comparison, the reflectance for a regular Mo/Si Bragg reflector structure as shown in Fig. 2a. The central part shows the Bragg reflection at 13.5 nm for normal incidence (0°) and curving to lower wavelengths for oblique incidence according to the condition[6]:

$$\lambda = 2d_{dl} \sqrt{n_{eff}^2 - \sin^2(\varphi)}$$

n_{eff} is the averaged refractive index of the Mo/Si structure. For grazing incidence, because $n_{eff} < 1$, total reflection occurs for angles large than α_{crit} , where

$$\sin(\alpha_{crit}) = n_{eff}$$

holds.

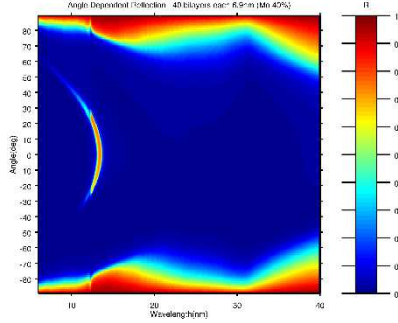


Figure 4: Dependence of the reflectance of a regular Mo/Si Bragg reflection mirror on the wavelength and on the angle of incidence. Positive values are for s-polarization (E-field parallel to layer surfaces) and negative values are for p-polarization.

For the superlattice structures shown in Figs. 2b) to 2d) additional reflections are seen at intermediate angles α_{refl} and wavelengths λ_{refl} (see Fig 5). For these reflections the relation

$$\sin(\alpha_{refl}) = \sqrt{n_{eff}^2 - k_{SL} \frac{\lambda_{refl}}{2D_{SL}}}$$

holds. k_{SL} is integer and is the index of the superlattice peak, $D_{SL} = n_{SL} d_{sl}$ is the period of the superlattice unit, e.g. $3 \times 6.9 \text{ nm}$ for SL-3.

As shown in Fig. 4 the spectrum of the reflectance around 13.5 nm narrows with reduced superlattice period which corresponds to more Mo layers being replaced by Si. It is narrowest for SL-2 where half of the Mo layer are replaced by Si.

The diagrams of Fig. 7 show in particular the angle dependence of the reflectance at 13.5 nm, the wavelength of the Sn plasma source. As the superlattice period increases, additional peaks appear in the intermediate angle range between the central peak around 0° angle of incidence and the strong reflection near 90° .

For s-polarization (electric field parallel to the layer surfaces, $n_{SL} - 1$ ($n_{SL} \times 6.9 \text{ nm}$ is the superlattice period) peaks are seen. For p-polarization fewer peaks are seen due to the absence of reflection at the Brewster angle.

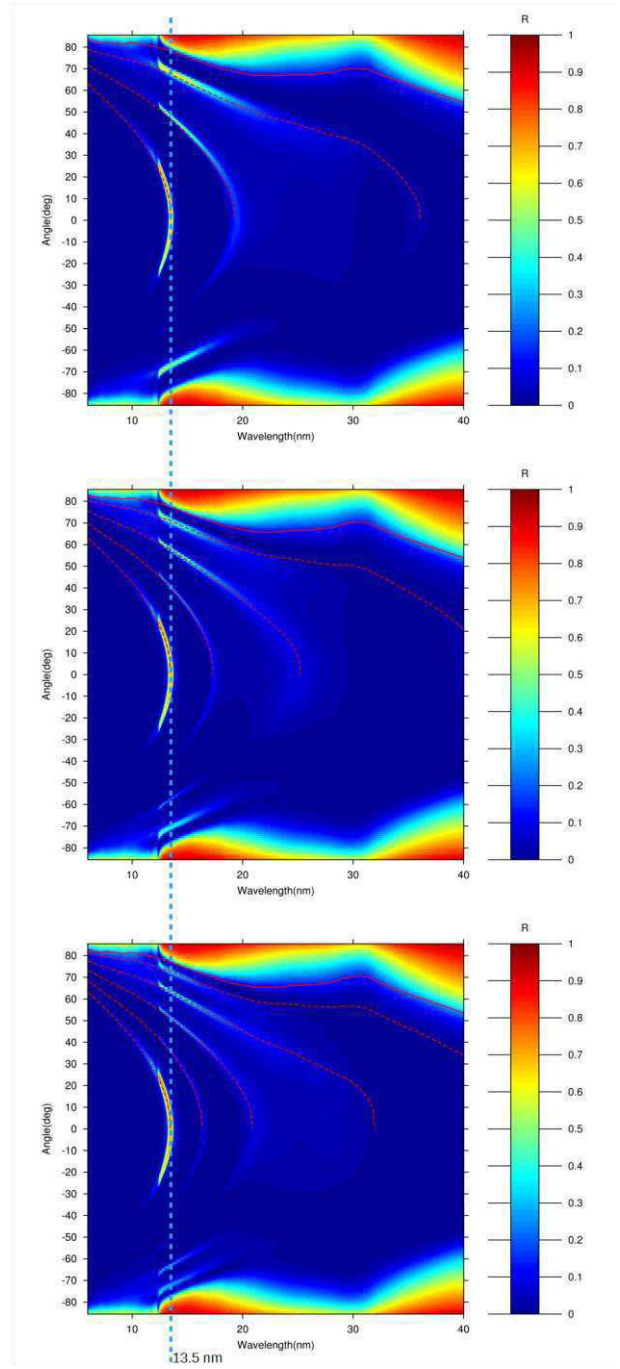


Figure 5: Dependence of the reflectance on the wavelengths λ_{refl} and on the angle of incidence α_{refl} for Mo/Si superlattice mirrors (SL-3 (top), SL-4 (center), and SL-5 (bottom)). Dashed red lines indicate theoretical position of the superlattice peaks. Positive values are for s-polarization (E-field parallel to layer surfaces) and negative values are for p-polarization. The blue dashed line indicates the peak wavelength of the Sn emission at 13.5 nm.

By alternating between superlattice period of 5 and 4 the number of intermediate peak is increased further (see Fig. 6). The introduction of grading the layer widths causes reflection in the whole intermediate range. There is a trade-off, however, as the peak reflectance at normal incidence is reduced.

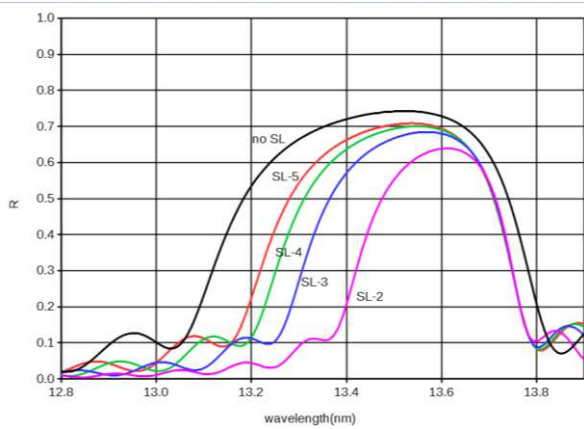


Figure 6: Reflectance of the regular structure (no SL) and of superlattices with superlattice periods 2 to 5 (SL-2 to SL-5) for normal incidence.

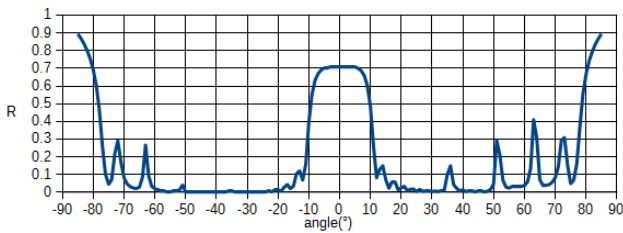
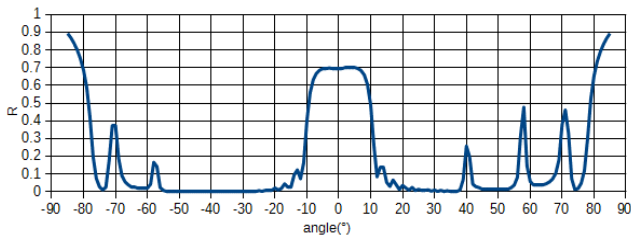
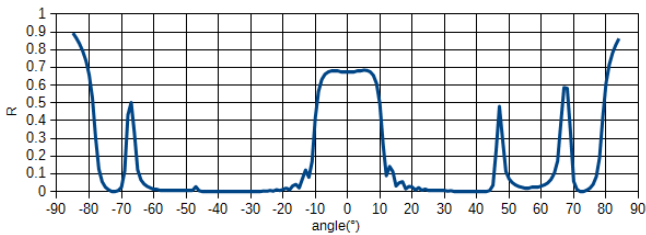


Figure 7: Angle dependence of the reflectance of the superlattice structures with superlattice periods 3 to 5 (top to bottom diagram) at 13.5 nm.

Summary

More complex PhCs than the 1D layer structure are explored. While the simple multilayer structure only shows, in addition to the reflection at normal incidence (0°), strong reflection at high angles corresponding to glancing incidence, in superlattices additional reflections appear at intermediate angles. More of these reflections appear by combining superlattices of different periods. By introducing a gradual increase of the layer thicknesses the intermediate range is covered so a wider range of incident angle is covered in the EUV optics; however the reflectance at normal incidence is reduced.

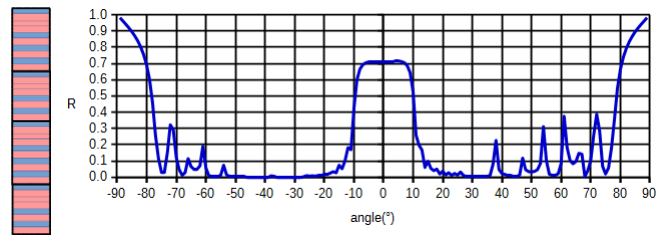


Figure 8: Angle dependence of the reflectance of the superlattice structure with alternating superlattice units of period 5 and 4 (shown at left) at 13.5 nm

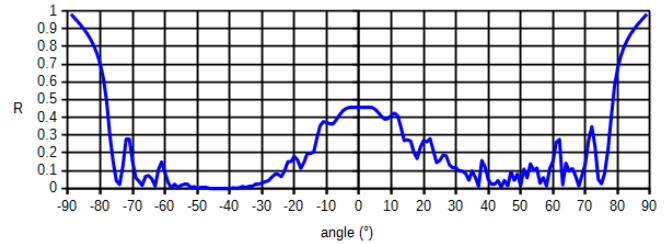


Figure 9: Angle dependence of the reflectance of the superlattice structure with alternating superlattice units of period 5 and 4 and with graded layer widths. The width is linearly increased from $d_{d1} = 6.9$ nm at the top to $d_{d1} = 9.66$ nm at the bottom of the mirror.

Conclusions

The narrowing of the reflectance spectrum of superlattice mirrors is useful where a sharper spectrum than produced by the EUV source is beneficial, e.g. in metrology.

The all-angle-reflectance is useful where a wide range of angles of incidence occurs, e.g., in optics with high numerical aperture in EUVL systems. With superlattices graded in this way, the thicknesses of the individual layers are varied one after another, but don't have to be varied for the off-axis regions of the mirror as it has to be done with the regular structure [7].

References

- [1] V. Baskshi, ed., "EUV Lithography", 2nd edition, Wiley (2018)
- [2] N. Stefanou, V. Yannopoulos, A. Modinos, Comput. Phys. Commun. **113**, 198 (1998).
- [3] N. Stefanou, V. Yannopoulos, A. Modinos, Comput. Phys. Commun. **132**, 198 (2000).
- [4] R. Meisels, F. Kuchar, Optics Express 25, 32215 (2017).
- [5] http://henke.lbl.gov/optical_constants/asf.html
- [6] <https://physics.nist.gov/PhysRefData/FFast/Text2000/sec01.html>
- [7] T. Feigl, S. Yulin, N. Benoit, N. Kaiser, Microel. Eng. 83, 703 (2006).

Simulation of Quantum Electron Transport

Josef Oswald
 josef.oswald@unileoben.ac.at

Introduction: In their pioneering work Chklovskii, Shklovskii and Glazman (CSG) addressed the local nature of edge channels in the integer quantum Hall effect regime [1]. Instead of narrow channels they get almost macroscopically (up to several hundred nm) wide compressible stripes (CS) that result from the electrostatic interaction based on Thomas-Fermi screening. Using a laterally resolved, self-consistent Hartree-Fock (HF) approximation we have most recently shown [2,3] that the well-known existence of an exchange enhanced Zeeman splitting is not compatible with the existence of wide regions of partly filled Landau levels (LL). We have demonstrated that many particle interactions lead to some sort of Hund's rule behavior that strongly counteracts a situation of simultaneously existing partly filled spin-up and spin-down LLs. Instead, the electron system undergoes a transformation to a mixture of clusters of full and empty LLs.

A continuous change of the total filling factor either by adding/removing electrons or changing the magnetic field leads to growing or shrinking clusters of fixed density. The boundaries of these clusters remain the only compressible parts of the electron system and thus they serve as transmitting channels for transport. From our results we draw the conclusion that on the microscopic level the many body interactions act towards re-establishing narrow channels of almost non-interacting single electrons, which seems to be at variation with the CSG picture. However, also a major part of most successful quantum Hall physics (e.g. the scaling theory) is based on models that rely on networks of narrow quantum channels such as the Chalker-Coddington network model [4].

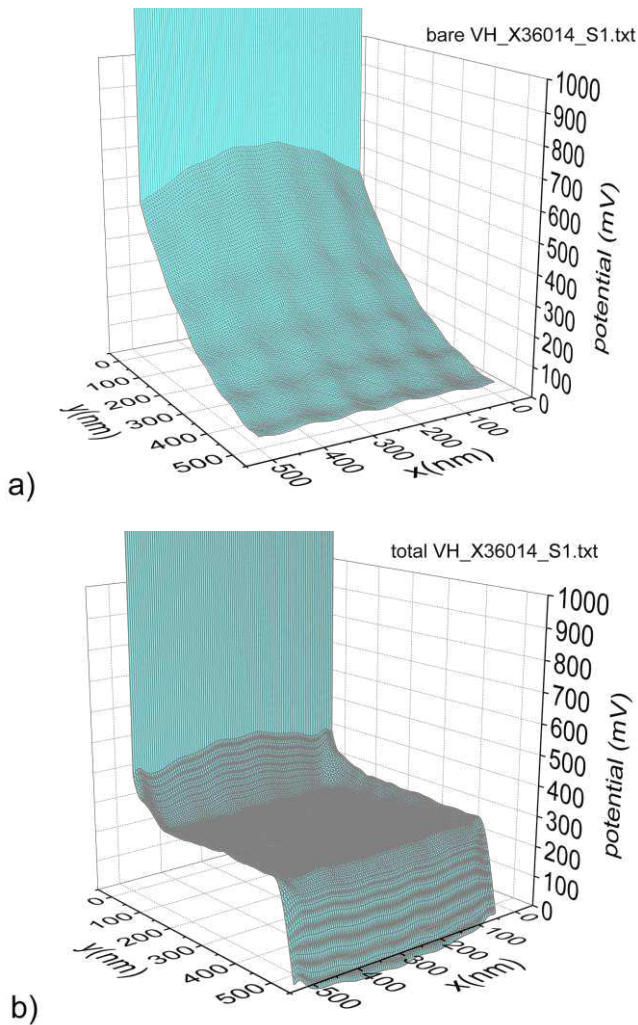


Figure 1: Bare (a) and screened (b) edge potential at $B=2.5$ T and $n = 1.3 \times 10^{11} \text{ cm}^{-2}$.

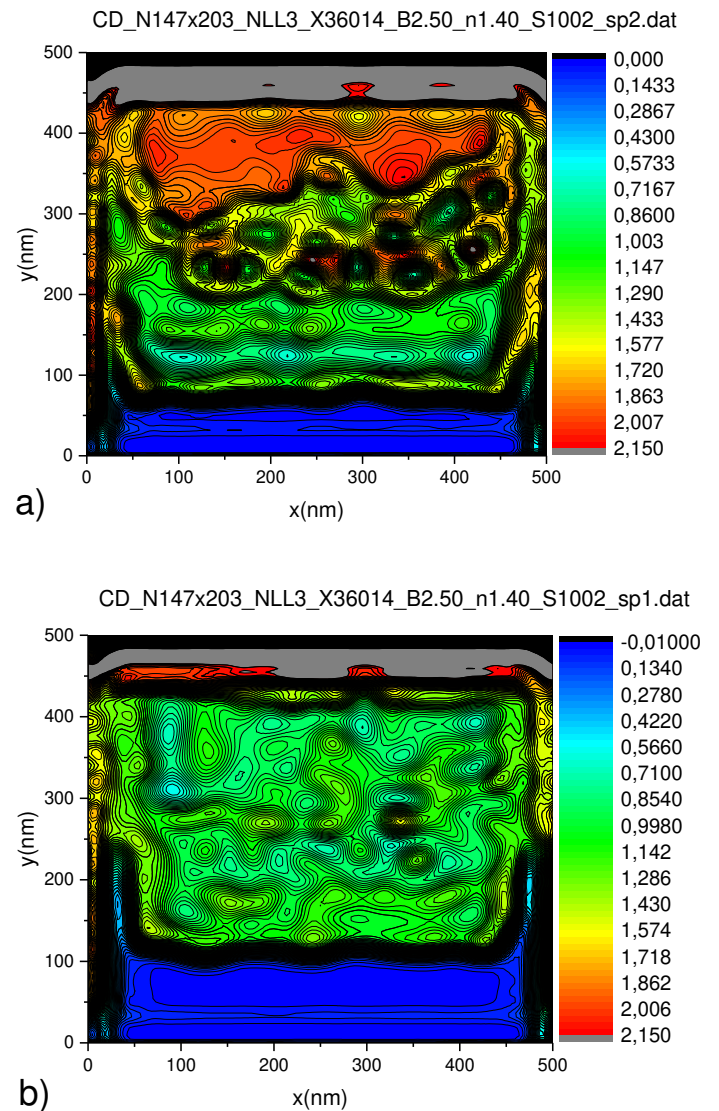
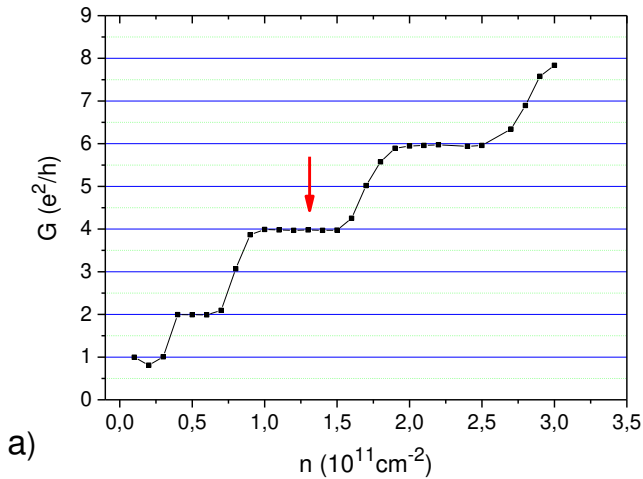


Figure 2: (a) Local filling factor distribution of spin-down electrons, which represents a partly filled 2nd LL by a mixture of clusters, that create a network of transmitting channels; (b) fully filled spin-up LL. Calculation for $B=2.5$ T and $n = 1.3 \times 10^{11} \text{ cm}^{-2}$.

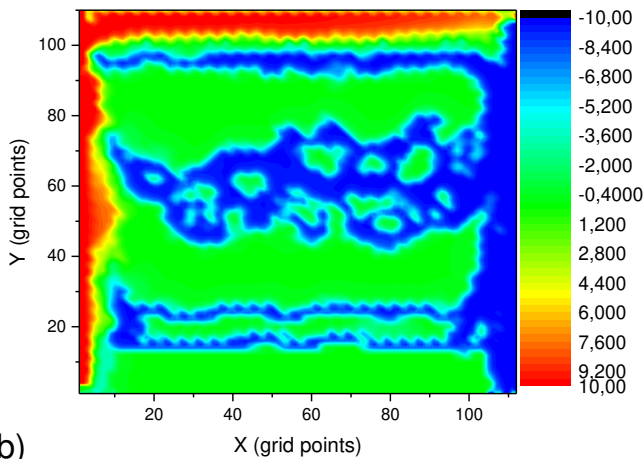
Topic 1: Compressible Stripes in the Integer Quantum Hall Effect regime: A need for re-interpretation even after 25 years¹

We propose a new view of the wide CS of CSG on the background of our most recent results. We obtained preliminary results for simulating just the edge region on one side of a Hall bar by using a large soft bare potential of about 1000 mV, while the opposite edge serves as a hard wall potential (Fig.1a). Additionally a random disorder potential of several mV amplitude is superimposed.



a)

laterally transmitted electrochemical potential via network model



b)

Figure 3: (a) two-point conductance as a function of electron density at fixed $B=2.5T$. The missing bulk region in the simulation might be responsible for the missing spin-splitting in transport, while spin-resolved edge stripes still appear at the soft edge; (b) lateral distribution of the injected non-equilibrium chemical potential for transport. At the position of the CS (edge potential terrace of Fig.1b) a network of “micro-channels” appears according to our non-equilibrium network model. The clockwise transmitted “blue” channels dissolve when arriving at the oppositely injected “red” potential. The vanishing bulk region is located close to the upper boundary, which can be understood to act as a hard wall potential.

Due to a modification of screening by just varying the size of the clusters of fully filled LLs at constant density, a Thomas-Fermi like screening behavior (like assumed by CSG) by creating edge potential terraces (see Fig.1b) recovers only on larger length scales of several hundred nanometers well above the typical cluster size. In contrast, the details of random potential fluctuations of a size equal or less than the typical cluster size remain almost unscreened. Due to the appearance of electron clusters of varying size, the on average homogeneously looking wide CS get an internal fine structure that creates a dense network of narrow channels which maintains the quantized transport (see Fig.2 and Fig.3). A complete sample with wide edge regions of several hundred nanometers on both sides and containing also a dominating bulk region like in real Hall bars, requires a total sample size of several micrometer. Such macroscopic samples at higher filling factors cannot be addressed by a pure laterally resolved, self-consistent Hartree-Fock approximation. Therefore a suitable multiscale approach has to be developed, which is the topic of future work.

Topic 2: Experimental evidence for sign reversal of the Hall coefficient in three-dimensional metamaterials

Kern et al [5] claim the observation of a sign reversal of the Hall coefficient as a three dimensional metamaterial effect. We point out that in Kern’s structure the sign reversal happens already in the individual building blocks of their crystal, which makes it’s identification as a metamaterial effect questionable. However, the understanding of metamaterial effects might be different for different systems and seems to lack a strict definition. As an example, in photonic crystals the periodicity of the host metamaterial and the interaction between the elementary building blocks is decisive, while this is not the case in Kern’s structure. Hence, a clarification is necessary.

From the topological point of view we assert that the individual elements of Kern’s structure are equivalent to the ring-like structure, which has been investigated by Mani et al [6] in the quantum Hall regime. By using a network model for magneto transport in the quantum Hall regime Oswald et al [7,8] have shown that the observed experimental behaviour can be modelled in agreement with the experiments. On the basis of these results we conclude, that the effect of sign reversal of the Hall coefficient in Kern’s metamaterial structure is the same like in Mani’s anti Hall-bar structure as numerically investigated by Oswald et al already more than 10 years ago [9].

Topic 3: Spatially resolved bubble and stripe many-body phases in the integer quantum Hall effect regime¹

While we propose a new view of the wide CS, which turns the homogeneously wide CS of CSG into stripes with an internal fine structure, we also demonstrate that for a weak long-range random disorder potential the same mechanism leads to bubble and stripe phases.

For strong disorder the cluster arrangement is triggered by the disorder potential, while for weak disorder, the necessary clusters for creating partly filled LLs arrange in a tentatively regular pattern, which appear as spaghetti like stripes for filling factors close to half filling and bubbles for filling factors far from half filling. In contrast to early but still widely accepted models [10] the structure of the boundaries of the bubble and stripe like clusters play an important role for their geometrical arrangement.

Cooperation:

Topic 1 and 3 are performed in cooperation with Rudolf A. Römer, *Department of Physics and Centre for Scientific Computing, University of Warwick, Coventry CV4 7AL, UK*

References:

- [1] D. B. Chklovskii, B. I. Shklovskii and L. I. Glazman, *Phys. Rev. B*, **46**, 4026 (1992)
- [2] J. Oswald and R. A. Römer, *EPL (Europhysics Letters)* **117**, 57009 (2017).
- [3] J. Oswald and R. A. Römer, *Phys. Rev. B* **96**, 125128 (2017)
- [4] J. T. Chalker and P. D. Coddington, *J. Phys. C: Solid State Phys.*, **21**, 2665 (1988)
- [5] Christian Kern, Muamer Kadic and Martin Wegener, *Phys. Rev. Lett.* **118**, 016601 (2017)
- [6] R. G. Mani, *Europhys. Lett.*, **36** (3), pp. 203-208 (1996)
- [7] M. Oswald, J. Oswald, and R. G. Mani, *Phys. Rev. B* **72**, 035334 (2005)
- [8] J. Oswald, M. Oswald, *Phys. Rev. B* **74**, 153315 (2006)
- [9] J. Oswald, *Phys. Rev. Lett* **120**, 149701 (2018, submitted August 2017)
- [10] M. M. Fogler, A.A. Koulakov, B.I. Shklovskii, *Phys. Rev. B*, **54**, 1853 (1996)

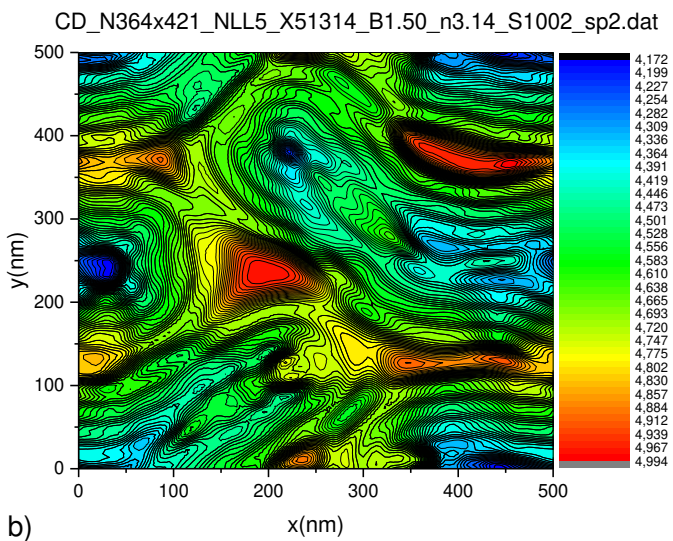
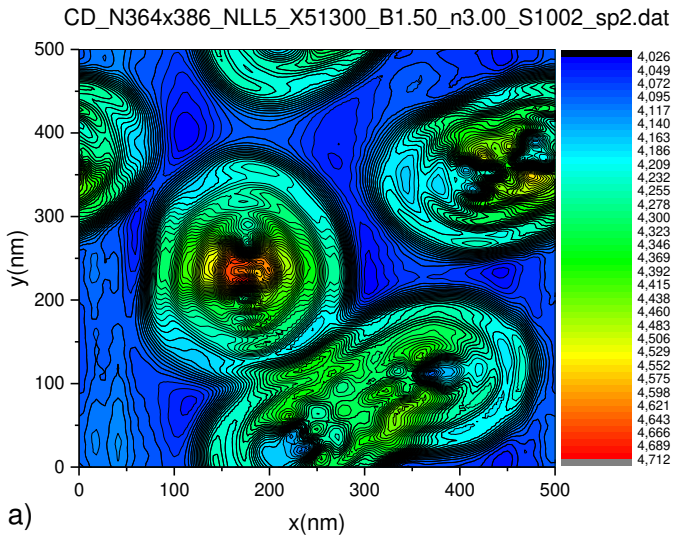


Figure 4: Simulation results for the local filling factor distribution of spin-down electrons for a low disorder structure, which represents a partly filled 5th LL a) far from half filling, which creates a bubble phase and b) close to half filling, which creates a stripe or spaghetti like phase.

3. Publication List

3.1 Original papers in SCI-listed journals

1. Balzer C., Waag A., Gehret S., Reichenauer G., Paris O., Putz F., Hüsing N., Gor G. Y., Bernstein N., and Neimark A. V., 'Adsorption-Induced Deformation of Hierarchically Structured Mesoporous Silica Effect of Pore-Level Anisotropy'. *Langmuir*, **33** (2017), 5592-5602.
2. Beltaos A., Bergren A. J., Bosnick K., Pekas N., Lane S., Cui K., Matković A., and Meldrum A., 'Visible light emission in graphene field effect transistors', *Nano Futures*, **1** (2017), 1-11.
3. Bermejo R., Daniel R., Schuecker C., Paris O., Danzer R., and Mitterer C., 'Hierarchical Architectures to Enhance Structural and Functional Properties of Brittle Materials', *Advanced Engineering Materials*, **19** (2017), 1600683.
4. Chien H.-T., Pözl M., Koller G., Challinger S., Fairbairn C., Baikie I., Kratzer M., Teichert C., and Friedel B., 'Effects of hole-transport layer homogeneity in organic solar cells – A multi-length scale study', *Surfaces and Interfaces*, **6** (2017), 4941-4947.
5. Chourdury S., Krüner B., Massuti-Ballester P., Tolosa A., Prehal C., Grobelsek I., Paris O., Borchardt L., and Presser V., 'Microporous novolac-derived carbon beads/sulfur hybrid cathode for lithium-sulfur batteries', *Journal of Power Sources*, **357** (2017), 198-208.
6. Dimitriev O. P., Grynko D. O., Fedoryak A. N., Doroshenko T., Kratzer M., Teichert C., Noskov Y., Ogurtsov N., Pud A., Balaz P., Balaz M., and Tesinsky M., 'Macroscopic versus microscopic photovoltaic response of heterojunctions based on mechanochemically prepared nanopowders of kesterite and n-type semiconductors', *Semiconductor Physics, Quantum Electronics & Optoelectronics*, **20(4)** (2017), 418-423.
7. Dohr M., Ehmann H. M. A., Jones A. O. F., Salzmann I., Shen Q., Teichert C., Ruzié C., Schweicher G., Geerts Y. H., Resel R., Sferrazza M., and Werzer O., 'Reversibility of temperature driven discrete layer-by-layer formation of dioctyl-benzothieno-benzothiophene films', *Soft Matter*, **13** (2017), 2322-2329.
8. Fritz-Popovski G., Morak R., Sharifi P., Amenitsch H., and Paris O., 'Pore Shape and Sorption Behaviour in Mesoporous Ordered Silica Films', *Journal of Applied Crystallography*, **49** (2016), 1713-1720.
9. Ganser C., Niegelhell K., Czibula C., Chemelli A., Schennach R., and Spirk S., 'Topography effects in AFM force mapping experiments on xylan-decorated cellulose thin films', *Holzforschung: International Journal of the Biology, Chemistry, Physics and Technology of Wood*, **70(12)** (2016), 1115-1123.
10. Ganser C., Popovski G., Morak R., Sharifi Rajabi P., Marmiroli B., Sartori B., Amenitsch H., Griesser T., Teichert C., and Paris O., 'Cantilever bending based on humidity-actuated mesoporous silica/silicon bilayers', *Beilstein Journal of Nanotechnology (Journal of Organic Nanotechnology)*, **7** (2016), 637-644.
11. Hartlieb P., Toifl M., Kuchar F., Meisels R., and Antretter T., 'Thermo-physical properties of selected hard rocks and their relation to microwave-assisted comminution', *Minerals Engineering*, **91** (2016), 34 - 41.
12. Kaynak B., Alpan C., Kratzer M., Ganser C., Teichert C., and Kern W., 'Anti-adhesive layers on stainless steel using thermally stable dipodal perfluoroalkyl silanes', *Applied Surface Science*, **416** (2017), 824-833.
13. Koczwarza C., Rumswinkel S., Prehal C., Jäckel N., Elsässer M. S., Amenitsch H., Presser V., Hüsing N., and Paris O., 'In Situ Measurement of Electrosorption-Induced Deformation Reveals the Importance of Micropores in Hierarchical Carbons', *ACS Applied Materials and Interfaces*, **9** (2017), 23319-23324.
14. Kondratenko S. V., Lysenko V. S., Kozyrev Y. N., Kratzer M., Storozhuk D. P., Iliash S. A., Czibula C., and Teichert C., 'Local charge trapping in Ge nanoclusters detected by Kelvin probe force microscopy', *Applied Surface Science*, **389** (2016), 783-789.
15. Kormoš L., Kratzer M., Kostecki K., Oehme M., Šikola T., Kasper E., Schulze J., and Teichert C., 'Surface analysis of epitaxially grown GeSn alloys with Sn contents between 15% and 18%.' *Surface and Interface Analysis*, **49** (2017), 297–302.

16. Kostoglou N., Koczwara C., Prehal C., Terziyska V., Babic B., Matovic B., Constantinides G., Tampaxis C., Charalambopoulou G., Steriotis T., Hinder S., Baker M. A., Polychronopoulou K., Doumanidis C. C., Paris O., Mitterer C., and Rebholz C., 'Nanoporous activated carbon cloth as a versatile material for hydrogen adsorption, selective gas separation and electrochemical energy storage', *Nano Energy*, **40** (2017), 49-64.
17. Kratzer M., and Teichert C., 'Thin film growth of aromatic rod-like molecules on graphene', *Nanotechnology*, **27(29)** (2016), 292001.
18. Manhart J., Ayalur-Karunakaran S., Oesterreicher A., Radl S. V., Moser A., Ganser C., Teichert C., Pinter G., Kern W., Grießer T., and Schlögl S., 'Design and application of photo-reversible elastomer networks by using the [4πs+4πs] cycloaddition reaction of pendant anthracene groups', *Polymer*, **102** (2016) 10-20.
19. Manhart J., Ayalur-Karunakaran S., Radl S. V., Oesterreicher A., Moser A., Ganser C., Teichert C., Pinter G., Kern W., Grießer T., and Schlögl S., 'Data on synthesis and thermo-mechanical properties of stimuli-responsive rubber materials of pendant anthracene groups', *Data in Brief*, **9** (2016), 524-529.
20. Matković A., Genser J., Lüftner D., Kratzer M., Gajic R., Puschnig P., and Teichert C., 'Epitaxy of highly ordered organic semiconductor crystallite networks supported by hexagonal boron nitride', *Scientific Reports*, **6** (2016), 38519.
21. Matković A., Kratzer M., Kaufmann B., Vujin J., Gajic R., and Teichert C., 'Probing charge transfer between molecular semiconductors and graphene', *Scientific reports*, **7** (2017), 9544.
22. Matković A., Vasić B., Pešić J., Prinz J., Bald I., Milosavljević A. R., and Gajic R., 'Enhanced structural stability of DNA origami nanostructures by graphene encapsulation', *New Journal of Physics*, **18(2)** (2016), 025016.
23. Meisels R., and Kuchar F., 'EUV Bragg reflectors with photonic superlattices', *Optics Express*, **25(26)** (2017), 32215-32226.
24. Mirkowska M., Kratzer M., Teichert C., and Flachberger H., 'Principal Factors of Contact Charging of Minerals for a Successful Triboelectrostatic Separation Process – a Review', *Berg- und hüttenmännische Monatshefte: BHM*, **161(8)** (2016), 359–382.
25. Morak R., Braxmeier S., Ludescher L., Balzer C., Putz F., Busch S., Hüsing N., Reichenauer G., and Paris O., 'Quantifying adsorption-induced deformation of nanoporous materials on different length scales', *Journal of Applied Crystallography*, **50** (2017), 1404-1410.
26. Nabavi, S.S. and Hartmann M.A., 'Weak reversible cross links may decrease the strength of aligned fiber bundles'. *Soft Matter*, **12** (2017) 2047-2055.
27. Natalio F., Fuchs R., Cohen S. R., Leitus G., Fritz-Popovski G., Paris O., Kappl M., and Butt H.-J., 'Biological fabrication of cellulose fibers with tailored properties', *Science*, **357(6356)** (2017), 1118-1122.
28. Oswald J., and Römer R. A., 'Manifestation of many-body interactions in the integer quantum Hall effect regime', *Physical Review : B, Condensed Matter and Materials Physics*, **96(12)** (2017), 125128.
29. Oswald J., and Römer R. A., 'Exchange-mediated dynamic screening in the integer quantum Hall effect regime', *EPL*, **117(5)** (2017), 57009.
30. Paris O., Lang D., Li J., Schumacher P., Deluca M., Daniel R., Tkadletz M., Schalk N., Mitterer C., Todt J., Keckes J., Zhang Z., Fritz-Popovski G., Ganser C., Teichert C., and Clemens H., 'Complementary high spatial resolution methods in materials science and engineering', *Advanced Engineering Materials*, **19(4)** (2017), 1600671.
31. Prehal C., Koczwara C., Jäckel N., Amenitsch H., Presser V., and Paris O., 'A carbon nanopore model to quantify structure and kinetics of ion electrosorption with in situ small-angle X-ray scattering', *Physical Chemistry, Chemical Physics : PCCP*, **19** (2017), 15549-15561.
32. Prehal C., Koczwara C., Jäckel N., Schreiber A., Burian M., Amenitsch H., Hartmann M. A., Presser V., and Paris O., 'Quantification of ion confinement and desolvation in nanoporous carbon supercapacitors with modelling and in situ X-ray scattering', *Nature Energy*, **2** (2017), 16215.
33. Prinz J., Matković A., Pešić J., Gajic R., and Bald I., 'Hybrid Structures for Surface-Enhanced Raman Scattering: DNA Origami/Gold Nanoparticle Dimer/Graphene', *Small*, **12(39)** (2016), 1-10.
34. Putz F., Morak R., Elsässer M. S., Balzer C., Braxmeier S., Bernardi J., Paris O., Reichenauer G., and Hüsing N., 'Setting directions: Anisotropy in hierarchically organized porous silica', *Chemistry of Materials*, **29** (2017), 7969-7975.

35. Reisinger M., Tomberger M., Zechner J., Daumiller I., Sartory B., Ecker W., Keckes J., Lechner R. T., 'Resolving alternating stress gradients and dislocation densities across $\text{Al}_x\text{Ga}_{1-x}\text{N}$ multilayer structures on Si(111)', *Applied Physics Letters*, **111(16)** (2017), 162103.
36. Roemhild K., Niemz F., Mohan T., Hribernik S., Kurecic M., Ganser C., Teichert C., and Spirk S., 'The Cellulose Source Matters—Hollow Semi Spheres or Fibers by Needleless Electrospinning', *Macromolecular Materials and Engineering*, **301(1)** (2016), 42-47.
37. Samusjew A., Kratzer M., Moser A., Teichert C., Krawczyk K., and Grießer T., 'Inkjet Printing of Soft, Stretchable Optical Waveguides through the Photopolymerization of High-Profile Linear Patterns', *ACS Applied Materials & Interfaces*, **9** (2017), 4941–4947.
38. Schrödl N., Bucher E., Gspan C., Egger A., Ganser C., Teichert C., Hofer F., and Sitte W., 'Phase decomposition in the chromium- and silicon-poisoned IT-SOFC cathode materials $\text{La}_{0.6}\text{Sr}_{0.4}\text{CoO}_{3-\delta}$ and $\text{La}_2\text{NiO}_{4+\delta}$ ', *Solid State Ionics*, **288** (2016), 14-21.
39. Schrödl N., Bucher E., Gspan C., Egger A., Ganser C., Teichert C., Hofer F., Sitte W., 'Phase decomposition in the chromium- and silicon-poisoned IT-SOFC cathode materials $\text{La}_{0.6}\text{Sr}_{0.4}\text{CoO}_{3-\delta}$ and $\text{La}_2\text{NiO}_{4+\delta}$ ', *Solid State Ionics*, **288** (2016) 14-21.
40. Sytnykt M., Yakunin S., Schöffberger W., Lechner R. T., Burian M., Ludescher L., Killilea N. A., YousefiAmin A., Kriegner D., Stangl J., Groiss H., and Heiss W., 'Quasi-epitaxial Metal-Halide Perovskite Ligand Shells on PbS Nanocrystals', *ACS nano*, **11(2)** (2017), 1246-1256.
41. Szajna K., Kratzer M., Wrana D., Mennucci C., Jany B. R., Buatier de Mongeot F., Teichert C., and Krok F., 'Influence of $\text{TiO}_2(110)$ surface roughness on growth and stability of thin organic films', *Journal of Chemical Physics*, **145** (2016), 144703.
42. Toifl M., Hartlieb P., Meisels R., Antretter T., Kuchar F., 'Numerical study of the influence of irradiation parameters on the microwave-induced stresses in granite', *Minerals Engineering*, **103-104** (2017), 78-92.
43. Toifl M., Meisels R., Hartlieb P., Kuchar F., and Antretter T., '3D numerical study on microwave induced stresses in inhomogeneous hard rocks', *Minerals Engineering*, **90** (2016), 29-42.
44. Van Opdenbosch D., Fritz-Popovski G., Planck J., Zollfrank C., and Paris O., 'Passive and active mechanical properties of biotemplated ceramics revisited', *Bioinspiration & Biomimetics*, **11** (2016), 065001.
45. Van Opdenbosch D., Fritz-Popovski G., Wagermaier W., Paris O., and Zollfrank C., 'Moisture-driven ceramic bilayer actuators from a biotemplating approach', *Advanced Materials*, **28** (2016), 5235-5240.
46. Vasić B., Matkovic A., and Gajić R., 'Phase imaging and nanoscale energy dissipation of supported graphene using amplitude modulation atomic force microscopy', *Nanotechnology*, **28** (2017), 1-14.
47. Vasić B., Matković A., Gajić R., and Stanković I., 'Wear properties of graphene edges probed by atomic force microscopy based lateral manipulation', *Carbon*, **107** (2017), 723-732.
48. Vasić B., Matković A., Ralević U., Belić M., and Gajić R., 'Nanoscale wear of graphene and wear protection by graphene', *Carbon*, **120** (2017), 137-144.
49. Yarema M., Xing Y., Lechner R. T., Ludescher L., Dordevic N., Lin W. M. M., Yarema O., and Wood V., 'Mapping the Atomistic Structure of Graded Core/Shell Colloidal Nanocrystals', *Scientific Reports*, **7(1)** (2017), 11718.
50. Zhang Y., De Falco P., Wang Y., Barbierie E., Paris O., Teririll N. J., Falkenberg G., Pugno N. M., and Gupta H.S., 'Towards in situ determination of 3D strain and reorientation in interpenetrating nanofibre composites', *Nanoscale*, **9** (2017), 11249-11260.
51. Zhang Y., Paris O., Terril N., and Gupta H. S., 'Uncovering three-dimensional gradients in fibrillar orientation in an impact-resistant biological armour', *Scientific Reports*, **6** (2016), 26249.

3.2 SCI listed Books and book contributions

1. Ganser C. and Teichert C., AFM based nanoindentation of cellulosic fibers', Tiwari A. and Natarajan S., Eds. in 'Applied Nanoindentation of Advanced Materials', Chichester: Wiley-VCH., p. 247-267, 2017.
2. Paris O. and Peterlik H., 'Single Carbon Fibres: Structure from X-ray Diffraction and Nanomechanical Properties', Paris O., Ed. in 'Structure and Multiscale Mechanics of Carbon Nanomaterials'. CISM Courses and Lectures, Springer Wien-Heidelberg-New York-Dordrecht-London p. 1-28, 2016.

3. Hartmann M., Todt M. and Rammerstorfer F.G., 'Atomistic and continuum modelling of graphene and graphene-derived carbon nanostructures', Paris O., Ed. in 'Structure and Multiscale Mechanics of Carbon Nanomaterials'. CISM Courses and Lectures, Springer Wien-Heidelberg-New York-Dordrecht-London p. 135-179, 2016.

3.3 Edited Books

1. Paris O., Editor, 'Structure and Multiscale Mechanics of Carbon Nanomaterials' CISM Courses and Lectures, Springer Wien-Heidelberg-New York-Dordrecht-London, 2016.

3.4 SCI listed conference proceedings

1. Czibula C., Ganser C., Kratzer M., Schennach R., Friedel B., and Teichert C., 'Exploring Paper/AgNW based composites for photovoltaic devices by atomic force microscopy methods' in 'Progress in Paper Physics Seminar 2016 Conference Proceedings', 2016, p. 213-216.
2. Czibula C., Ganser C., Kratzer M., Brumbauer F., Kräuter M., Shanmugam K., Batchelor W., Penn M., Ebner M., Pramstrahler M., Pilat F., Chien H.-T., Schennach R., Friedel B., and Teichert C., 'Silver Nanowires: A versatile tool for conductive paper', Söderberg D. and Batchelor W. Eds. in 'Advances in Pulp and Paper Research', Oxford, vol 2. Oxford 2017, p. 723-737.
3. Czibula C., Ganser C., Tscharnuter D., Schöberl T., Teichert C., and Hirn U., 'Investigating the transversal viscoelastic properties of paper fibers by Atomic Force Microscopy', Kazakov Y. Ed. in 'Proceedings 4th International Conference in memory of Professor Valery Komarov', Arkhangelsk 2017, p. 74-79.
4. Kasper E. and Teichert C., 'Ion assisted epitaxy: Methods, effects and applications' in 'Proceedings of the International Conference on Integrated innovative development of the Zarafshan region: Achievements, challenges and prospects' (IDZ). Navoi, Uzbekistan, 2017, p. 221-223.
5. Kozic D., Konetschnik R., Maier-Kiener V., Schönggrundner R., Brunner R., Kiener D., Antretter T., and Gänser H.-P., 'Fracture and Material Behavior of Thin Film composites' in '17th International Conference on Thermal, Mechanical and Multi-Physics Simulation and Experiments in Microelectronics and Microsystems (EuroSimE)', IEEE. 2016, p. 1-6.
6. Teichert C., Genser J., Matkovic A., Kratzer M., Gajic R., Léoni T., Siri O., Becker C., Lüftner D., and Puschnig P., 'Ordering of crystalline organic nanostructures on two-dimensional materials' in 'Book of Abstracts "Nanoscale Pattern Formation at Surfaces"', Helsinki, June 26-28 2017. p. 36-37.
7. Toifl M., Hartlieb P., Meisels R., Antretter T., and Kuchar F., 'Numerical study of the influence of irradiation parameters on the microwave-induced stresses in granite for industrial applications' in 'Comminution '16 – Proceedings', 2016.

3.5 Other publications

1. Morak R., Braxmeier S., Balzer C., Ludescher L., Putz F., Busch S., Hüsing N., Reichenauer G. and Paris O. 'Adsorption-induced deformation of silica monoliths with hierarchical porosity', Scientific Report in MLZ Annual Report 2017.
2. Oswald J., 'Linking Non-equilibrium Transport with the Many Particle Fermi Sea in the Quantum Hall Regime', Book chapter in 'Research Advances in Quantum Dynamics', p.131-163, INTECH, Rijeka, 2016.
3. Paris O. 'Hybride Superkondensatoren durch innovative Materialkonzepte'. Science Brunch Grundlagenforschung: Photovoltaik + Speichermaterialien, Klima und Energiefonds, Wien, 2017.
4. Prehal C., Koczwarra C., Jäckel N., Schreiber A., Burian M., Amenitsch H., Hartmann M. A., Presser V., and Paris O., 'Combining modeling and in situ X-ray scattering to quantify confinement and desolvation in nanoporous carbon supercapacitors' in ELETTRA Highlights. 2017.
5. Teichert C., 'Heteromolecular phases: Opposite interaction matters'. *Nature Materials*. **16(6)** (2017), 604-606.

4. Presentations

4.1 Talks at conferences

1. Czibula C., Ganser C., Hirn U., and Teichert C., 'AFM based dynamic mechanical analysis of viscoelastic properties of cellulose fibers', ÖPG Jahrestagung, Wien 26.-29.09.2016.
2. Czibula C. M., Ganser, C., Teichert, C, Hirn U., 'Using atomic force microscopy to investigate the transversal viscoelastic properties of paper fibers', Paper & Biorefinery 2017, Graz, 31.05.-01.06.2017.
3. Fritz-Popovski, G., Morak, R., Sharifi, P., Amenitsch, H., and Paris, O. 'Pore Shape Determination in Mesoporous Ordered Silica Films', ECM-30, Basel 28.08.-01.09.2016.
4. Ganser C., Czibula C., Hirn U., Teichert C., 'Humidity dependent mechanical properties of cellulose materials investigated by atomic force microscopy', EPNOE, Sophia-Antipolis, 13.-14.10.2016.
5. Ganser C., Czibula C., Manhart J., Radl S., Schlögl S., Hirn U., and Teichert C., 'Measurements of viscoelasticity and adhesion force of polymer materials with large radius AFM tips', ÖPG Jahrestagung, Wien 26.-29.09.2016.
6. Koczwar, C., Prehal, C., Rumswinkel, S., Jäckel, N., Elsässer, M. S., Amenitsch, H., Hartmann, M. A., Hüsing, N., Presser, V., and Paris, O., 'In situ small angle X-ray scattering as a novel tool to study ion electrosorption in supercapacitor electrodes', ISEE CAP 2017: 5th International Symposium on Enhanced Electrochemical Capacitors, Jena, Germany, 10.-14.07.2017.
7. Koczwar, C., Prehal, C., Rumswinkel, S., Jäckel, N., Burian, M., Elsässer, M. S., Amenitsch, H., Hüsing, N., Presser, V., and Paris, O., 'Ion electrosorption in supercapacitor electrodes studied by in-situ small-angle X-ray scattering', NESY Winterschool & Symposium 2017: 10th European NESY Winterschool & Symposium on Neutron and Synchrotron Radiation, Altaussee, Austria, 06.-10.03.2017.
8. Koczwar, C., Prehal, C., Rumswinkel, S., Jäckel, N., Elsässer, M. S., Amenitsch, H., Hüsing, N., Presser, V., and Paris, O., 'Electrode swelling during ion electrosorption in carbon based supercapacitors', Gemeinsame Jahrestagung von SPG und ÖPG, Geneva, Switzerland, 21.-25.08.2017.
9. Kratzer, M. 'Organic thin film growth on graphene and other 2D materials.' Energy Materials Nanotechnology (EMN) Meeting, Dubrovnik, Croatia, 4.-7-5-2016 (**invited**)
10. Kratzer, M. Lasnik, M., Bombieri, F., Röhrig, S., Deluca, M., and Teichert, C., 'Analysing the orientation distribution function of ferroelectric domains using Vector Piezo Response Force Microscopy'. DPG Spring Meeting 2017, Dresden, Germany, 19.-24.3.2017.
11. Kratzer, M., Dimitriev, O. P., Grynko, D.O., Fedoryak, A.M., Doroshenko, T. P., Teichert, C., Balaz, P., Tesinsky, M., and Hegedus, M., 'AFM based characterization of Ketserite n-type semiconductor powder bulk heterojunctions'. EMRS 2017 Fall Meeting, Warsaw, Poland, 18.-21-09.2017.
12. Kratzer, M., Klima, S., Matkovic, A., Genser, J., and Teichert, C. 'Graphene and other 2D materials as substrates for organic thin film growth'. Joint Vacuum Confernece (JVC 15) Portoroz, Slovenia, 6.-10.6.2016.
13. Kratzer, M., Matkovic, A., Genser, J., Lüftner, D., Puschnig, P., Gajic, R., and Teichert, C., 'Epitaxial growth of organic crystal networks on ultra-thin hexagonal boron nitride'. ECOS 33, Szeged, Hungary, 27.08.-01.09.2017.
14. Kuchar F., and Meisels R., 'Bragg meets Moore: Photonic Crystals for the Extreme Ultraviolet'. 62th Metallkunde-Kolloquium, Lech am Arlberg, Austria, 11.-13.04.2016.
15. Lechner, R.T., Ludescher, L., Fritz-Popovski, G., Dirin, D., Kovalenko, M.V., and Paris O. 'Core/Shell Structure of Spherical and Non-Spherical Nanocrystals revealed by anomalous SAXS and WAXS', Nanoscience with Nanocrystals NaNaX 7, Marburg, Germany, 4.-8.4. 2016
16. Lechner, R.T., 'Shape, Chemical and Crystalline Structure of Nanocrystals and their Impact on the Supercrystal Structure of Colloidal Superlattices' 30th Meeting of the European Crystallographic Association: ECM-30, Basel, Switzerland, 28.8.-1.9. 2016 (**invited**)
17. Lechner, R.T., NESY for Energy: Neutron and Synchrotron Radiation Characterisation of Nanostructures for Energy Materials, invited talk, NESY Symposium: Future Possible Use of Neutron and Synchrotron Sources by the Austrian User Community, Graz, Austria, 15.-16.9. 2016 (**invited**)

18. Lechner, R.T., 'Colloidal Crystallization Studied by In-situ Synchrotron SAXS and Computer Simulations', 66. Jahrestagung der Österreichischen Physikalischen Gesellschaft ÖPG 2016, Wien, Austria 27.-29.9. 2016 **(invited)**.
19. Lechner, R.T., Burian, M., Karner, C., Amenitsch, H., Yarema, M., Heiss W., and Delago, C. 'Revealing 3D Colloidal Supercrystal Growth Conditions by combining in-situ Synchrotron SAXS and MC-simulations', NaNaX 8, Braga, Portugal, 3.-7.7. 2017.
20. Ludescher L., Putz F., Elsässer M. S., Morak R., Balzer C., Hüsing N., Reichenauer G., and Paris O., 'Investigation of local pore structure and sorption induced deformation in hierarchical mesoporous silica by nanobeam x-ray diffraction', InterPore, Cincinnati, Ohio, USA, 09.-12.05.2016.
21. Matković A., Kratzer M., Genser J., Kaufmann B., Vujin J., Gajic R., and Teichert C., 'Thin Film Growth of Organic Rod-Like Conjugated Molecules on 2D Materials', NanoFIS, Graz, Austria, 27.-29.06.2016.
22. Matković A., Kratzer M., Genser J., Kaufmann B., Vujin J., Gajic R., and Teichert C., 'Early Stage Growth of Organic Rod-Like Conjugated Molecules on 2D Materials', NanoSEA2016, Taormina, Italy, 03.-08.07.2016.
23. Matković A., Kratzer M., Genser J., Kaufmann B., Vujin J., Vasić B., Gajic R., and Teichert C., 'Epitaxy of Highly Ordered Conjugated Organic Semiconductor Crystallite Networks on Graphene Based Devices', ICSFS18, Dresden, Germany, 28.08.-02.09.2016.
24. Matković A., Kratzer M., Genser J., Kaufmann B., Vujin J., Vasić B., Gajic R., and Teichert C., 'Gated Growth of Organic Rod-Like Conjugated Molecules on Graphene and Hexagonal Boron Nitride Based Devices', ÖPG, Vienna, Austria 27.-29.09.2016.
25. Meisels, R., 'Investigation of complex photonic structures in the extreme ultraviolet', Gemeinsame Jahrestagung von SPG und ÖPG, Geneva, Switzerland, 21.-25.08.2017.
26. Meisels, R., and Kuchar, F., 'Numerical Studies on the Application of Photonic Crystals for EUV mirrors', ÖPG Jahrestagung, Vienna, 27.-29.08.2016.
27. Morak R., Paris O., Balzer C., Waag A., Reichenauer G., Putz F., Elsässer M. S., and Hüsing N., 'Sorption-Induced Deformation of Silica Monoliths with Hierarchical and Anisotropic Porosity', 40th International Conference and Expo on Advanced Ceramics and Composites, Daytona Beach, USA, 24.-29.01.2016.
28. Oswald J., 'Probing condensed many particle quantum states in the quantum Hall effect regime', EMN MEETING ON QUANTUM 2016: Energy, Materials and Nanotechnology, 8/04/16 - 11/04/16, Phuket, Thailand **(invited)**.
29. Oswald J., 'Manifestation of many-body interactions in the integer quantum Hall effect', 66. Jahrestagung der Österreichischen Physikalischen Gesellschaft, 27.9.2016-29.8.2016, Wien.
30. Oswald J., 'The role of many particle interactions in the integer quantum Hall effect regime', Joint Annual Meeting of SPS and ÖPG, 21-25 August 2017 in Geneva.
31. Oswald J., 'Many particle interactions in the integer quantum Hall effect regime', 2nd International Conference on Quantum Physics and Quantum Technology, Sept 25-26 2017 Berlin, Germany **(invited)**.
32. Paris O., 'Watching ions in supercapacitors at work by in-situ X-ray scattering', *CESEP 17 7th International Conference on Carbon for Energy Storage and Environmental Protection*, Lyon, France 23-26. October 2017 **(invited Keynote Lecture)**.
33. Paris O., 'In-situ small-angle X-ray scattering on nanoporous materials for energy applications', *Symposium D1 "Materials Science with Synchrotron Radiation X-rays" EUROMAT 2017*, Thessaloniki, Greece, 17 - 22 September, 2017 **(Plenary Lecture)**.
34. Paris O., 'In-operando X-ray scattering during charging/discharging of supercapacitors', 9th *NanoNet Austria Meeting*, Leoben Austria, 16.11.2016 **(invited)**.
35. Paris O., 'In-operando SAXS for energy applications', C. Prehal, C. Koczwara, R.T. Lechner, H. Amenitsch, V. Presser, *Symposium SAXS on Nanosystems: Current trends and perspectives; 20 Years of the Austrian SAXS beamline*, ICTP, Trieste, Italy 10.-12.10.2016 **(invited)**.
36. Prehal, C., Koczwara, C., Jäckel, N., Schreiber, A., Burian, M., Amenitsch, H., Hartmann, M. A., Presser, V., and Paris, O., 'Quantifying local ion rearrangement in nanoporous carbon supercapacitors using in-situ small angle X-ray scattering', 67th ISE Annual Meeting, The Hague, Netherlands, 21.-26.08.2016.
37. Teichert, C., 'Interfaces of organic semiconductor molecules with 2D materials', 3rd International Symposium on Surfaces and Interfaces of sustainable, advanced materials, SIPS 2017, Cancun, Mexico, 22. – 26.10.2017 **(Plenary Lecture)**.

38. Teichert, C., 'Organic crystalline nanoneedles on 2D materials and their optoelectronic properties', PHOTONICA 2017, Belgrade, Serbia, 28.08.-01.09., 2017 (**invited**).
39. Teichert, C., 'Facet analysis of crystalline nano- and microstructures by atomic force microscopy', 2017 International Workshop on Nanomaterials and Nanodevices, Xi'an, China, 07-09.07.2017 (**invited**).
40. Teichert, C., 'Organic nanodevices on van der Waals materials', 2017 International Workshop on Nanomaterials and Nanodevices, Beijing, China, 03-06.07.2017 (**Plenary Lecture**).
41. Teichert, C., 'Sensing cleanliness and defect structure of various graphene substrates with small organic molecules', 5th World Congress of Advanced Materials (WCAM-2016), Symposium on Graphite and Graphene, Chongqing, China, 06-08.06.2016 (**invited**).
42. Teichert, C., 'Advanced AFM based mechanical and electrical characterization of nanostructured materials in controlled environment', DPG-Frühjahrstagung, Regensburg, 06-11.03.2016 (**invited**).
43. Teichert, C., 'Exploring the potential of graphene as transparent electrode material for organic semiconductor devices', 3rd IEEE International Conference on Devices, Circuits and Systems – ICDCS'16, Coimbatore, India, 03-05.03.2016 (**Plenary Lecture**).
44. Toifl M., Hartlieb P., Meisels R., Antretter T., and Kuchar F., 'Numerical study of the influence of irradiation parameters on the microwave-induced stresses in granite for industrial applications', Comminution '16, Cape Town, South Africa, 11.-14.04.2016.

4.2 Invited talks at external institutions: Seminars

1. Kratzer, M., 'Organic thin film growth on 2D materials', Faculty of Physics, University of Vienna, Vienna, Austria 16.11.2016.
2. Kratzer, M., 'Growth of para-hexaphenyl on clean and modified TiO₂(110) surfaces', V. Lashkaryov Institute of semiconductor Physics, NASU, Kiev, Ukraine 20.12.2016.
3. Paris, O., 'When space becomes tight: molecules and ions in nanoconfinement', Anorganisch-Chemisches Kolloquium, Universität Hamburg, 06.02.2017.
4. Paris, O., 'Functionality through hierarchical structuring: from nature to materials science', Biologisches Kolloquium Freiburg, 24.10.2016.
5. Paris, O., 'Sorptions induced deformation of nanoporous materials: from basic experiments to potential applications', INM-Kolloquium, Institut für Neue Materialien, Saarbrücken, 13.07.2016.
6. Paris, O., 'Sorptions induced deformation of nanoporous materials: from basic experiments to potential applications', Seminaire LIPHY, Université Joseph Fourier, Grenoble 29.06.2016.
7. Paris, O., 'When space becomes tight: understanding and controlling fluid-solid interactions in nanopores', Physik Kolloquium, Institut für Halbleiter- und Festkörperphysik, JKU Linz, 23.06.2016.
8. Paris, O., 'Insights into the outstanding performance of biological and bioinspired materials by X-ray micro- and nanobeam diffraction', Seminar Series: Selected research topics in Biomedical Engineering; Department of Biomedical Engineering, Univ. Basel, 21.04.2016.
9. Teichert, C., 'Ion bombardment induced rippled substrates as templates for organic thin film growth', Seminar, Department of Physics, Sook-Myung Women's University, Seoul, Korea, 19.08.2016.
10. Teichert, C., 'Topographic and electrical nanometer structure characterization by atomic force microscopy and conductive AFM', Tutorial, Department of Physics, Sook-Myung Women's University, Seoul, Korea, 18.08.2016,
11. Teichert, C., 'Electrical and photoelectric characterization of semiconductor nanostructures using atomic-force microscopy based techniques', Seminar, State Key Laboratory of Solidification Processing, Northwestern Polytechnical University, Xi'an, PR China, 10.06.2016.
12. Teichert, C., 'Nanometer structure characterization by atomic force microscopy', Tutorial, Karunya University, Coimbatore, Tamil Nadu, India, 04.03.2016.
13. Teichert, C., 'Growth of rod-like organic molecules on 2D materials', Seminar, Institut für Festkörperphysik, TU Graz, 01.03.2017.
14. Teichert, C. 'Functionalizing 2D materials by organic molecules', Seminar, Institute of Ion Beam Physics and Materials Research, Helmholtz-Zentrum Dresden-Rossendorf, Germany, 02.05.2017.
15. Teichert, C. 'Organic semiconductor nanostructures on van der Waals materials', Kolloquium, Department of Physics, TU Chemnitz, Germany, 03.05.2017.

16. Teichert, C., '2D materials as substrates for organic thin films', Seminar, Fachgruppe Oberflächen- und Grenzflächenphysik, Institut für Physik, Martin-Luther-Universität Halle-Wittenberg, Germany, 04.05.2017.
17. Teichert, C., 'Topographic, electric, and photoelectric characterization of semiconductor nanostructures', Seminar, Institut für Angewandte Physik, Johannes-Kepler-Universität Linz, 22.05.2017.
18. Teichert, C., 'Facet analysis of crystalline nano- and microstructures by atomic force microscopy', 24.05.2017.
19. Teichert, C., 'Characterization of semiconductor nanostructures using atomic-force microscopy based techniques', Seminar, State Key Laboratory of Solidification Processing, Northwestern Polytechnical University, Xi'an, PR China, 10.07.2017.
20. Teichert, C., 'Exploring growth and electronic properties of organic nanostructures on two-dimensional materials', Seminar, University of Nova Gorica, Slovenia, 14.09.2017.
21. Teichert, C., 'Structure and properties of organic nanoneedles grown on van der Waals materials', Seminar aus Physikalischer und Theoretischer Chemie, Institut für Chemie, Karl Franzens Universität Graz, 06.10.2017.
22. Teichert, C., 'Advanced AFM based electrical characterization on the nanometer scale', Seminar, Institute of Applied Physics, Abbe Center of Photonics Friedrich-Schiller-Universität Jena, Germany, 13.11.2017.
23. Teichert, C., 'Structure and properties of crystalline organic nanoneedles grown on two-dimensional materials', Seminar, Institute of Physics, Jagiellonian University, Krakow, Poland, 28.11.2017.

4.3 Posters

1. Fritz-Popovski, G., Morak, R., Sharifi, P., Amenitsch, H., and Paris, O. 'Pore Shape and Lattice Deformation in Mesoporous Films', Workshop "Future Possible Use of Neutron and Synchrotron Sources by the Austrian User Community", Graz, 15.09.-16.09.2016.
2. Ganser C., Czibula C., Tscharnutter D., Teichert C., and Hirn U. 'A combination of a viscoelastic material model with contact mechanics to study cellulosic materials with AFM', Linz Winterworkshop 03.-06.02.2017.
3. Genser J., Matkovic A., Lüftner D., Kratzer M., Gajic R., Puschnig P., and Teichert C. 'Epitaxy of Highly Ordered Conjugated Organic Semiconductors Supported by Hexagonal Boron Nitride', 66. Jahrestagung der Österreichischen Physikalischen Gesellschaft, Vienna, Austria, 27.-29.09.2016.
4. Genser J., Matkovic A., Lüftner D., Kratzer M., Siri O., Puschnig P., Becker C., and Teichert C. 'Epitaxy of highly ordered conjugated organic semiconductors supported by hexagonal boron nitride', 16th IUVESTA School on Nanophysics, Devet Skal 2017, Devet Skal, Czech Republic, 12.-16.06.2017.
5. Koczwaro C., Prehal C., Rumswinkel S., Elsässer M. S., Amenitsch H., Hüsing N., and Paris O., 'Ion electrosorption in hierarchically ordered carbon studied by in-situ small angle X-ray scattering', Nanosystems: Current trends and perspectives, 20 years of the Austrian SAXS beamline., Trieste, Italy, 10.-12.10.2016.
6. Lechner R.T., Prehal C., Koczwaro C., Popovski G., and Paris O., 'Characterisation of Nanostructures for Supercapacitors, Batteries and Solar Cells using advanced Synchrotron Scattering Techniques', BESSY II Foresight Workshop on Energy Materials Research, Berlin, Germany, 10.-11.10. 2016.
7. Meisels R., and Kuchar F., 'Photonic Crystals for the Extreme Ultraviolet', Mauterndorf Winterschool 2016, Mauterndorf, Austria, 21.-26.02.2016.
8. Morak R., Ludescher L., Paris O., Hüsing N., Putz F., Braxmeier S., Waag A., Balzer C., Reichenauer G., Busch S., and Heinemann A., 'Simultaneous measurement of macroscopic strain and mesopore deformation of silicas with hierarchical porosity', InterPore, Cincinnati, Ohio, USA, 09.-12.05.2016.
9. Oswald J., 'Towards an all-inclusive numerical model for the integer quantum Hall effect regime', 19th International Winterschool: New Developments in Solid State Physics, Mauterndorf, Austria, 21- 26.02.2016.

10. Prehal C., Koczwara C., Amenitsch H., Rumswinkel S., Hüsing N., Hartmann M. A., Presser V., and Paris O., 'In-operando SAXS as a novel method to understand ion electrosorption in confined geometry', NESY Symposium, Graz, Austria, 15-16.09.2016.
11. Prehal C., Koczwara C., Jäckel N., Amenitsch H., Hartmann M. A., Presser V., and Paris O., 'Combining in situ small angle X-ray scattering and atomistic modelling to study ion charge storage in nanoporous carbon supercapacitors', SAXS Excites, Graz, Austria 26.09.2017.
12. Prehal C., Koczwara C., Jäckel N., Amenitsch H., Presser V., and Paris O. 'Structure and kinetics of ions in nanoporous carbon supercapacitors studied by in situ X-ray scattering and atomistic modelling', XXVI International Materials Research Congress in Cancún, México, 20.-25.08.2017.
13. Prehal C., Koczwara C., Lechner R., Jäckel N., Amenitsch H., Presser V., and Paris O. 'In situ monitoring of nanomaterials for energy storage', Evaluierung Werkstoffwissenschaft, Leoben, Austria, 08.06.2017.
14. Samusjew A., Krawczyk K., Kratzer M., and Grießer T., 'Inkjet Printing of Elastomeric Optical Waveguides', Printing for Fabrication 2016: Materials, Applications, and Processes, The 32nd International Conference on Digital Printing Technologies, Manchester, UK, 12.-16.09. 2016.
15. Simon K., Manhart J., Ayalur-Karunakaran S., Moser A., Ganser C., Oesterreicher A., Pinter G., Teichert C., Kern W., Grießer T., and Schlögl S., 'Photoreversible Crosslinking of Elastomeric Materials Comprising Spatially Resolved Switchable Characteristics', 4th European Symposium of Photopolymer Science (ESPS), Leipzig, Germany, 11.-14.09.2016.
16. Simone R., Grießer T., Edler M., Kern W., Rath T., Trimmel G., Pavitschitz A., Teichert C., Simbrunner C., Schwabegger G., and Sitter H. 'A Novel UV Tunable and Patternable Polyaniline Derivate as a Charge Injection Layer in OLEDs', 4th European Symposium of Photopolymer Science (ESPS), Leipzig, Germany, 11.-14.09.2016.
17. Teichert C., 'Organic semiconductor nanostructure devices on two-dimensional materials', 7th Bonn Humboldt Award Winners' Forum "Fundamental Concepts and Principles of Chemical Energy Conversion", Bonn, Germany, 11.-13.10.2017.
18. Teichert C., Genser J., Matkovic A., Kratzer M., Gajic R., Siri O., Becker C., Lüftner D., and Puschnig P., 'Growth of polar molecules on ultrathin hexagonal boron nitride', Gemeinsame Jahrestagung von SPG und ÖPG 2017, Geneva, Switzerland, 21.-25.08.2017.

4.4 Awards

- **Ganser, Christian:** Research award for a two years stay in Japan by the Japanese Society for the Promotion of Science (JSPS), 2017.
- **Genser, Jakob:** Poster Prize at the 66th Annual Meeting of the Austrian Physical Society 2016 for his work on 'Epitaxy of highly ordered conjugated semiconductor molecules supported by hexagonal boron nitride', 27. - 29.9.2016.
- **Ludescher, Lukas:** Marshall Plan Scholarship for a three month stay at the New Jersey Institute of Technology 2017.
- **Matković, Aleksandar:** Lise-Meitner-award by the Austrian Science fund, 2017.
- **Prehal, Christian:** Award of Excellence of the Bundesministeriums für Wissenschaft, Forschung und Wirtschaft für ausgezeichnete Dissertationen
- **Prehal, Christian:** Fonda-Fasella 2017 Award for his work on "Ion charge storage in supercapacitor nanopores quantified by modeling and in situ SAXS" done at Elettra Sincrotrone Trieste.
- **Prehal, Christian:** Christian Doppler Preis des Landes Salzburg for technical sciences and physics, 2017.

5. Research Projects

5.1 §26 – Projects (FWF-Projects)

Project: Deformation of hierarchical and anisotropic porous solids by fluid adsorption
Funded by: FWF (I1605-N20)
Start: 2 June 2014
Duration: 30 June 2018
Project leader: O. Paris
Co-Applicant: N. Hüsing - FB Chemie und Physik der Materialien, Paris-LodronUniversität Salzburg
Internat.Partner: G. Reichenauer – Center for Applied Energy Research, Würzburg (DE)
Coworker(s): C. Prehal, L. Ludescher, R. Morak
Funding: € 175.000,-- (Institute of Physics)

Project: Growth of polar organic moecules on graphene and saphire
Funded by: FWF (I 1788-N20 FWF-ANR bilateral project)
Start: 1 Dec. 2014
Duration: 31 Dec, 2018
Project leader: C. Teichert
Co-Applicant: C. Becker, CNRS + University Aix-Marseille, France
Coworker(s): M. Kratzer, A. Matkovic, B. Kaufmann, J. Genser
Funding: € 275.000,--

Project: Tuning ordering of organic nanostructures on 2D materials
Funded by: FWF (M 2323-N36) Lise Meitner-Programms
Start: 1. Jan. 2018
Duration: 31 Dec. 2019
Project leader: A. Matkovic
Co-Applicant: C.Teichert
Funding: € 153.340,--

Project: Microwave-induced modifications of thermal and mechanical properties of rocks and their consequences for rock fragmentation
Funded by: FWF (TRP 284-N30 Translational-Research-Program)
Start: 1 April, 2013
Duration: 31 March, 2016
Project leader: T. Antretter (Institut für Mechanik)
Co-Applicant: F. Kuchar, R. Meisels
Funding: € 70.000,-- (inkl. 20% Overhead)

Project: Bridging length scales to analyse and enhance the performance of piezoceramics for commercial actuators
Funded by: FWF(TRP 302-N20)
Start: 1.9. 2013
Duration: 31 Aug 2016
Project leader: M. Deluca (MCL Leoben)
Co-Applicant: C.Teichert
Coworker(s): M. Kratzer, M. Lasnik
Funding: € 27.500,--

5.2 §27 – Projects (FFG, EU,...)

Project:	Hybride Superkondensatoren durch innovative Materialkonzepte Programm: Energieforschung (e!MISSION)
<i>Funded by</i>	Österreichischer Klima- und Energiefonds, FFG Projekt 848808
<i>Start</i>	1. June 2015
<i>Duration</i>	30. Sept. 2018
<i>Project leader</i>	O. Paris
<i>Project partner</i>	N. Hüsing, - FB Chemie und Physik der Materialien, Paris-LodronUniversität Salzburg
<i>Coworker(s)</i>	C. Prehal, C. Koczwarra, H. Schönmaier, S. Stock, L. Hammerschmid
<i>Funding:</i>	€ 336.242,-- (Institute of Physics)
Project:	In-situ SAXS/GISAXS of solid-gas interactions in nanoporous materials and at nanostructured surfaces
<i>Funded by:</i>	COMET K2 MPPE: Projekt A2.19
<i>Start:</i>	01 Oct 2014
<i>Duration:</i>	July 2016
<i>Project leader:</i>	O. Paris
<i>Project partner(s)</i>	Materials Center Leoben Forschung GmbH Bruker AXS Analytical X-ray Systems GmbH Montanuniversität Leoben, Lehrstuhl für Materialphysik,
<i>Coworker(s):</i>	R. Morak, G. Popovski, C. Prehal
<i>Funding:</i>	Ca. € 257.189,-- (Institute of Physics)
Project:	Innovative microstructural design of low voltage varistors
<i>Funded by</i>	COMET K2 MPPE: Project A7.22
<i>Start:</i>	01 July 2017
<i>Duration:</i>	Sept. 2020
<i>Project leader:</i>	P. Supancic (Institut für Struktur- und Funktionskeramik)
<i>Project partner(s)</i>	EPCOS OHG, Deutschlandsberg (EPCOS) Montanuniversität Leoben, Institut für Struktur- und Funktionskeramik (ISFK) Montanuniversität Leoben, Institut für Physik (IP) Materials Center Leoben Forschung GmbH (MCL)
<i>Coworker(s):</i>	C. Teichert, M. Kratzer
<i>Funding:</i>	€ 23.245,81

5.3 Participation in CD Laboratories

Project:	CD Labor Faserquellung (Fiber Swelling)
<i>Funded by:</i>	Christian Doppler Gesellschaft
<i>Start:</i>	1. Dec. 2015
<i>Duration:</i>	Maximum 7 years
<i>Project leader:</i>	U. Hirn, TU Graz
<i>Co-Project leader</i>	C. Teichert
<i>Coworker(s):</i>	C. Ganser, C. Czibula, L. Weninger
<i>Funding:</i>	€ 150.000,--

5.4 Other Projects

- Project:** **Nanometer scale electrical investigation of silicon materials for solar energy conversion**
Funded by: ÖAD/ Wissenschaftlich-Technisches Abkommen mit Tschechien, 2014-2015 (Cz Sp 04/2014)
Start: 1 March 2014
Duration: until 29 Feb 2016
Project leader: C. Teichert
Co-Applicant: A. Fejfar, Institute of Physics, Czech Academy of Sciences, Prague, Czech Republic
Coworker(s): M. Kratzer, C. Czibula, J. Genser, K. Gradwohl., L. Kormos
Funding: € 5.388,--
- Project:** **Two-dimensional materials as templates for the growth of organic semiconductors**
Funded by: ÖAD/ Wissenschaftlich-Technisches Abkommen mit Serbien, 2016-2017 (SRB 09/2016)
Start: Jan 1 2016
Duration: until Dec 31 2017
Project leader: C. Teichert
Co-Applicant: B. Vasic, Institute of Physics, University of Belgrade, Serbien
Coworker(s): M. Kratzer, C. Czibula, J. Genser, K. Gradwohl, B. Kaufmann, A. Matkovic
Funding: € 6.930,--
- Project:** **Untersuchung der Alterung organischer Dünnschichten auf SiO₂,TiO₂ und Graphen auf der Nanometerskala**
Funded by: ÖAD/ Wissenschaftlich-Technisches Abkommen mit Polen, 2014-2015 (PL 05/2014)
Start: 1 Apr 2014
Duration: until 31 Mar 2016
Project leader: M. Kratzer
Co-Applicant: F. Krok, Institute of Physics, Jagiellonian University, Krakow, Poland
Coworker(s): J. Genser, S. Klima, C. Czibula, C. Teichert
Funding: € 5.231,--
- Project:** **Nanodraht-Einkristall basierte organisch-inorganische Heterokontakte für Photovoltaik- und Sensorikanwendungen**
Funded by: ÖAD/ Wissenschaftlich-Technisches Abkommen mit der Ukraine, 2015-2016 (UA 07/2015)
Start: 1 Jan 2015
Duration: until 31 Dec 2016
Project leader: M. Kratzer
Co-Applicant: D. Grynko, V. Lashkaryov Institute of Semiconductor Physics, Kiev, Ukraine
Coworker(s): M. Mirkowska, S. Klima, C. Czibula, C. Teichert
Funding: € 8.000,--
- Project:** **Growth and characterization of ZnTe-based crystals for terahertz emitters and sensors**
Funded by: ÖAD/ Wissenschaftlich-Technisches Abkommen mit der PR China, 2016-2018 (CN 02/2016)
Start: 1 Sept 2016
Duration: until 30 Nov 2018
Project leader: C. Teichert
Co-Applicant: Y. Xu, Northwestern Polytechnical University, PR China
Coworker(s): K. Gradwohl, M. Kratzer A. Matkovic
Funding: € 9.910,--

5.5 Funded experiments at large scale facilities

In addition to funded projects by national and international research grants, the Institute of Physics was again very successful in acquiring measurement time for experimental work at large scale facilities for synchrotron radiation and neutrons. The allocation of measurement time requires submitting proposals for the planned experiments, which are then reviewed by international panels and beamtime is granted on the basis of scientific excellence. Within the reporting period, we were able to get 11 beamtimes and a total of 56 days of beamtime were granted to the Institute of Physics in the past two years.

2016

Main proposer	Co Proposer(s)	Proposal Title	Facility	Days
Christian PREHAL	Koczwara, Paris (<i>Physics, MUL</i>), Rumswinkel, Hüsing (<i>Univ. Salzburg</i>), Krüner, Schreiber, Presser (<i>INM Saarbrücken</i>)	In-situ SAXS Studies of Electrical Double-Layer Capacitors: the Role of the electrolyte concentration	SAXS ELETTRA Trieste	5
Christian KOCZWARA	Prehal, Paris (<i>Physics, MUL</i>), Rumswinkel, Hüsing (<i>Univ. Salzburg</i>), Presser, (<i>INM Saarbrücken</i>)	In-operando SAXS Studies on Hybrid Supercapacitors: the role of the negatively polarized electrode	SAXS ELETTRA Trieste	5
Gudrun REICHENAUER (<i>ZAE Bayern</i>)	Morak, Ludescher, Paris (<i>Physics MUL</i>), Scherdel (<i>ZAE Bayern</i>)	Sorption induced deformation of monolithic silica with hierarchical porosity: a combined USANS and dilatometric study	SANS MLZ Munich	4
Gudrun REICHENAUER (<i>ZAE Bayern</i>)	Morak, Ludescher, Paris (<i>Physics MUL</i>), Braxmeier (<i>ZAE Bayern</i>)	Sorption induced deformation of monolithic silica with hierarchical porosity: a combined SANS and dilatometric study	SANS MLZ Munich	6
				20

2017

Christian PREHAL	Prehal, Paris (<i>Physics, MUL</i>), Presser, (<i>INM Saarbrücken</i>), Rumswinkel, Hüsing (<i>Univ. Salzburg</i>)	In situ anomalous SAXS/WAXS study on nanoporous carbon supercapacitors	ID02 ESRF Grenoble	2
Dirk MÜTER (<i>Univ. Kopenhagen</i>)	Ludescher, Paris (<i>Physics, MUL</i>), Hüsing (<i>Univ. Salzburg</i>), Reichenauer, Balzer (<i>ZAE Bayern</i>), Soerensen (<i>Univ. Kopenhagen</i>)	Nanotomography of hierarchically organized porous silica monoliths: a necessary step towards quantification of sorption induced deformation at all scales	ID16NI ESRF Grenoble	2
Christian KOCZWARA	Prehal, Paris (<i>Physics, MUL</i>), Presser, (<i>INM Saarbrücken</i>), Rumswinkel, Hüsing (<i>Univ. Salzburg</i>)	In-operando SAXS Studies on Supercapacitors: the influence of micropores on the swelling of the electrodes	SAXS ELETTRA Trieste	6
Christian KOCZWARA	Prehal, Paris (<i>Physics, MUL</i>), Kostoglu, Mitterer (<i>Functional Materials, MUL</i>), Rebholz (<i>Univ. Cyprus</i>)	In-operando SAXS Studies on few-layer graphene as a supercapacitor electrode: the influence of surface functionalization	SAXS ELETTRA Trieste	7
Rainer T. LECHNER	M. Sytnyk (<i>FAU Nürnberg-Erlangen</i>)	In-situ SAXS/WAXS experiments to study the growth of organic nanocrystals in millisecond time-resolution	SAXS ELETTRA Trieste	7
Oskar PARIS	Ludescher, Morak, (<i>Physics, MUL</i>), Hüsing, Putz (<i>Uni Salzburg</i>), Reichenauer, Balzer, Braxmeier (<i>ZAE Bayern</i>)	Adsorption-induced deformation of monolithic carbons with hierarchical porosity: assessing the impact of micro- versus mesopores	SANS MLZ Munich	6
Cyril PICARD (<i>Univ. Grenoble</i>)	Ludescher, Paris (<i>Physics, MUL</i>), Michel (<i>Univ. Grenoble</i>)	Forced water intrusion into deformable hydrophobic nanopores	D16 ILL Grenoble	6
				36

6. Teaching

6.1 Courses held in the years 2016 and 2017

Winter Term 2015/2016

Number	Title	Hours per week / Type		Lecturer
460.129	Anleitung zu wissenschaftlicher Arbeit auf dem Gebiet der Physik von Halbleitern und Nanosystemen	4	PV	Paris O, Teichert C
460.060	Bauprinzipien biologischer Materialien	1,5	VO	Paris O
460.111	Einführung in die Oberflächen- und Dünnschichtprozesse	2	VO	Teichert C
460.094	Halbleiterwerkstoffe	2	VO	Meisels R, Teichert C
460.104	Herstellung einkristalliner Schichten - Epitaxie	2	VO	Kratzer M
460.066	Industrielle Herstellungstechniken der Mikroelektronik	2	VO	Ganitzer P
460.003	Konversatorium zu Physik I	1	KV	Paris O
460.072	Physik der Mikro- und Nanoelektronik-Bauelemente	2	VO	Meisels R
460.007	Physik IA	1,75	VO	Paris O
460.008	Physik IB	1,75	VO	Paris O
460.030	Physik Praktikum I (18 groups)	2	UE	Ganser C, Kratzer M, Lechner R.T, Meisels R, Morak R, Oswald J, Popovski G
460.000	Physik 0	0,5	IV	Paris O
460.114	Quantenmechanik (2 groups)	2,5	IV	Oswald J
460.001	Rechenübungen zu Physik IA und IB (24 groups)	2	UE	Angerer P, Brunner R, Eck S, Ganser C, Hofstätter M, Kaufmann B, Koczwar C, Kratzer M, Lechner R.T, Morak R, Prehal C, Putz B, Teichert C, Waldner P, Wießner M
460.004	Repetitorium Physik	1	RP	Paris O
460.022	Repetitorium Physik I	1	RP	Oswald J
460.121	Seminar aus Halbleiterphysik und Nanotechnologie	2	SE	Meisels R, Oswald J, Paris O, Teichert C
460.200	Seminar Bachelorarbeit	4	SE	Paris O, Teichert C
460.070	Solarzellen	2	VO	Brunner R

Summer Term 2016

Number	Title	Hours per week / Type		Lecturer
460.132	Anleitung zu wissenschaftlicher Arbeit auf dem Gebiet der Physik von Halbleitern und Nanosystemen	4	PV	Meisels R, Oswald J, Paris O, Teichert C
460.108	Anwendung von Computersimulationen in der Metall- und Biophysik	2	VO	Hartmann M
460.461	Einführung in die Synchrotronstrahlung	1	VO	Paris O
460.102	Elektronische und mechanische Eigenschaften von Heterostruktur-Bauelementen	2	VO	Kasper E
460.110	Grundprinzipien der Quantenphysik	2	VO	Oswald J
460.105	Magnetische Eigenschaften von Nanowerkstoffen	2	VO	Lechner R
460.010	Physik II	2	VO	Paris O
460.016	Physik III	2	VO	Teichert C
460.03	Physik Praktikum I (2 groups)	2	UE	Meisels R, Oswald J
460.054	Physik Praktikum II (8 groups)	2	UE	Kratzer M, Lechner R.T, Meisels R
460.055	Physik Praktikum IIA für Kunststofftechnik (3 groups)	2	UE	Lechner R.T
460.113	Physik von Fullerenen, Graphen und Carbon Nanotubes	2	VO	Teichert C
460.069	Physikalische Messtechnik (3 groups)	2	IV	Meisels R, Oswald J
460.103	Rastersondentechniken zur Charakterisierung von Festkörperoberflächen	2	VO	Teichert C
460.009	Rechenübungen zu Physik II (21 groups)	1	UE	Brunner R, Ganser C, Kaufmann B, Koczwar C, Kratzer M, Lechner R, Ludescher L, Meisels R, Morak R, Popovski G, Prehal C, Waldner P
460.048	Rechenübungen zu Physik III (2 groups)	1	UE	Kratzer M, Teichert C
460.004	Repetitorium Physik	1	RP	Paris O
460.022	Repetitorium Physik I	1	RP	Oswald J
460.122	Seminar aus Halbleiterphysik und Nanotechnologie	2	SE	Meisels R, Oswald J, Paris O, Teichert C
460.462	Synchrotronstrahlung in der Materialforschung	2	UE	Lechner R, Paris O
420.102	Einführung in die Werkstoffwissenschaft	0,1875	SE	Paris O, Teichert C

Winter Term 2016/2017

Number	Title	Hours per week / Type		Lecturer
460.129	Anleitung zu wissenschaftlicher Arbeit auf dem Gebiet der Physik von Halbleitern und Nanosystemen	4	PV	Paris O, Teichert C
460.060	Bauprinzipien biologischer Materialien	1,5	VO	Paris O
460.111	Einführung in die Oberflächen- und Dünnschichtprozesse	2	VO	Teichert C
460.094	Halbleiterwerkstoffe	2	VO	Meisels R, Teichert C
460.104	Herstellung einkristalliner Schichten - Epitaxie	2	VO	Kratzer M
460.066	Industrielle Herstellungstechniken der Mikroelektronik	2	VO	Ganitzer P
460.003	Konversatorium zu Physik I	1	KV	Paris O
460.072	Physik der Mikro- und Nanoelektronik-Bauelemente	2	VO	Meisels R
460.000	Physik 0	0,5	IV	Paris O
460.007	Physik IA	1,75	VO	Paris O
460.008	Physik IB	1,75	VO	Paris O
460.030	Physik Praktikum I (16 groups)	2	UE	Ganser C, Kratzer M, Lechner R, Meisels R, Oswald J
460.114	Quantenmechanik (2 groups)	2,5	IV	Oswald J
460.001	Rechenübungen zu Physik IA und IB (22 groups)	2	UE	Ganser C, Koczwar C, Kratzer M, Lechner R, Ludescher L, Meisels R, Morak R, Popovski G, Prehal C, Putz B, Romaner L, Spieckermann F, Teichert C, Waldner P
460.004	Repetitorium Physik	2	RP	Koczwar C, Paris O
460.022	Repetitorium Physik I	1	RP	Oswald J
460.121	Seminar aus Halbleiterphysik und Nanotechnologie	2	SE	Meisels R, Oswald J, Paris O, Teichert C
460.200	Seminar Bachelorarbeit	4	SE	Paris O, Teichert C
460.070	Solarzellen	2	VO	Brunner R
460.076	Übungen zu Charakterisierung von Werkstoffen der Elektronik	2	UE	Lechner R, Meisels R, Oswald J, Teichert C

Summer Term 2017

Number	Title	Hours per week / Type		Lecturer
460.132	Anleitung zu wissenschaftlicher Arbeit auf dem Gebiet der Physik von Halbleitern und Nanosystemen	4	PV	Paris O, Teichert C
460.461	Einführung in die Synchrotronstrahlung	1	VO	Paris O
460.102	Elektronische und mechanische Eigenschaften von Heterostruktur-Bauelementen	2	VO	Kasper E
460.110	Grundprinzipien der Quantenphysik	2	VO	Oswald J
460.105	Magnetische Eigenschaften von Nanowerkstoffen	2	VO	Lechner R.T
460.010	Physik II	2	VO	Paris O
460.016	Physik III	2	VO	Teichert C
460.054	Physik Praktikum I (2 groups)	2	UE	Kratzer M, Lechner R
460.055	Physik Praktikum II (6 groups)	2	UE	Kratzer M, Lechner R
460.056	Physik Praktikum IIA für Kunststofftechnik (2 groups)	2	UE	Kratzer M
460.113	Physik von Fullerenen, Graphen und Carbon Nanotubes	2	VO	Teichert C
460.069	Physikalische Messtechnik (8 groups)	2	IV	Meisels R, Oswald J
460.103	Rastersondentechniken zur Charakterisierung von Festkörperoberflächen	2	VO	Teichert C
460.009	Rechenübungen zu Physik II (18 groups)	1	UE	Brunner R, Koczwarra C, Kratzer M, Lechner R, Ludescher L, Meisels R, Morak R, Prehal C, Romaner L, Spieckermann F
460.048	Rechenübungen zu Physik III (2 groups)	1	UE	Kratzer M, Teichert C
460.020	Repetitorium Physik	1	RP	Koczwarra C, Paris O
460.022	Repetitorium Physik I	1	RP	Oswald J
460.122	Seminar aus Halbleiterphysik und Nanotechnologie	2	SE	Meisels R, Oswald J, Paris O, Teichert C
460.100	Strukturforschung mit Röntgen- und Neutronenstreuung an Europäischen Großforschungsanlagen	2	VO	Keckes J, Paris O
460.462	Synchrotronstrahlung in der Materialforschung	2	UE	Lechner R.T, Paris O
460.100	Strukturforschung mit Röntgen- und Neutronenstreuung an Europäischen Großforschungsanlagen	2	VO	Keckes J, Lechner R
420.102	Einführung in die Werkstoffwissenschaft	0,19	SE	Paris O, Teichert C

Winter Terms 2017/2018

Number	Title	Hours per week / Type		Lecturer
460.140	Anleitung zu wissenschaftlichen Arbeiten auf dem Gebiet der Physik von Nanomaterialien	2	PV	Paris O
460.143	Anleitung zu wissenschaftlichen Arbeiten auf dem Gebiet der Physik von Halbleiternanostrukturen und Festkörperoberflächen	2	PV	Teichert C
460.060	Bauprinzipien biologischer Materialien	1,5	VO	Paris O
460.004	Einführung in die montanistischen Wissenschaften	1	VO	Paris O, Clemens H, Friesenbichler W, Holzer C, Kern W, Pinter G, Schledjewski R, Schuecker C, Zsifkovits H, Bernhard C, Sachsenhofer R, Hofstätter H, Lehner M, Pomberger R, Flachberger H, Antrekowitsch H, Kienberger T, Grün F
460.111	Einführung in die Oberflächen- und Dünnschichtprozesse	2	VO	Teichert C
460.094	Halbleiterwerkstoffe	2	VO	Meisels R, Teichert C
460.104	Herstellung einkristalliner Schichten - Epitaxie	2	VO	Kratzer M
460.003	Konversatorium zu Physik I	1	KV	Kratzer M, Lechner R
460.072	Physik der Mikro- und Nanoelektronik-Bauelemente	2	VO	Meisels R
460.000	Physik 0	0,5	IV	Paris O
460.007	Physik IA	1,75	VO	Paris O
460.008	Physik IB	1,75	VO	Paris O
460.030	Physik Praktikum I (14 groups)	2	UE	Kratzer M, Lechner R, Meisels R, Oswald J, Popovski G
460.114	Quantenmechanik (2 groups)	2,5	IV	Oswald J
460.001	Rechenübungen zu Physik IA und IB (15 groups)	2	UE	Kaufmann B, Koczwarra C, Kratzer M, Lechner R, Ludescher L, Meisels R, Morak R, Popovski G, Prehal C, Teichert C
460.004	Repetitorium Physik	1	RP	Koczwarra C, Oswald J
460.121	Seminar aus Halbleiterphysik und Nanotechnologie	2	SE	Meisels R, Oswald J, Paris O, Teichert C
460.200	Seminar Bachelorarbeit	4	SE	Paris O, Teichert C
460.070	Solarzellen	2	VO	Brunner R
460.076	Übungen zu Charakterisierung von Werkstoffen der Elektronik	2	UE	Lechner R, Meisels R, Oswald J, Teichert C

6.2 Teaching Personnel

The faculty staff is quite heavily involved in teaching. One Univ. Prof. and three Ao. Profs. all teach on average 10 hours per week each semester, and the Senior Lecturers reached even teaching loads of 12-14 hours per week each semester. The two PhD students financed by University had a teaching obligation of up to 4 hours per week each semester. Due to the high number of parallel groups in physics exercises and/or physics practical training, in addition all other (german speaking) PhD students and postdocs were involved in teaching by typically 2 hours per week each semester, and we needed additionally some help from external lecturers, which were recruited from other Chairs at the MUL, or from external research institutions such as the Materials Center Leoben (MCL) or the Erich Schmid Institute of the Austrian Academy of Sciences (ESI-ÖAW)

We gratefully acknowledge the help from

- Dr. C. Ganser, MSc. B. Kaufmann, MSc. S. Nabavi, Dr. C. Prehal, Dr. G. Popovski, Institut für Physik
- Dr. M. Hofstätter, Institut für Struktur- und Funktionskeramik
- Dr. P. Angerer, Dr. S. Eck, Dr. R. Brunner, Dr. L. Romaner, Materials Center Leoben
- Dipl.Ing. K. Grundner, Dipl.Ing. B. Putz, Dr. F. Spieckerman, Lehrstuhl für Materialphysik & ESI-ÖAW
- Dipl.Ing. C. Bodor, Lehrstuhl für Spritzgießen von Kunststoffen
- Dr. M. Battisti, Lehrstuhl für Kunststoffverarbeitung
- Dipl.Ing. A. Moser, Lehrstuhl für Werkstoffkunde und Prüfung der Kunststoffe
- Dr. P. Waldner, Lehrstuhl für Physikalische Chemie

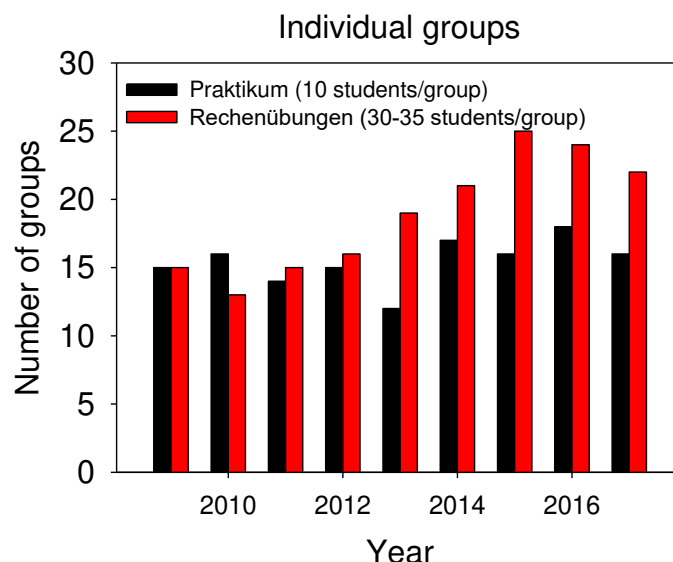
In addition, we are very grateful to

- Univ.Prof. Dr. E. Kasper, Institut für Halbleitertechnik, Universität Stuttgart, Germany
- Dr. P. Ganitzer, Infineon Technologies Austria AG, Villach
- Dr. R. Brunner, Materials Center Leoben

who support the Institute by delivering important lectures in the elective topic “Werkstoff der Elektronik und Physik funktionaler Materialien”.

Also the SAXS Beamline group at the ELETTRA synchrotron radiation source in Trieste is gratefully acknowledged for the help within the practical training course “Synchrotron Radiation in Materials Science” which took place again in both reporting years in Trieste

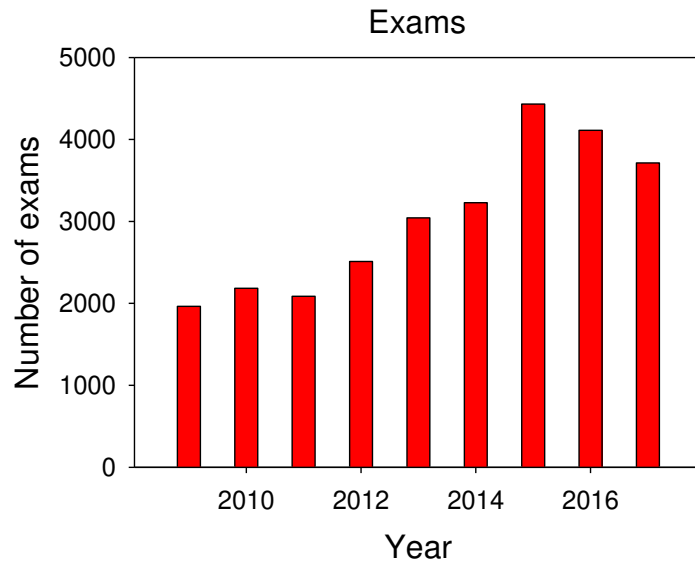
- Dr. H. Amenitsch, Dr. B. Marmioli, Dr. B. Sartori, Institute of Inorganic Chemistry, TU Graz and ELETTRA Synchrotron, Trieste.



The statistics shows the development of the number of parallel teaching classes (groups) in the winter terms for exercises and practical training in Physics since 2009.

6.3 Exams

LV.Nr.	Titel	2016	2017
460.000	Physik 0	461	354
460.001	Rechenübungen zu Physik IA & IB	688	559
460.003	Konversatorium zu Physik I	68	24
460.004	Repetitorium Physik I	3	9
460.022		2	1
460.005	Physik IA	6	
460.007		689	677
460.006	Physik IB	67	
460.008		520	491
460.009	Rechenübungen zu Physik II	546	489
460.010	Physik II	453	477
460.016	Physik III	53	54
460.020	Repetitorium Physik	0	12
460.030	Physik Praktikum I	190	188
460.048	Rechenübungen zu Physik III	55	50
460.054	Physik Praktikum II	74	55
460.055	Physik Praktikum IIA für Kunststofftechnik	33	22
460.060	Bauprinzipien biologischer Materialien	15	17
460.066	Industrielle Herstellungstechniken der Mikroelektronik	1	0
460.067	Mechanisch-Physikalische Messtechnik	5	1
460.069	Physikalische Messtechnik	30	81
460.070	Solarzellen	13	10
460.072	Physik der Mikro- und Nanoelektronik-Bauelemente	1	0
460.076	Übungen zu Charakterisierung von Werkstoffen der Elektronik	2	0
460.094	Halbleiterwerkstoffe	40	30
460.100	Strukturforschung mit Röntgen- und Neutronenstreuung an Europäischen Großforschungsanlagen	0	4
460.102	Elektronische und mechanische Eigenschaften von Heterostruktur-Bauelementen	3	2
460.103	Rastersondentechniken zur Charakterisierung von Festkörperoberflächen	8	14
460.104	Herstellung einkristalliner Schichten - Epitaxie	2	5
460.105	Magnetische Eigenschaften von Nanowerkstoffen	2	1
460.110	Grundprinzipien der Quantenphysik	2	1
460.111	Einführung in die Oberflächen- und Dünnschichtprozesse	5	4
460.113	Physik von Fullerenen, Graphen und Carbon Nanotubes	3	3
460.114	Quantenmechanik	51	61
460129	Anleitung zu wissenschaftlicher Arbeit auf dem Gebiet der Physik von Halbleitern und Nanosystemen	0	1
460.460	Exkursion: Synchrotronstrahlung in der Materialforschung /	12	11
460.462	Synchrotronstrahlung in der Materialforschung		
460.461	Einführung in die Synchrotronstrahlung	2	5
460.200	Bachelorprüfungen	2	0
	Diplomprüfungen/Masterprüfungen	5	1
	Total number of exams	4.112	3.714



The diagram shows the development of the annual number of exams taken by the Institute of Physics. As compared to 2009-2011 this number has essentially doubled. Even though the absolute peak of 2015 has not been reached anymore in 2016 and 2017, close to 4000 exams were still taken in both years during the reporting period.

7. Bachelor-, Diploma- and Doctoral Theses

7.1 Bachelor Theses

Kevin GRADWOHL
Supervisor: C. Teichert
Finished: Oct 2016

Kristallmorphologie von Lithium-Eisen Phosphat Mikropartikeln untersucht mit Rasterkraft - Mikroskopie

Hannah SCHÖNMAIER
Supervisors: O. Paris, C. Prehal
Finished: Oct. 2016

In-situ Röntgentransmissionsmessungen zur Untersuchung der Ionenkonzentration in nanoporösen, kohlenstoffbasierten Superkondensatoren

7.2 Diploma/Master Theses

Finished

Jakob Alexander GENSER
Supervisor: C. Teichert
Finished: Nov 2016

Growth of para-hexaphenyl on exfoliated hexagonal boron nitride flakes

Patrice KREIML
Supervisor: C. Teichert
Finished: March: 2016

Investigation of water absorption of cellulose fibers by gravimetric analysis and atomic force microscopy

Michael LASNIK
Supervisor: C. Teichert,
M. Kratzer, M. Deluca
Finished: Feb 2016

Determination of the Orientation Distribution Function of PZT Ceramics by Piezoresponse Force Microscopy

Lukas LUDESCHER
Supervisor: R.T. Lechner, O. Paris
Finished: Feb 2016

On the chemical and crystalline structure of CdSe/CdS core-shell nanocrystals

Caterina CZIBULA
Supervisor: C. Teichert
Finished: June 2016

Exploring chemical contrast on cellulosic materials with atomic force microscopy

Guanpeng LIN
Supervisor: C. Teichert
Finished: Sept 2017

Wachstumsmorphologien des polaren organischen Moleküls Dihydrotetraazaheptacen auf Graphen

Ongoing

Michael HUSZAR
Supervisor: C. Teichert
Since: June 2015

AFM and KPFM investigation of high-strength Aluminium brazing sheets

Aydan CICEK
Supervisor: C. Teichert,
A. Matkovic
Since: April 2017

Growth morphologies of dihydro-tetraaza-acenes on sapphire surfaces

7.3 Doctoral Theses

Finished

Christian PREHAL
Supervisor: O Paris
Finished: Aug 2017

Ion electrosorption in nanoporous carbons

Roland J. MORAK
Supervisor: O. Paris
Finished: Nov 2017

Sorption induced deformation of hierarchical porous materials

Monika MIRKOWSKA
Supervisor: H. Flachberger, Chair
of Mineral Processing/ C. Teichert
Finished: Dec 2016

Triboelectric charge behavior of minerals at microscale for
understanding the triboelectrostatic separation process

Ongoing

Christian KOCZWARA
Supervisor: O. Paris
Since: Sept 2015

Hybrid supercapacitors

Lukas LUDESCHER
Supervisor: O. Paris
Since: March 2016

Fluid-solid interactions in nanoporous materials

Caterina CZIBULA
Supervisor: C. Teichert
Since: Aug 2016

Exploring chemical contrast on cellulosic materials with atomic
force microscopy

7.4 Habilitation Theses

Markus HARTMANN
Mentor: O. Paris
Finished: November 2016

Monte Carlo Simulations in Materials Science: Mechanics of carbon
and polymer nanostructures

8. Incomings: Invited Guests (Seminar)

YEAR 2016

- Thu., 15. Dezember 2016 (together with the Department Allgemeine Analytische und Physikalische Chemie) **Kolloquium zu den Nobelpreisen 2016 aus Physik und Chemie**
- Prof. Leonhard Grill**
(Institut für Chemie, Bereich Physikalische Chemie, Karl-Franzens-Universität Graz)
“Moleküle als Nanomaschinen: Mechanische Funktionen auf der atomaren Skala” Der Nobelpreis für Chemie 2016 geht an Jean-Pierre Sauvage, Fraser Stoddart und Bernard Feringa für die "Entwicklung und Synthese molekularer Maschinen". Damit können einzelne Moleküle bei Energiezufuhr von außen gesteuert werden, um kontrollierte Bewegungen auszuführen und Arbeit zu verrichten.
- Prof. Ronny Thomale**
(Lehrstuhl für Theoretische Physik 1, Julius-Maximilians-Universität Würzburg) **“Topologische Quantenzustände von Materie”** Der Nobelpreis für Physik 2016 geht an die drei britischen Wissenschaftler David J. Thouless, F. Duncan M. Haldane und J. Michael Kosterlitz für die „theoretische Entdeckung topologischer Phasen und Phasenübergänge“ zur Beschreibung exotischer Materiezustände wie Suprafluidität, Quanten-Hall-Effekt und topologische Isolatoren.
- Tue., 13. Dezember 2016 **Dr. Benoit Coasne**
(Laboratoire Interdisciplinaire de Physique, CNRS/Université Grenoble Alpes, Grenoble, France)
“Adsorption and Transport in Multiscale Porous Media”
- Tue., 6. Dezember 2016 **Dr. Raul D. Rodriguez**
(Technische Universität Chemnitz, 09107 Chemnitz, Germany, www.ters-team.com)
“TERS: Imaging at the nanoscale with atomic force microscopy and Raman spectroscopy”
- Tue, 29. November 2016 **Prof. Conrad Becker**
(Aix-Marseille Université, CNRS, CiNaM – UMR 7325 Marseille, France)
“Single molecule chemistry by STM”
- Mo, 28. November 2016 **Dr. Olivier Siri**
(CiNaM, UMR 7325 CNRS, Aix-Marseille Université, France)
“Synthesis of rod-like molecules”
- Thu, 22. September 2016 Honorary Colloquium on the occasion of the 75th Birthday of Em.O.Univ.-Prof. **Friedemar Kuchar** & the 60th Birthdays of Ao.Univ.Profs. **Roland Meisels** and **Josef Oswald**
“From Quantum Hall Effect via Photonic Crystals to Microwave Supported Cracking of Rocks”
- Em. Univ. Prof. Günther Bauer**, Linz: “Von Villach über Wien, Oxford, Washington und Buffalo nach Leoben”
Em. Univ. Prof. Bernhard Kramer, Bremen: “Quanta, Waves, and all that Fuzz”
Prof. Rados Gajic, Belgrade: “Superconductivity in Novel 2D Materials”
Prof. Kurt Hingerl, Linz: “Coherence, Decoherence and Resulting Depolarization”
Prof. Peter Moser / Dr. Philipp Hartlieb, Leoben “New Technologies for the Excavation of Raw Materials”
- Mo, 25. Juli 2016 **Ass. Prof. Michael Grünwald**
(Chemistry Department at the University of Utah, USA)
“Self-assembly and structural transformations of semiconductor nano-materials - insights from computer simulation“

- Tue, 21. Juni 2016 **Prof. Matthias Batzill**
(Department of Physics, University of South Florida, Tampa, FL 33620, USA)
"Interfaces and Defects in 2D Materials: Graphene and MoSe₂"
- Tue, 14. Juni 2016 **Assoc.-Prof. Dr. Peter Puschnig**
(Institut f. Physik, FB Theoretische Physik, Karl-Franzens-Universitaet Graz, Austria)
"Structural and electronic properties of organic/metal interfaces investigated with photoemission tomography"
- Tue, 7. Juni 2016 **Dr. Paul Zaslansky**
(Julius Wolff Institut (JWI) Charité - Universitätsmedizin Berlin, Berlin, Germany)
"How teeth work: X-ray insights into the micro and nano structures of human dentine"
- Tue, 31. Mai 2016 **Ass. Prof. Dr. Eric Daniel Głowacki**
(Institute of Physical Chemistry, JKU Linz)
"Back to basics - solutions for next generation electronics and bioelectronics from 19th century dye chemistry"
- Mi, 11. Mai 2016 **Prof. Leonhard Grill**
(Physical Chemistry Department. Institute of Chemistry, University of Graz)
"Manipulation of single functional molecules on surfaces - from switches to wires"
- Tue, 15. März 2016 **Dr. Aleksandar Matkovic**
(Institut für Physik, Montanuniversität Leoben)
"Scanning Probe Microscopic and Spectroscopic Investigations of Graphene"
- Tue, 1. März 2016 **Prof. Volker Presser**
(INM – Leibniz-Institut für Neue Materialien gGmbH, Nanotechnologie Funktionaler Energiespeichermaterialien, Universität des Saarlandes, Saarbrücken, Deutschland)
"Capacitive Deionization an Emerging Water Treatment Technology"
- Tue, 9. Februar 2016 **Dr. Antonin Fejfar**
(Institute of Physics of Czech Academy of Sciences, Prague)
"Correlative microscopy of nanostructures for solar cells"
- Fr, 5. Februar 2016 **Prof. Martin Müller**
(Institut für Werkstofforschung, Zentrum für Material- und Küstenforschung GmbH, Helmholtz-Zentrum Geesthacht, Deutschland)
"Understanding Engineering Materials in Nature"
- Tue, 26. Jänner 2016 **Ao.-Prof. Peter Knoll**
(Institut für Physik, Karl-Franzens-Universität Graz)
"Antiferromagnetic NiO nano-particles: general properties and magnetic behavior"
- Tue, 19. Jänner 2016 **Prof. Bohuslav Rezek**
(Institute of Physics, Czech Academy of Sciences, Prague, CZ and Faculty of Electrical Engineering, Czech Technical University, Prague, CZ)
"Understanding Opto-Electronic Properties of Diamond Nanoparticles by Scanning Probe Methods"

YEAR 2017

- Tue, 19. Dezember 2017 **Ass.-Prof. Dr. Notburga Gierlinger**
(Institut für Biophysik, BOKU Wien)
“Raman scattering and scanning probe approaches on biological materials: principles & prospects”
- Thu, 14. Dezember 2017 **Kolloquium zu den Nobelpreisen 2017 aus Physik und Chemie**
(together with the
Department Allgemeine
Analytische und
Physikalische Chemie)
- Prof. Peter C. Aichelburg**
(Fakultät für Physik, Gravitationsphysik, Universität Wien)
„Gravitationswellen: In 100 Jahren von der Theorie zur Beobachtung“
Der Nobelpreis für Physik 2017 geht an die drei US-Forscher Rainer Weiss, Barry Barish und Kip Thorne für den ersten direkten Nachweis im All entstehender Gravitationswellen.
- Prof. Ferdinand Hofer**
Institut für Elektronenmikroskopie und Nanoanalytik, Technische Universität Graz
„Kryo-Elektronenmikroskopie: Hochauflösende Struktur-untersuchungen an Biomolekülen und Biomaterialien“
Der Nobelpreis für Chemie 2017 geht an die drei Wissenschaftler Joachim Frank (USA), Richard Henderson (UK) und Jacques Dubochet (Schweiz) für die „Entwicklung der Kryo-Elektronenmikroskopie“.
- Tue, 12. Dezember 2017 **Prof. Ulrike Diebold**
(Institute of Applied Physics, TU Wien, Vienna, Austria)
“Surface Science of Oxides: Atomic-Scale Insights Relevant for Applications”
- Thu, 7. Dezember 2017 **Dr. Borislav Vasic**
(Institute of Physics, University of Belgrade, Belgrade, Serbia)
“Nanoscale properties of graphene studied by atomic force microscopy”
- Tue, 5. Dezember 2017 **Prof. Martin Sterrer**
(Institut für Physik der KFU Graz)
“Ultrathin MgO(001) layers on Ag(001): A playground for studying adsorption structures and charge transfer phenomena”
- Thu, 23. November 2017 **Dr. Mihai Irimia-Vladu**
(Institute for Surface Technologies and Photonics, Joanneum Research
Forschungsgesellschaft mbH, Biological and Biologically-inspired Materials for
Electronics Fabrication, Weiz)
“Biological and Biologically-inspired Polymers and Small Molecules for Sustainable Electronics”
- Tue, 7. November 2017 **Dr. Emanuel Schneck**
(Max Planck Institute of Colloids and Interfaces, Biomaterials Department, Potsdam, Germany)
“Studying Single and Interacting Soft Interfaces with X-Rays, Neutrons, and Computer Simulations”
- Tue, 31. Oktober 2017 **Dr. Stefan Freunberger**
(Institute for Chemistry and Technology of Materials, TU Graz)
“Energy storage beyond the horizon: Materials and mechanism”
- Mo, 17. Juli 2017 **DIANA Minisymposium: Deformation of hierarchical and anisotropic porous solids by fluid adsorption**

Dr. John Dunlop

(Max Planck Institute of Colloids & Interfaces, Department of Biomaterials, Potsdam, Germany)

“Hygroscopic plant motion - the materials design of natural actuators”

Ass.-Prof. Gennady Gor

(New Jersey Institute of Technology, Department of Chemical, Biological and Pharmaceutical Engineering, Newark, USA)

“What can we learn about elasticity of nanoporous material from elasticity of fluid in its pores?”

Prof. Alexander Neimark

(Rutgers University, Department of Chemical and Biochemical Engineering, New Brunswick, USA)

“Adsorption induced deformation from the standpoint of classical poromechanics”

Mo, 3. Juli 2017

Dr. Gregor Hlawacek

(Institute of Ion Beam Physics and Materials Research Ion Beam Center, Helmholtz-Zentrum Dresden-Rossendorf, Dresden, Germany)

“Helium and Neon ion based microscopy and nanofabrication“

Tue., 27. Juni 2017

Prof. Alberta Bonanni

(Institute of Semiconductor and Solid State Physics, JKU Linz, Austria)

“III-nitrides: nano-spinodal decomposition, spin-orbitronics and piezoelectro magnetization effects”

Tue., 20. Juni 2017

Prof. Yadong Xu

(Northwestern Polytechnical University in Xi'an, China)

“Secondary phase particles and the extended defects in group II-VI telluride semiconductors”

Tue., 13. Juni 2017

Dr. Armin Hoell

(Institut Nanospektroskopie, BESSY, Helmholtz Zentrum Berlin, Germany)

“ASAXS as a synchrotron based method and some materials science applications”

Tue., 30. Mai 2017

Dr. Daniel Lüftner

(KFU Graz)

“Characterization of the interface geometry of organic adsorbates ”

Tue., 16. Mai 2017

Ao.-Prof. Egbert Zojer

(Institute of Solid State Physics, Graz University of Technology, NAWI Graz)

“Electrostatic Design of Low-Dimensional Organic Materials”

Tue., 9. Mai 2017

Prof. Jörg Kröger

(Technische Universität Ilmenau

Fakultät für Mathematik und Naturwissenschaften

Institut für Physik, Ilmenau, Deutschland)

"Exploring Nano-Chemistry and Quantum Physics on Surfaces with a Scanning Tunnelling Microscope"

Tue., 11. April 2017

Ass. Prof. Dirk Mütter

(NanoGeoScience section, University of Copenhagen, Dänemark)

"Nanoscale characterisation of natural porous materials using high-resolution X-ray tomography"

Tue., 4. April 2017

Prof. Udo Schwingenschlögl

(King Abdullah University of Science and Technology (KAUST), Physical Science and

Engineering Division, Thuwal , Saudi Arabia)

“Potential and limitations of 2D materials: Insights from computational theory”

Tue,, 21. März 2017

Prof. Oliver Diwald

(Department of Chemistry and Physics of Materials, University of Salzburg, Austria)

“Thin water films as reactive interfaces for nanomaterials growth”

Tue,, 31. Jänner 2017

Prof. Andreas Magerl

(Lehrstuhl für Biophysik, FAU Erlangen-Nürnberg, Erlagen, Deutschland)

“ Dynamical diffraction, key to see nanoprecipitates in silicon and to widen neutron backscattering spectroscopy”

Tue,, 10. Jänner 2017

Ass.-Prof. Dr. Heinz Amenitsch

(TU Graz, Anorganische Chemie, Elettra - Sincrotrone Trieste S.C.p.A., Italien)

“Energy Materials at the Austrian SAXS Beamline”

9. Outgoings: Foreign Research Visits of Institute Members

Cicek , A.	23.12.2017- 29.12.2017	Institute of Physics, University of Belgrade, Belgrade (Serbia). Research Visit within the framework of the ÖAD Project SRB09/2016
Czibula, C.	18.12.2016- 22.12.2016	Lashkaryov Institute of Semiconductor Physics, NASU, Kiev (Ukraine). Research Visit within the framework of the ÖAD Project UA07/2015
	26.02.2017- 04.03.2017	Institute of Physics, Jagiellonian University Krakow (Poland). Research Visit within the framework of the ÖAD Project PL06/2016
	19.11.2017- 24.11.2017	V. Lashkaryov Institute of Semiconductor Physics, NASU, Kiev (Ukraine). Research Visit within the framework of the ÖAD Project UA07/2015
Ganser, C.	18.07.2016 - 22.07.2016	Institute of Physics, University of Belgrade (Serbia), research visit within the framework of ÖAD Project SRB 09/2016
	03.10.2016 - 07.10.2016	Institute of Physics, University of Belgrade (Serbia), research visit within the framework of ÖAD Project SRB 09/2016
Gradwohl, K.	08.07.2017- 16.07.2017	School of Mat. Sci. & Eng., Northwestern Polytechnical University, Xi'an, China.). Research Visit within the framework of the ÖAD Project CN02/2016
Koczwar, C.	10.02.2016 - 14.02.2016	SAXS Beamline, Synchrotron ELETTRA Trieste (Italy)
	14.03.2016 - 19.03.2016	SAXS Beamline, Synchrotron ELETTRA Trieste (Italy)
	10.04.2016 - 13.04.2016	SAXS Beamline, Synchrotron ELETTRA Trieste (Italy)
	06.10.2016 - 13.10.2016	SAXS Beamline, Synchrotron ELETTRA Trieste (Italy)
	23.07.2017 - 26.07.2017	ID02, ESRF Grenoble (France)
	31.08.2017 - 08.09.2017	SAXS Beamline, Synchrotron ELETTRA Trieste (Italy)
	11.11.2017 - 27.11.2017	SAXS Beamline, Synchrotron ELETTRA Trieste (Italy)
	Kratzer, M.	18.12.2016- 22.12.2016
26.02.2017- 04.03.2017		Institute of Physics, Jagiellonian University Krakow (Poland). Research Visit within the framework of the ÖAD Project PL06/2016
06.07.2017- 08.07.2017		CINAM-CNRS Marseille (France), Research Visit within the framework of the FWF Project I1788-N20
10.07.2017- 14.07.2017		Institute of Physics, University of Belgrade, Belgrade (Serbia). Research Visit within the framework of the ÖAD Project SRB0906/2016
19.11.2017- 24.11.2017		V. Lashkaryov Institute of Semiconductor Physics, NASU, Kiev (Ukraine). Research Visit within the framework of the ÖAD Project UA07/2015

Lechner, R.T.	05.12.2017- 11.12.2017	SAXS Beamline, Synchrotron ELETTRA Trieste (Italy)
	24.04.2017- 29.04.2017	SAXS Beamline, Synchrotron ELETTRA Trieste (Italy)
Matković, A	06.03.2016.- 10.03.2016	Institute of Physics, University of Belgrade, Belgrade (Serbia). Research Visit within the framework of the ÖAD Project SRB 09/2016
	06.07.2017.- 08.07.2017	CINAM-CNRS Marseille (France), Research Visit within the framework of the FWF Project I1788-N20
Prehal, C.	14.03.2016 - 19.03.2016	SAXS Beamline, Synchrotron ELETTRA Trieste (Italy)
	10.04.2016 - 13.04.2016	SAXS Beamline, Synchrotron ELETTRA Trieste (Italy)
	06.10.2016 - 13.10.2016	SAXS Beamline, Synchrotron ELETTRA Trieste (Italy)
	23.07.2017 - 26.07.2017	ID02, ESRF Grenoble (France)
	11.11.2017 - 27.11.2017	SAXS Beamline, Synchrotron ELETTRA Trieste (Italy)
Teichert, C.	27.02.2016- 07.03.2016	Karunya-University, Coimbatore, Tamil Nadu, Indien
	18.12.2016- 22.12.2016	Lashkaryov Institute of Semiconductor Physics, NASU, Kiev (Ukraine). Research Visit within the framework of the ÖAD Project UA07/2015
	09.07.2017- 16.07.2017	School of Mat. Sci. & Eng., Northwestern Polytechnical University, Xi'an (China). Research Visit within the framework of the ÖAD Project CN02/2016
	27.08.2017- 01.09.2017	Institute of Physics, University of Belgrade, Belgrade (Serbia). Research Visit within the framework of the ÖAD Project SRB09/2016
	26.11.2017- 29.11.2017	Institute of Physics, Jagiellonian University Krakow (Poland). Research Visit within the framework of the ÖAD Project PL06/2016

10. Conference Organisation

10.1 Organisation of Conferences, Workshops or Schools

Kuchar, Friedemar

- 19th International Winterschool on New Developments in Solid State Physics, Feb 21 – 26, 2016, Castle of Mauterndorf, A-5570 Mauterndorf, Province of Salzburg, Austria (with G. Bauer, F. Schäffler, A. Rastelli)

Lechner, Rainer T. & Paris, Oskar

- 10th European NESY Winter-School & Symposium on Neutrons and Synchrotron Radiation including topical highlight lectures on Biological Systems, Altaussee (Austria), March 6-10, 2017, Austria

Teichert, Christian

- Since 2007 Co-Organizer of the Annual Nobel Prize Colloquium

10.2 Organisation of Symposia or Sessions at Conferences

Teichert, Christian

- Co-Chair des International Scientific Committee “Nanometer Structures” IVC-20, Busan, South Korea, Aug. 21 - 26, 2016.
- Vice-Chair Organizing Committee, 14th IUVESTA School on Nano-Optics, Braga, Portugal, Apr. 11- 15 2016.
- Co-Organizer 84th IUVESTA Workshop on Surface Micro-Spectroscopy and Spectro- Microscopy of Electrical Phenomena, Rehovot, Israel, Sept. 2 - 5 2018.

10.3 Membership of Program Committees & Advisory Boards of Meetings

Lechner, Rainer T. & Paris, Oskar

- Member of the Program Committee: 10th European NESY Winter-School & Symposium on Neutrons and Synchrotron Radiation, Altaussee (Austria), March 6-10, 2017, Austria

Paris, Oskar

- Member of the Program Committee of the NESY User Meeting: Future possible use of neutron and synchrotron sources by the Austrian user community, TU Graz, September 15-16, 2016, Austria

Teichert, Christian

- Member International Steering Committee, Intl. Conference on Nanoscience + Technology (ICN+T 2016), Busan, South Korea, Aug. 21 - 26, 2016.
- Member International Program Committee, 19th International Winterschool on New Developments in Solid State Physics, Mauterndorf, Feb. 21 - 26, 2016.
- Member of Scientific International Committee of 1st International Workshop Science & Entrepreneurship NanoFabrication, NanoDevices and NanoMetrology”, June 19-20 2017, Eindhoven, NL.
- Member International Program Committee, 9th International Workshop on Nanoscale Pattern Formation at Surfaces, Helsinki, Finland, June 26 – 28, 2017.
- Member International Program Committee, 20th International Winterschool on New Developments in Solid State Physics, Mauterndorf, Feb. 25 – March 22, 2018.
- Member International Steering Committee and Intl. Program Committee, Intl. Conference on Nanoscience + Technology (ICN+T 2018), Brno, Tschechische Republik, July 22 - 27, 2018

11. University Administration

Kratzer, Markus

- Betriebsrat (Member)
- Habilitationskommission Schlögl 2017 (Member)

Lechner, Rainer T.

- Sicherheitsvertrauensperson (SVP)

Oswald, Josef

- Betriebsrat (Member)
- Labour union (national representative)
- ULV (organization of the university staff for science and art, national representative)

Paris, Oskar

- Institute Chair: since 2009
- Dean of Studies: since October 2017
- Vice Dean of Studies: 2011-2017
- Vice-Delegate of the Delegate Assembly of the Austrian Science Foundation (FWF) (2015-2019).
- MUL representative at OEAWI (Österreichische Agentur für Wissenschaftliche Integration)
- Member of the task force „Forum Lehre“, Österreichische Universitätenkonferenz (UNIKO): since October 2017
- Curriculum Committee “Werkstoffwissenschaften” (Member, Vice Chair)
- Curriculum Committee “Kunststofftechnik” (Substitute Member)
- Member of the task force „§98-Professur Energietechnik“
- Member of the steering group „Evaluierung des Fachbereichs Werkstoffwissenschaften“
- Berufungskommission Biologische Physik (University of Salzburg, external Member)
- Habilitationskommission Deluca (Member)
- Habilitationskommission Hartman (Member and Reviewer)
- Habilitationskommission Holec (Member)
- Habilitationskommission Gegenhuber (Member)
- Habilitationskommission Daniel (Member)

Teichert, Christian

- Deputy Institute Chair
- Curriculum Committee “Werkstoffwissenschaften” (Member)
- Curriculum Committee “Kunststofftechnik” (Substitute Member)
- Habilitation Committee M. Hartmann 2016 (Member)

12. Advisory- & Editorial Boards, Review Committees, Membership, etc.

Kratzer, Markus

- Reviewer for Elsevier BV, Nature Scientific Report, Journal of Physical Chemistry C, ACS Applied Materials and Interfaces, Journal of Material Science, Nanotechnology, Engineering.

Lechner, Rainer T.

- Reviewer for Mater. Chem. Phys., Chem. Phys. Letters, MMM Annual Conference Proceedings
- Reviewer for Polish National Science Centre (NCN)
- National Delegate for the European Synchrotron User Organisation (ESUO)
- Member of the Austrian Physical Society and the Neutrons and Synchrotron Radiation division (NESY)

Meisels, Ronald

- Reviewer for Optics Express.

Oswald, Josef

- Reviewer for Physics Letters A, Europhysics Letters, Physical Review B.

Paris, Oskar

Scientific Boards and Memberships

- Austrian Observer at the Council of the European Synchrotron Radiation Facility ESRF.
- Chairman of the ESRF Advisory Board of the Austrian Academy of Sciences.
- Member of the Commission for International Large Scale Research of the Austrian Academy of Sciences.
- Member of the ILL Advisory Board of the Austrian Academy of Sciences.
- Member of the Scientific Advisory Board „Freiburger Zentrum für interaktive Werkstoffe und Bioinspirierte Technologien“.
- Member of the Austrian National Committee for Crystallography (OeNKK).
- Member of the Austrian Physical Society (ÖPG), German Physical Society (DPG), Austrian Chemical-Physical Society (CPG).

Memberships in Scientific Review Committees

- German BMBF-Gutachterausschuss: Erforschung kondensierter Materie an Großgeräten.
- Scientific Proposal Reviews: ESRF Grenoble, MLZ, Munich
- Beamline Review: ID02 beamline ESRF (member)

Reviewer for grant proposals and scientific publications

- Grant Proposals: Minerva Foundation (Israel)
- Habilitation theses: M. Hartmann (MUL), Svea Mayer (MUL)
- PhD theses: JB Forien (TU Berlin), C. Balzer (Univ. Würzburg), C. Prehal (MUL), R. Morak (MUL)
- Reviewer for peer-reviewed journals: Langmuir, Angewandte Chemie International Edition, European Physics Letters, Bioinspiration & Biomimetics, Journal of Synchrotron Radiation.

Popovski, Gerhard

- Reviewer for Journal of Physical Chemistry Letters.
- Reviewer for German (DFG) and Swiss (SNF) Science Funds.

Teichert, Christian

- Since 2016 Editorial Board Member of “Scanning” Hindawi/Wiley
- Since 2017 Member of Proposal Review Panel for Center of Functional Nanomaterials-Brookhaven Natl. Lab., US
- 2013-08/2016 Chair and since 09/216 Vice Chair of the Nanometer Structure Division of the International Union of Vacuum Science, Technology and Application IUVSTA
- Since 2013 Board Member of the Austrian Physical Society (ÖPG)
- Reviewer for numerous journals among them Nature Materials, Scientific Reports, Nano Letters, Applied Physics Letters, New Journal of Physics, 2D Materials, Nanotechnology, Physical Review B, J. Physical Chemistry, Surface Science, Beilstein J. of Nanotechnology, Cellulose, ...
- Reviewer for German (DFG) Austrian Academic Exchange Service (ÖAD)
- Member of the Austrian Physical Society (ÖPG), the Austrian Vacuum Society (ÖGV), the American Vacuum Society (AVS), the German Physical Society (DPG), the Materials Research Society
- Juror of the Austrian Young Physicists Tournament (AYPT)

13. Picture gallery



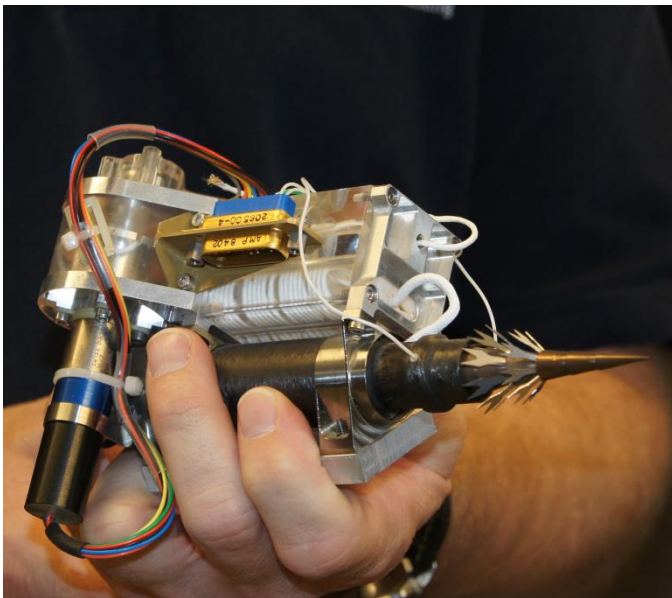
Jakob Genser: The Poster Prize at the 66th Annual Meeting of the Austrian Physical Society is awarded by the President of the Society Eberhard Widmann, (left) and the organizer Christoph Dellago, (center) to Jakob Genser (right).



Dancing goblins on a curtain of decorated graphene by A Matković: This image won the second prize of the “When Art Meets Science Competition” of the 6th International Conference on Nanostructures and Nanomaterials Self-Assembly, 2016.



10th European NESY Winter School & Symposium on Neutron and Synchrotron Radiation including topical highlight lectures on Biological Systems Altaussee (Austria), March 6-10, 2017



Visit of the Institut für Weltraumforschung (Space Research Institute) of the Austrian Academy of Sciences in Graz, September 21st 2016



Habilitation of Markus Hartmann, November 2016



50th birthday of Oskar Paris, January 2017



Symposium on occasion of Fridemar Kuchar's 75th birthday (and Ronald Meisel's and Josef Oswald's 60th birthday), September 2016



R. T. Lechner with students on an excursion to ELETTRA, Trieste 2017



Rigorosum Prehal, September 2017



Rigorosum Morak, November 2017



Fonda-Fasella 2017 award given to Christian Prehal in Trieste.



Christan Doppler Preis des Landes Salzburg 2017 awarded to Christian Prehal in Salzburg



Nobel Prize Colloquium 2017: Presentations by Peter C. Aichelburg (Faculty of Physics, University of Vienna) on gravitational waves and by Ferdinand Hofer (Institute of Electron Microscopy and Nanoanalysis, TU Graz) on cryo-electron microscopy.



Christmas Party 2017

Back cover image:
6P nanoneedles on ultrathin hBN (A. Matković, et al., Scientific Reports 2016)

